Catecholamines synthesizing enzymes in vascular cells and their hypoxic regulation

AMIR RAFIQ

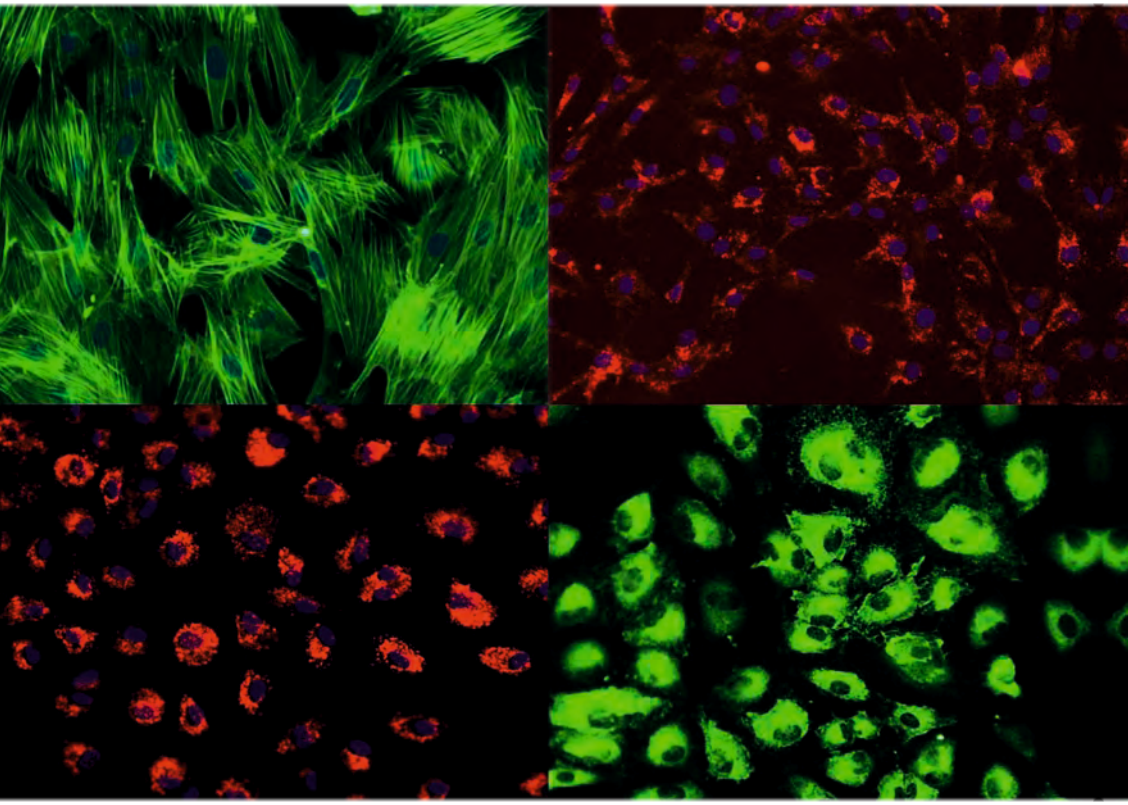

INAUGURALDISSERTATION zur Erlangung des Grades eines **Doktors der Humanbiologie**
des Fachbereichs Medizin der Justus-Liebig-Universität Gießen

édition scientifique
VVB LAUFERSWEILER VERLAG

1. Auflage 2012

1st Edition 2012

Printed in Germany

édition scientifique
VVB LAUFERSWEILER VERLAG

STAUFENBERGRING 15, D-35396 GIESSEN
Tel: 0641-5599888 Fax: 0641-5599890
email: redaktion@doktorverlag.de

www.doktorverlag.de

Catecholamines synthesizing enzymes in vascular cells and their hypoxic regulation

INAUGURALDISSERTATION

zur Erlangung des Grades eines
Doktors der Humanbiologie
des Fachbereichs Medizin
der Justus-Liebig-Universität Gießen

vorgelegt von

Amir Rafiq

aus Lahore, Pakistan

Gießen (2011)

Aus dem Institut für Anatomie und Zellbiologie
des Fachbereichs Medizin
der Justus-Liebig-Universität Gießen
Leiter/Direktor: Prof. Dr. Wolfgang Kummer

Gutachter: Prof. Dr. Wolfgang Kummer
Gutachter: Prof. Dr. Norbert Weismann
Tag der Disputation: 19.04.2012

Dedicated to

My Parents

Table of contents

List of Figures:

List of Tables:

List of Abbreviations

AP-1	Activating protein -1
BSA	Bovine serum albumin
CaMPK	Calcium- and calmodulin-dependent protein kinase
CNS	Central nervous system
CRE	cAMP response element
DβH	Dopamine-β-hydroxylase
DA	Dopamine
DAPI	4’,6-diamidino-2-phenylindole dihydrochloride
DAT	Dopamine transporter
DDC	Dopa decarboxylase
DMEM	Dulbecco's Modified Eagle Medium
DTT	Dithiothreitol
DT	Dopamine transport mechanism e.g. PMAT, DAT and OCT-2
E	Epinephrine
EDTA	Ethylendinitrilo-N, N, N´, N´, -tetra-acetic acid disodium salt
ERK	Extracellular signal-regulated protein kinase
FITC	fluorescein isothiocyanate
HAEC	Human aortic endothelial cells
HAOSMC	Human aortic smooth muscle cells
HIF	Hypoxia-inducible factor
HMVEC-L	Human micovascular endothelial cells-lung
HPAEC	Human pulmonary artery endothelial cells
LAT	L-type amino acid transporter
L-DOPA	L-3, 4-dihydroxyphenylalanine
LPS	Lipopolysaccharide
MAPKAPK	MAPK-activated protein kinase
MSK	Mitogen- and stress-activated protein kinase
NE	Norepinephrine
NMT	N-methyl transferase
OCT-2	Organic cation transporter
PBS	Phosphate buffered saline
PDPK	Proline-directed protein kinase,

PKA	Protein kinase A
PKC	Protein kinase C
PKG	Protein kinase G
PMAT	Plasma monoamine transporter
PNMT	Phenylethanolamine-N-methyltransferase
PPs	Protein phosphatases
PRAK	p38-regulated/activated kinase
PVDF	Polyvinylidene fluoride
SDS	Sodium dodecyl sulphate
SDS-PAGE	SDS polyacrylamide gel electrophoresis
Ser	Serine
SMA	Superior mesenteric artery
TH	Tyrosine hydroxylase
TTBS	Tween tris buffered saline
β2-MG	β2-microglobulin

I Introduction

I.1 Catecholamines

Catecholamines (dopamine, norepinephrine and epinephrine) are physiologically important as they are involved in a number of body functions and also act as neurotransmitters. Dopamine acts as a very important neurotransmitter in various processes in the central nervous system (CNS). It is also an active player in kidney function and also Norepinephrine acts as a neurotransmitter in the CNS and of postganglionic sympathetic neurons. Epinephrine is a hormone released from the adrenal gland and also serves as neurotransmitter of brainstem neurons (Kuhar et al., 2006).

I.1.1 Chemical structure

The peculiarity of catecholamines is having an amine group, and a nucleus made of a catechol ring (a benzene ring with two attached hydroxyl groups), thus they are called “catecholamines” (Feldman et al. 1997).

I.1.2 Catecholamine biosynthesis

Catecholamines are synthesized from a single precursor, tyrosine, a non-essential amino acid (Fig. 1). Catecholamine synthesis was first described by Blaschko in 1939. Later, tyrosine hydroxylase (TH) was characterized as mediating the rate limiting enzymatic step of the synthesis pathway (Nagatsu et al., 1964). The first enzymatic step in the catecholamine synthesis is catalyzed by TH, also known as tyrosine 3-monooxygenase. It catalyzes the conversion of tyrosine into L-3,4-dihydroxyphenylalanine (L-DOPA). This enzymatic step is the rate limiting enzymatic step of the catecholamine synthesis pathway. Tetrahydrobiopterin, iron and molecular oxygen act as cofactors for the activity of this enzyme. The next step is the conversion of L-DOPA into dopamine, which is catalyzed by L-aromatic amino acid decarboxylase (AADC) also known as dopa decarboxylase (DDC). Pyridoxal phosphate acts as a cofactor for this enzyme (Feldman et al. 1997). The next enzymatic step is catalyzed by dopamine-β-hydroxylase (DβH), a copper containing soluble and membrane bound enzyme (Wallace et al., 1973), which converts dopamine into noradrenaline or norepinephrine (NE). Ascorbate and molecular oxygen act as cofactors for this enzyme

(Fig. 1). The last enzymatic step of this pathway is catalyzed by phenylethanolamine-N-methyltransferase (PNMT), which converts norepinephrine (NE) = noradrenaline into epinephrine (E) = adrenaline by adding a methyl group to the amino group. S-adenosylmethionine acts as cofactor for the enzymatic activity (Kuhar et al., 2006; Kvetnanský et al., 2009).

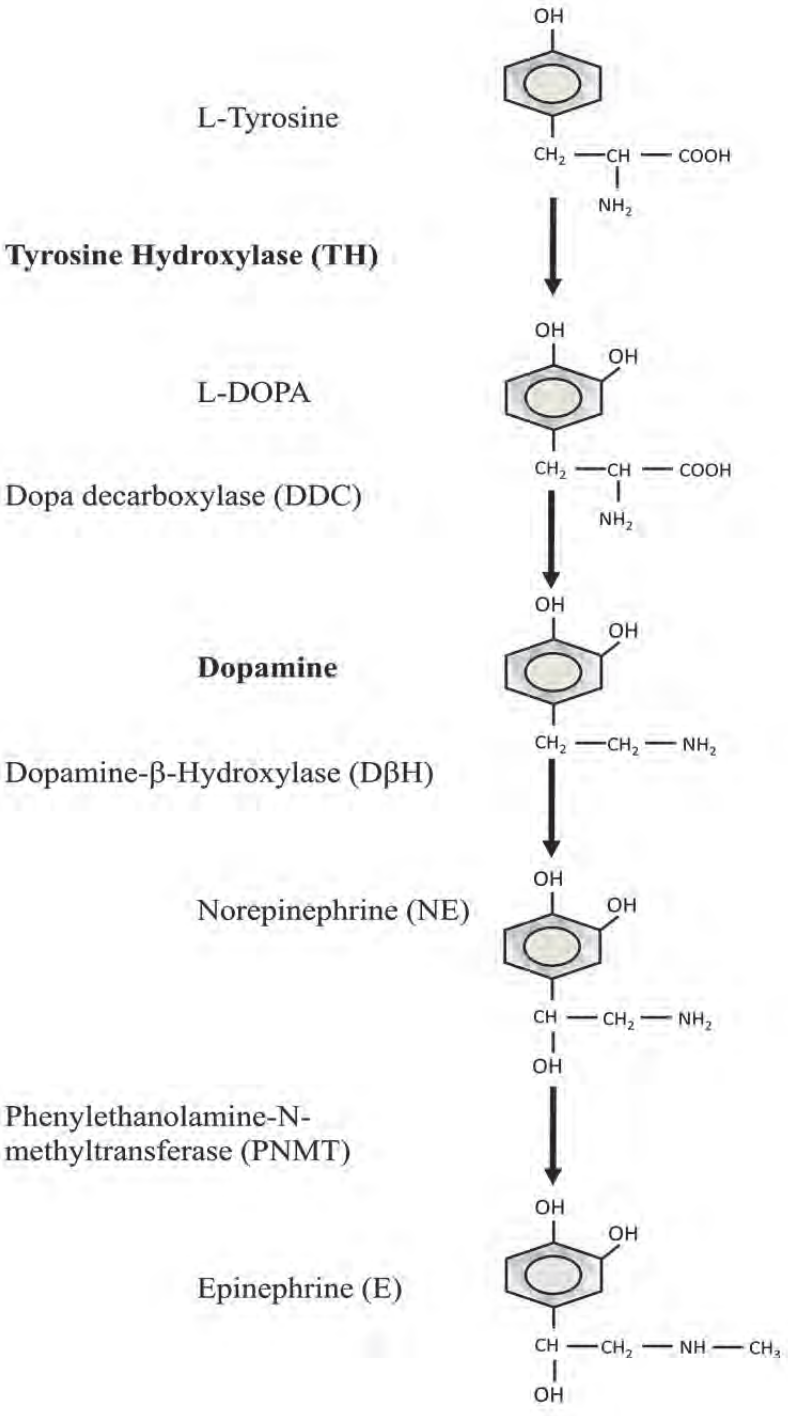

Fig. 1: Schematic diagram of catecholamine biosynthesis pathway and its enzymatic steps.

I.1.3 Characteristics of catecholamine synthesizing enzymes

TH is a hetrodimeric enzyme; each subunit has a molecular weight of about 60 kDa. It is a soluble enzyme, various cytoplasmic metabolites or substances can modulate the activity of TH, e.g. phosphatidylserine, polyanions and heparin sulfate. Analogs of tyrosine, e.g. α-methyl-p-tyrosine, act as competitive inhibitors for the TH activity. Primarily, it converts tyrosine to L-DOPA but it can also catalyze the conversion of phenylalanine to tyrosine (Kuhar et al., 2006).

DDC is the final enzymatic step in the dopamine synthesizing neuron in the CNS. It is of clinical significance in patients suffering from Parkinson disease. The patients are given excess of L-DOPA to increase the dopamine synthesis in surviving dopaminergic nerve terminals. α-Methyldopa is a potent inhibitor of its enzymatic activity. **DβH** is a tetrameric glycoprotein consisting of 77 and 73 kDa subunits. This enzyme is mainly confined to the inner membrane of vesicles although a minor amount is also present freely within the vesicles. This enzyme is also released along with norepinephrine from the nerve endings or from the adrenal gland and it is present in plasma (Kuhar et al., 2006). **PNMT** is the terminal enzyme of catecholamine synthesis pathway, which is mainly present in the endocrine cells of the adrenal medulla but also in some brainstem neurons. The enzyme activity is affected by corticosteroids in the adrenal gland and in superior cervical ganglia (Bohn et al., 1984).

I.2 Non-neuronal catecholamine synthesis

It has been reported that catecholamine synthesis is not confined to neurons and the adrenal gland. Instead, other cells/tissues in the body also express the entire or parts of the enzymatic machinery involved in catecholamine synthesis. This non-neuronal catecholamine synthesis is of particular interest in various body functions such as in immune response, renal function and regulation of vascular tone.

Recently, catecholamine synthesis in adipocytes has been reported. Vargovic et al., 2011 has reported that adipocytes from various body parts posses all the required enzymatic machinery to sysnthesize *de novo* catecholamines (Vargovic et al., 2011).

Certain cells of immune system, e.g. lymphocytes, can synthesize catecholamines *de novo* and also store them (Bergquist et al., 1994; Musso et al., 1996). Recently, Flierl et al. (2007) have shown that alveolar macrophages and blood neutrophils are capable of *de novo* catecholamine synthesis. Expression levels of

mRNAs for TH and DβH mRNA are upregulated in these cells after exposure to lipopolysaccharide (LPS) for 4 h. TH mRNA expression is reported in rat spleen, which is another non-neuronal site of catecholamine synthesis, and the catecholamines synthesized in spleen are involved in immune response (Kubovcáková et al., 2001). Furthermore, it is also reported that catecholamiens and their metabolites are present in lymphocytes, where they might modulate the function of T cells and B cells (Bergquist et al., 1994). The presence of DDC is also reported in kidney, liver and spleen (Lovenberg et al., 1962; Rahman et al., 1981; Lindström and Sehlin, 1983; Adam et al., 1986). Human peripheral leukocytes express functionally active DDC, which is able to convert L-DOPA into dopamine (Kokkinou et al., 2009).

PNMT mRNA expression has been reported in rat spleen and thymus (Andreassi II et al., 1998), in rat lung (Kennedy et al., 1993), and during rat embryonic development it is mainly present in the heart (Ebert et al., 1996). Ziegler and coworkers have reported non-adrenal PNMT enzymatic activity in various rat tissues such as hypothalamus, brain stem, heart, eyelid, muscle and kidney. The activity level in various tissues from rat is reported to be hypothalamus > atria > brain stem > ventricle > eyelid > muscle > kidney (Ziegler et al., 2002). PNMT expression and enzyme activity have also been detected in various human organs such as lung, kidney, heart, liver, spleen and pancreas. Nonspecific N-methyl transferase (NMT) is also reported in various human organs (Kennedy et al., 1995).

Endocrine and exocrine cells of the rat pancreas can also synthesize and release the catecholamine dopamine. Following chemical sympathectomy, TH presence is reported in rat pancreas (Mezey et al., 1996). Furthermore, Kawamura and coworkers reported TH mRNA expression and enzyme activity in rat aorta, vas deferens and lung. Chemical sympathectomy studies with 6-hydroxydopamine showed persistence of dopamine and TH activity in aorta, vas deferens, stomach and lung, suggesting a non-neuronal synthesis of dopamine and possibly other catecholamines in these organs (Kawamura et al., 1999).

Non-neuronal catecholamine (NE and E) synthesis in the rat kidney was reported by Silva et al., in 1979 using the isolated perfused kidney model. Proximal tubular cells of the kidney were also reported to synthesize dopamine (Chan 1976). DiMarco et al., in 2007 have shown synthesis and release of all catecholamines from various kidney epithelial cell lines, e.g. LLC-Pk_1, MDCK and mIMCD-3. These renal

epithelial cell lines express the enzymatic machinery for catecholamine synthesis and they are also able to release these catecholamines (DiMarco et al., 2007).

I.3 Vascular effects of catecholamines

I.3.1 Vascular effects of dopamine

Dopamine is profoundly involved in the regulation of blood pressure, sodium balance, kidney and adrenal gland function, and is considered to be involved in the pathogenesis of hypertension (Hussain and Lokhandwala, 1998; Jose et al., 1998; Muhlbauer et al., 2000; Jose et al., 2002). Dopamine has vasodilator effects in the systemic circulation. Injecting dopamine in the dog renal artery causes vasodilation (McNay et al., 1965), and similar effects were observed in humans (McDonald et al., 1964). This vasodilator effect in arteries differs from that of NE and E as it cannot be blocked by α-adrenergic antagonists (McNay and Goldberg, 1966). Dopaminergic vasodilation is mediated by specific dopamine receptors. The first evidence for such vascular dopamine receptors was provided by Goldberg et al. in 1978 (Goldberg et al., 1978). Later on it was shown that specific dopamine receptors are present in the vasculature of canine paw pads, dopamine released from nerve terminals causes vasodilation, and this response is independent from adrenergic receptors (Bell and Stubbs, 1978).

In arteries, presence of D_1-like receptors (D_1 and D_3) is well reported on smooth muscle cells of arteries and they mediate a vasodilator response (Hussain and Lokhandwala, 2003). D_2-like receptors are localized prejunctionally in arteries, and stimulation of these receptors inhibits the release of NE, thereby augmenting the vasodilator effect of D_1-like receptors (Goldberg et al., 1978; Lokhandwala and Hegde, 1990). D_2 and D_4 receptors have also been reported to be localized in human and rat heart atria (Ricci et al., 1998).

In the kidney dopamine plays an important role by regulating the sodium excretion, increasing diuresis and vasodilation, resulting in reduced renal resistance (Bello-Reuss et al., 1982; Lokhandwala and Hegde, 1990; Ricci et al., 1993). D_2 receptors present in kidney cause vasodilatation by reducing the sympathetic vasoconstrictor effect (Rump and Schollmeyer, 1993; Cheung and Barrington, 1996).

I.3.2 Structure and types of dopamine receptors

On the basis of pharmacological properties dopamine receptors were first classified in two types: D_1 (dopamine is required in micro-molar concentration) and D_2 (dopamine is required in nano-molar concentration) receptors (Goldberg et al., 1978; Kebabian and Calne, 1979). The D_1 receptor is highly expressed in the brain (Derray et al., 1990; Fremeau et al., 1991; Weiner et al., 1991).

In the canine circulatory system, initial findings suggested that arterial blood pressure, heart rate and blood flow in the renal and femoral arteries are regulated by dopamine receptors D_1 and D_2. In another classification scheme, the dopamine receptors were classified on the basis of their location: Postjunctional D_1 receptors are involved in direct vasodilation in the renal artery, and the prejunctional D_2 receptors on the postganglionic sympathetic nerve terminals have an inhibitory effect on the norepinephrine release, which augments vasodilation mediated by the D_1 receptor in the femoral artery and also results in decreased cardiac contraction (Goldberg et al., 1978).

Pharmacological studies suggested that, in blood vessels, the D_1 receptor is predominantly localized in the tunica media (middle layer), which mainly comprises of smooth muscle cells. In contrast, D_2 receptors are mainly present on sympathetic nerve endings and are involved in inhibition of NE release. In the kidney, D_1 receptors are ubiquitously localized and are involved in regulation of various kidney functions. D_2 receptors are also localized in kidney (Missale et al., 1998).

Dopamine receptors have seven transmembrane domains and are members of the G-protein coupled receptor family. Based on molecular cloning and pharmacologic studies, dopamine receptors are classified in two different groups: the D_1-like, which consists of subtypes D_1 and D_3, and the D_2-like, consisting of subtypes D_2, D_4 and D_5 (Vallone et al., 2000).

I.3.3 Vascular effects of norepinephrine and epinephrine

Norepinephrine is the predominant catecholamine in the arteries of rat and rabbit (Head et al., 1982). Both NE and E cause vasoconstriction in canine coronary arteries (Berne, 1958). These effects are mediated by adrenergic receptors which are also G-protein coupled receptors with 7 transmembrane domains. There are two main groups of adrenergic receptors first explained by Ahlquist in 1948, α and β, which are further subdivided.

I.3.4 α-Adrenergic receptors

α-Adrenergic receptors are further subdivided into α_1 and α_2, which are involved in various functions; among them are vasoconstriction of coronary arteries (Woodman and Vatner, 1987), vasoconstriction of veins (Elliott, 1997) and decreased motility of smooth muscle cells in gastrointestinal tract (Sagrada et al., 1987). They are distributed overall in the body (Kuhar et al., 2006).

I.3.5 β-Adrenergic receptors

β-Adrenergic receptors are widely distributed in the body and play a major role for maintaining homeostasis in the CNS and in cardiovascular, pulmonary and endocrine systems (Brodde, 2008). There are three types of β-adrenergic receptors: β_1, β_2 and β_3. In human, β_1 is localized in heart, kidney, cerebral cortex and hypothalamus, β_2 is localized in lung, liver, cerebellum, hippocampus, cerebral cortex, smooth muscles and olfactory bulb, while β_3 is localized in fat tissue and brain (Kuhar et al., 2006).

I.4 Oxygen sensing, hypoxia and gene regulation

Oxygen is an essential molecule for all higher organisms, since it is the main terminal electron acceptor in mitochondrial oxidative phosphorylation. It also acts as substrate or cofactor for various metabolic enzymes. It is necessary that O_2 supply must be regulated. Any kind of changes (hypoxia, hyperoxia) causes alterations in the cellular and tissue metabolism. All the cells of the body are able to detect and respond to changes in O_2 in their microenvironment. A reduced supply of O_2 to tissue or cell causes major pathological changes, such as stroke or myocardial infarction. All the higher organisms have developed mechanism to cope with low supply of O_2. Hypoxia is defined as a condition where oxygen demand for steady state cell metabolism is higher than oxygen supply. Such exposure to lowered pO_2 results in a specific regulation of the cellular transcription machinery. Hypoxia can arise in a variety of developmental, physiological, and pathological states. Different tissues and organs of the mammalian body behave differently in response to acute (seconds to minutes) and chronic (hours to days) hypoxia. Acute response usually involves hyperventilation, increased cardiac output, vasodilation in systemic arteries, pulmonary vasoconstriction and activation of glucose uptake by cells to enhance energy production. In most of tissues, chronic

hypoxia effects erythropoiesis, angiogenesis and neovascularization, tissue remodeling and activation of glucose metabolism and transport (Lopez-Barneo et al., 2001).

Hypoxia causes regulation of a number of physiologically important genes in vasculature, among which are erythropoietin, vascular endothelial growth factor and TH (Zhu et al., 2002). Hypoxic response is studied in various cell lines and it is reported that all mammalian cells possess one or more oxygen sensing mechanism or oxygen sensor responding to lowered O_2. Various cell types within the body are specialized to sense changes in pO_2, e.g. carotid body and airway neuroepithelial bodies. However, it is difficult to proclaim one or more specific O_2 sensor (Wenger, 2000). The discovery of oxygen regulated transcription factors was a major advancement in the field of O_2 sensing. Hypoxia-inducible factors (HIFs) are well studied for their role in the regulation of gene expression for maintaining O_2 homeostasis. HIF-1, an O_2 regulated transcription factor, is ubiquitously expressed and is involved in cellular responses to low pO_2. HIF-1 plays a vital role as metabolic regulator which allows rapid adaptation to oxygen availability. It was initially discovered that HIFs are able to bind to hypoxia response elements in the 3´ flanking region of the erythropoietin gene at low intracellular oxygen tension. HIF-1 and HIF-2 are heterodimeric transcription factors composed of one of two HIF proteins (HIF-1α or HIF-2α) and HIF-1β, also known as aryl hydrocarbon receptor nuclear translocator (Gardner and Corn, 2008). HIF proteins are members of basic helix-loop-helix-Per-Arnt-Sim family of transcription factors. HIF proteins have conserved domains which include a basic helix-loop-helix region for DNA binding and two per-arnt-sim domains meant for dimerization and target gene specificity (Semenza and Wang 1992; Maxwell et al., 1993; Wang and Semenza 1993; Semenza, 1999; Wang et al., 1995; Semenza 2000). In normoxic conditions, HIF-1α is consistently present in cells whereas HIF-1α is not detectable during normoxia because it is rapidly degraded after being synthesized. Hypoxia causes rapid stabilization and activation of HIF-1α which is detectable in less than 30 min, and peak response takes 4-8 hours. Upon normoxia, activity decays very rapidly, having a half life of about 5 min (Jiang et al., 1996). Hypoxia increases the HIF-1 activity at multiple levels. It increases HIF-1α transcription, mRNA stabilization and nuclear translocation. The most important effect of hypoxia on HIF-1α is preventing its degradation. The low levels of HIF-1α during normoxia are due to ubiquitination and proteasomal degradation, and these are blocked during hypoxia. Exogenous H_2O_2 can inhibit the increased HIF activity by hypoxia while sulfhydryl oxidation reverses hypoxic activation (Ema et al.,

1999; Huang et al., 1998; Salceda and Caro, 1997). In some pathological states, certain gene products also play a role in the ubiquitination and subsequent degradation of HIF-1α, one such example is the von Hippel-Lindau (VHL) tumor suppressor gene product pVHL. In VHL-defective cells, HIF-1α is consistently expressed and stabilized (Maxwell et al., 1999; Kroll et al., 1999). It is also observed that hypoxia induced HIF-1α activity is blocked by rotenone, an inhibitor of mitochondrial complex I (Semenza 1999; Chandel et al., 1998).

Activating protein-1 (AP-1) is another transcription factor which is involved in various functions; one of them is catecholamine biosynthesis (Shaulian and Karin, 2001). Growth factors, proinflammatory cytokines, UV radiation and hypoxia can activate AP-1, which can regulate various targets (Cummins and Taylor, 2005). It is known that hypoxia activates AP-1 in vessels which results in regulation of various genes, including TH (Milhorn et al., 1997), vascular endothelial growth factor (Salnikow et al., 2002) and endothelial nitric oxide synthase (Hoffmann et al., 2001).

I.4.1 Hypoxic regulation of TH expression

The carotid body is an arterial chemoreceptor; it is a small, paired organ of neuroectodermal origin. It is located at the carotid bifurcation. During fetal life, sympathoadrenal progenitors from the superior cervical ganglia migrate to form this organ. It is innervated by afferent sensory nerve fibers from the glossopharyngeal nerve, and contains a profuse network of blood vessels. The carotid body is the most abundantly perfused organ of the body. It is made of type I cells or glomus cells, which are wrapped with processes of glia-like type II cells (Kameda, 2005; Lopez-Barneo, 2001). The carotid body can rapidly detect any changes in chemical composition of the blood. It is well known that the carotid body can be activated by hypoxia, hypercapnia and acidosis. Furthermore, it is also activated by low glucose (Peers & Buckler, 1995; Pardal and Lopez-Barneo, 2002; Lopez-Barneo, 2001; Garcia-Fernandez et al., 2007; Zhang et al., 2007). The type I cells or glomus cells contain secretory vesicles having ATP, dopamine, acetylcholine and many others neurotransmitters (Nurse, 2005). The dopamine released from secretory vesicles is probably involved in vasodilation in response to low pO_2. Hypoxic regulation of TH expression has been extensively studied in the carotid body. Hypoxia causes up-regulation of TH mRNA expression in the carotid body up to 500% after 6 h of hypoxic exposure. This hypoxic response is

restricted to type I cells of the carotid body (Millhorn et al., 1993). Hypoxia also increases TH enzyme activity in the carotid body (Czyzyk-Krzeska et al., 1992).

The PC12 cell line is derived from rat adrenal pheochromocytoma (Greene and Tischler, 1976). This cell line expresses high levels of catecholamines, especially dopamine. It is extensively used to study catecholamine synthesis and release mechanism by using different stimulants. An up-regulation of TH mRNA levels and increased mRNA stability are also observed in hypoxia exposed PC12 cells (Czyzyk-Krzeska et al., 1994). An O_2 responsive sequence of the TH gene promoter is involved in the enhanced TH mRNA expression and its stability (Norris and Millhorn, 1995). Additionally, PNMT expression in mouse phechromocytoma cells is upregulated in response to hypoxia (Evinger et al., 2000).

HIFs are also involved in the regulation of TH gene expression in PC12 cells by interacting with the hypoxia response elements located in the proximal region of the TH promoter (Schnell et al., 2003). TH mRNA transcription is mainly dependent on cAMP response element (CRE) activity. In PC12 cells, basal transcription level of TH is mediated by transcription factors activity at partial dyad (-17 bp), CRE (-45bp), and AP-1 (-205 bp) while induced transcription is mainly regulated by CRE activity, while very small contributions are from AP-1 and hypoxia response element 1 (-225 bp), and this differential regulation is independent of the inducing stimulus (Lewis-Tuffin et al., 2004).

I.5 TH regulation by phosphorylation

Dopamine synthesis is also regulated by phosphorylation of TH at various serine (ser) residues such as ser-19, ser-31 and ser-40 sites. TH is phosphorylated at ser-40 mainly by protein kinase A (PKA) in response to forskolin and cyclic Adenosine mono phosphate analogues, and by protein kinase G (PKG) in response to nitric oxide and cyclic guanosine monophosphate analogues while protein kinase C (PKC) acts directly or indirectly in response to phospholipase C activators (Fig. 2, Dunkley et al., 2004).

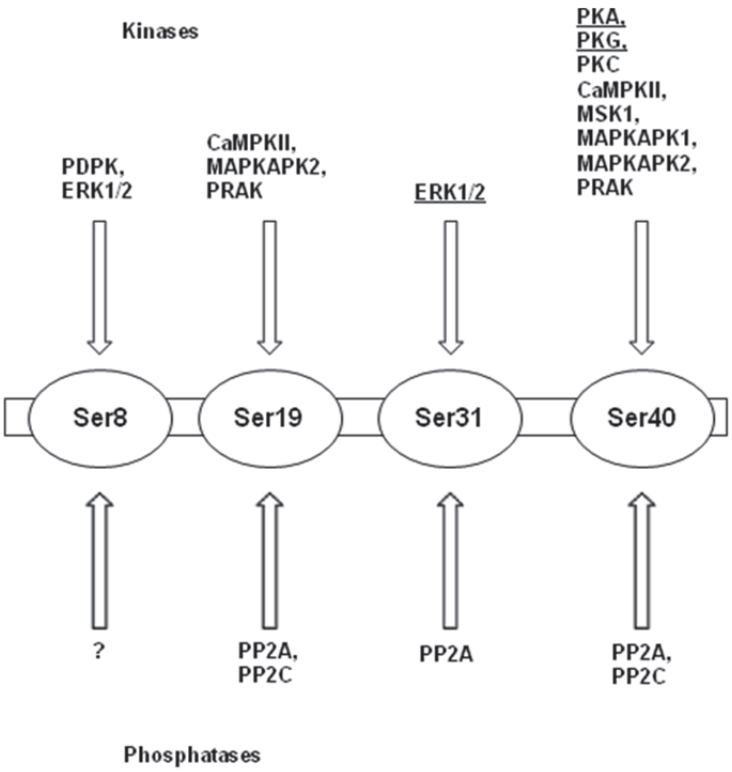

Fig. 2: The protein kinases and protein phosphatases (PPs) capable of modulating TH phosphorylation in vitro and in situ. The protein kinases and PPs able to phosphorylate and dephosphorylate TH in vitro at serine residue Ser8, Ser19, Ser31 and Ser40 are shown. These four sites are all phosphorylated in situ. There is good evidence that the kinases shown in bold and underlined are able to phosphorylate TH in situ but the evidence is incomplete for depolarizing stimuli. There is enough evidence that the kinases shown in bold but not underlined are able to phosphorylate TH in situ. CaMPK, calcium- and calmodulin-stimulated protein kinase; ERK, extracellular signal-regulated protein kinase; MAPKAPK, MAPK-activated protein kinase; MSK, mitogen- and stress-activated protein kinase; PDPK, proline-directed protein kinase; PKA, protein kinase A; PKC, protein kinase C; PKG, protein kinase G; PRAK, p38-regulated/activated kinase (Dunkley et al., 2004).
(Adapted from Dunkley et al., 2004, under permission license nr. 2639590089628 from John Wiley and sons Inc.)

Calcium and calmodulin-dependent protein kinase II (CaMPKII) is most likely responsible for the phosphorylation at ser-19 site in response to depolarizing agents and increases intracellular calcium. Extracellular signal-regulated protein kinase (ERK) is mainly responsible for the phosphorylation at ser-31 site of TH in response to various stimuli. The phosphorylation rate of TH at ser-31 is relatively slower as compared to ser-19 and ser-40. The fourth phosphorylation site ser-8 is reported to be less significant (Dunkley et al., 2004).

1.6 Catecholamine synthesis in arteries

Little is known about the expression and hypoxic regulation of catecholamine synthesis enzymes in the arterial system. Our workgroup previously showed, by using radio-immunoassay, dopamine and other catecholamines in control and chemically sympathectomized rat aorta and superior mesenteric artery (SMA). Dopamine content was unaffected by chemical sympathectomy, whereas levels of norepinephrine and epinephrine were significantly reduced in arteries from chemically sympathectomized rats (Fig. 3).

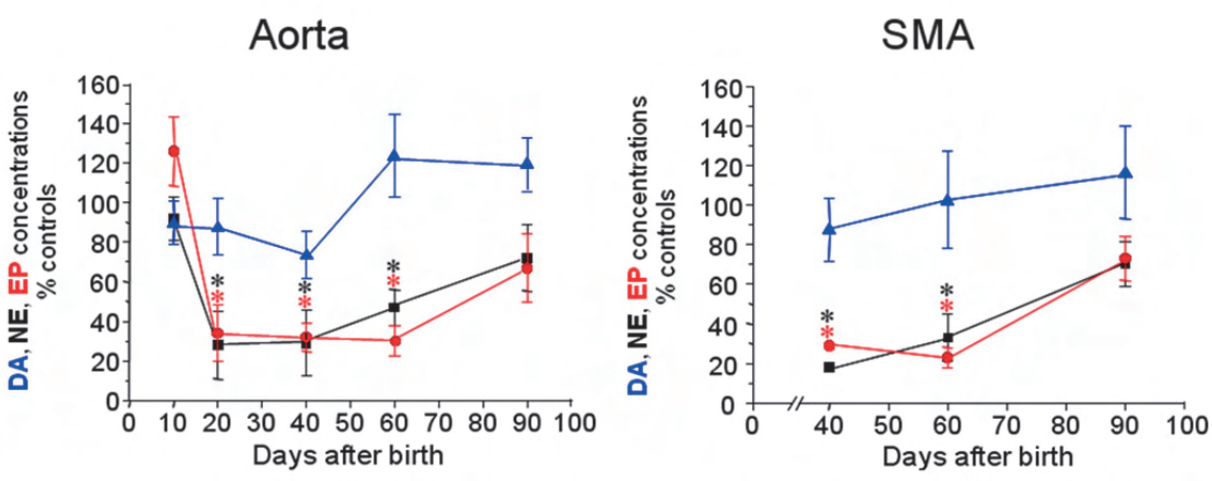

Fig. 3: Catecholamines content of chemically sympathectomized (6-hydroxydopamine) rat aorta and SMA. ∗, ∗ vs respective control value (n = 6-9). The significance level was set as P<0.05. DA; Dopamine, NE; Norepinephrine and EP; Epinephrine (Kuncová et al., 2007) unpublished data from Dr. Jitka Kuncová, Institute of Physiology, Medical Faculty Pilsen, Charles University Prague, Czech Republic)

Functional studies with isolated perfused rat SMA showed an endothelium-dependent vasodilation in U46619-preconstricted SMAs when pO_2 in the superfusion medium was lowered from 150 to 125 mmHg. This vasodilation was blocked by the specific dopamine D_1 receptor antagonist SCH-23990. This vasodilatory response was still observed when endothelium was removed, although its magnitude was less as compared to the response with endothelium. This suggested a role of locally synthesized dopamine in mediating vasodilation in response to lowering pO_2 in rat SMA.

I.7 Aim of the study

The main focus of the study was to identify the source of catecholamine synthesis in cells of the vascular wall (endothelial and smooth muscle cells) and to further elaborate the hypoxic up-regulation of catecholamine synthesizing enzymes gene expression in these cells.

The following questions were specifically addressed:

- Do intact arteries express the catecholamine synthesizing enzymes?
- Do isolated and cultured vascular cells express the catecholamine synthesizing enzymes?
- What is the influence of hypoxia on this enzymatic machinery in isolated and cultured vascular cells?

II Material and Methods

II.1 Cell culture

To isolate endothelial cells, adult female wistar rats weighing 240-260 g (for lung microvascular endothelial cells n=7, and for aortic endothelial cells n=6) were used. The rats were obtained from the animal facility of the Institute for Physiology, Justus-Liebig-University Giessen.

II.1 Lung microvascular endothelial cell culture

Day 1: Preparation of anti-RECA antibody coupled dynabeads®

In order to couple anti-RECA antibody to dynabeads® (Dynal A.S., Oslo, Norway), 25 µl of dynabeads® were taken in a 1.5 ml test tube and the test tube was placed in a magnetic particle concentrator (Dynal MPC®-E, Dynal A.S., Oslo, Norway) for ~3 min. The dynabeads® attached to the wall of the test tube facing the magnet and then the supernatant was removed. Then, 1 ml of wash buffer (phosphate buffered saline [PBS] pH 7.4 and 0.1 % bovine serum albumin [BSA], filter sterilized) was added and gently mixed with the dynabeads®. The test tube was placed again in the magnetic particle concentrator for ~3 min and the supernatant was removed. This wash process was repeated 3 times.

Then, mouse anti-RECA antibody (Clone HIS52, Serotec, U.K.) was diluted 1:100 in wash buffer I, mixed gently with the dynabeads® and this mixture was placed overnight at 2-8°C.

Day 2: Isolation of rat lung endothelial cells

The beads were again washed 2 times with wash buffer I. The rats were sacrificed by inhalation of isoflurane (Baxter, Unterschleißheim, Germany). The thorax was opened and 0.2 ml of heparin (5000 IU/ml, Ratiopharm, Ulm, Germany) was injected into the left ventricle of the heart. To perfuse the pulmonary vasculature, a small opening was made into the right ventricle and a cannula was inserted. An opening was also made into the left atrium as an outlet of perfusion. The animal was perfused with rinsing solution consisting of polyvinylpyrrolidone 12.5 g, NaCl 4.5 g and procainhydrochloride 2.5 g dissolved in 500 ml water, to which 500 µl of heparin was added prior to use. This rinsing solution was followed by ice-cold DMEM medium (PAA Laboratories GmbH, Marburg, Germany) with 1% penicillin/streptomycin (P/S; PAA Laboratories GmbH, Marburg, Germany).

After perfusion, the lung was removed and placed in a petri dish with 15 ml of DMEM medium with 10% P/S. In a laminar flow cabinet, the lung was cut into small pieces with a small scissor. These pieces were placed in collagenase solution (0.5% collagenase, 0.5% bovine serum albumin and 10% P/S in DMEM, sterile filtered) with continuous agitation at room temperature for 45 min. The mixture was filtered through a 20-30 μm pore size filter. The filtrate was collected in a 50 ml sterile tube (Greiner Bio-One GmbH, Frickenhausen, Germany) and centrifuged at 377xg for 5 min. The supernatant was removed and the pellet was resuspended in 10 ml of DMEM medium with 10% P/S and centrifuged at 377xg for 5 min. This process was repeated again and the cell pellet was resuspended in a 1 ml volume of DMEM medium with 10% P/S and transferred to 2 ml sterile test tube. Anti-RECA antibody coupled dynabeads® were added to this test tube and incubated at 2-8°C for 30 min. The test tube was placed in the magnetic particle concentrator for ~4 min, the supernatant was removed and the endothelial cell-anti-RECA antibody-dynabeads® complexes were washed with DMEM medium with 10% P/S. This wash process was repeated 2 times. After washing, the endothelial cell-anti-RECA antibody-dynabeads® complexes were transferred to a 75 cm^2 cell culture flask (NUNC, New York, USA) with 10 ml of endothelial cell growth medium MV (Promo cell, Heidelberg, Germany). The medium was replaced every 2^{nd} day and the cells were trypsinized when confluent. Cells were trypsinized according to the process described in II.3.

II.2 Aortic endothelial cell culture

Day 1

The day 1 procedure for coupling of anti-RECA antibody to dynabeads® was the same as for isolation of lung endothelial cells (II.1)

Day 2

The rats were sacrificed by inhalation of isoflurane (Baxter, Unterschleißheim, Germany). The thorax was opened and 0.2 ml of heparin (5000 IU/ml, Ratiopharm, Ulm, Germany) was injected into the left ventricle of the heart. In order to perfuse the systemic vasculature, a small opening was made into the left ventricle and a cannula was inserted. An opening was also made into the right atrium as an outlet of perfusion. The animal was perfused with rinsing solution, followed by ice-cold DMEM medium with 1% P/S.

After perfusion, the aorta was removed and placed in a petri dish with 15 ml of DMEM medium with 10% P/S. In a laminar flow cabinet, the aorta was cut into small pieces with a small scissor. These pieces were placed in collagenase solution (0.5% collagenase, 0.5% bovine serum albumin and 10% P/S in DMEM, sterile filtered) with continuous agitation at room temperature for 45 min. The mixture was filtered through a 20-30 μm pore size filter. The filtrate was collected in a 50 ml sterile tube (Greiner Bio-One GmbH, Frickenhausen, Germany) and centrifuged at 377xg for 5 min. The supernatant was removed and the pellet was resuspended in 10 ml of DMEM medium with 10% P/S and centrifuged at 377xg for 5 min. This process was repeated again and the cell pellet was resuspended in a 1 ml volume of DMEM medium with 10% P/S and transferred to 2 ml sterile test tube. Anti-RECA antibody coupled dynabeads® were added to this test tube and incubated at 2-8°C for 30 min. The test tube was placed in the magnetic particle concentrator for ~4 min, the supernatant was removed and the endothelial cell-anti-RECA antibody-dynabeads® complexes were washed with DMEM medium with 10% P/S. This wash process was repeated 2 times and then the endothelial cell-anti-RECA antibody-dynabeads® complexes were transferred to a 75 cm^2 cell culture flask (NUNC, New York, USA) with 10 ml of endothelial cell growth medium MV (Promo cell, Heidelberg, Germany). The medium was replaced every 2^{nd} day and the cells were trypsinized when confluent.

II.3 Trypsinisation of cells

Cells were trypsinized at 90% confluency. The medium was removed, the cells were washed with a small amount (3 ml) of trypsin solution (PAA Laboratories GmbH, Marburg, Germany) and then 5 ml of trypsin solution was added and the flask was placed at 37°C in an incubator until all the cells were detached (~5 min). Then, 5 ml of prewarmed endothelial cell growth medium was added to the flask. The contents were mixed with a 10 ml plastic pipette and transferred to a 15 ml sterile centrifuge tube and centrifuged at 377xg for 5 min. The supernatant was removed and the cell pellet was resuspended in 3 ml of prewarmed endothelial cell growth medium.

Cells from one 75 cm^2 flask were usually splitted to 4 flasks (each 75 cm^2) for expansion.

II.4 Characterization of endothelial cells

EC were characterized by 1,1'-dioctadecyl-3,3,3',3'-tetramethyl-indocarbocyanine perchlorate labeled acetylated low density lipoprotein (DiI-Ac-LDL; Paesel & Lorei, Hanau, Germany) uptake and by immunolabelling for von Willebrand factor (vWF).

II.4.1 DiI-Ac-LDL uptake

EC were cultured in 8-well cell culture slide (NUNC, New York, USA) for 48 hours. EC were incubated with DiI-Ac-LDL, 10 μg/ml at 37°C for 4 hours. Then, the EC were washed with pre-warmed cell growth medium followed by 5 min wash with PBS, were fixed using 4% PFA for 10 min and washed with PBS 2 x 10 min. For nuclear labeling, the EC were incubated with 4',6-diamidino-2-phenylindole dihydrochloride (DAPI; 1 mg/ml Sigma, St. Louis, USA 1:5000 diluted in PBS) for 10 min, followed by washing with PBS 2 x 10 min. The slides were covered with Mowiol 4-88 (Calbiochem, Darmstadt, Germany) and stored at 4°C until microscopy.

II.4.2 Immunolabelling for vWF

EC were cultured in 8-well sterile culture slides (NUNC, New York, USA). At 80-90 % confluency, cells were washed with PBS for 5 min and fixed with ice cold methanol (Merck, Darmstadt, Germany) for 15 min, followed by incubation with blocking solution (5% BSA and 5% normal goat serum in PBS) for 1 h at room temperature.

The EC were incubated overnight at room temperature with rabbit-anti-human vWF antibody (cat # A0082, Dako Cytomation, Glostrup, Denmark), diluted 1:300 in PBS with 0.05 M NaCl and 0.01% NaN_3 (PBS+NaCl+NaN_3). After overnight incubation with primary antibody, the EC were washed with PBS 2 x 10 min and incubated with secondary antibody (FITC-conjugated goat-anti rabbit IgG; Cappel, Aurora, USA) diluted 1:400 in PBS+NaCl+NaN_3, for 1 h at room temperature. The EC were again washed with PBS 2 x 10 min. For nuclear labeling, the EC were incubated with DAPI (1 mg/ml; 1:5000 diluted in PBS) for 10 min, followed by washing with PBS 2 x 10 min. The EC were post-fixed with 4% paraformaldehyde (PFA) for 10 min, washed 2 x 10 min with PBS and cover-slipped with mowiol 4-88. Slides were kept at 4°C until microscopy.

II.5 Isolation of aortic smooth muscle cells

The rats were sacrificed by inhalation of isoflurane (Baxter, Unterschleißheim, Germany). The thorax and the abdomen were opened and 2 ml of heparin (5000 IU/ml, Ratiopharm, Ulm, Germany) was injected into the left ventricle of the heart. In order to perfuse the systemic vasculature, a small opening was made into the left ventricle and a cannula was inserted. An opening was also made into the right atrium as an outlet of perfusion. The animal was perfused with rinsing solution, followed by ice-cold DMEM medium with 1% P/S.

The aorta was removed and placed in ice-cold DMEM medium. With the help of a dissecting microscope the surrounding tissues were removed and the aorta was cut into two parts: thoracic and abdominal aorta.

The aorta was cut open longitudinally and the endothelium was removed with the help of a cotton swab. Then, the opened aorta was cut into small pieces (1-2 mm) and placed in a sterilized 24-well plate (Greiner Bio-One GmbH, Frickenhausen, Germany). Smooth muscle growth medium (Dulbecco's Modified Eagle Medium: Nutrient Mixture F-12 [DMEM/F12; Invitrogen GmbH, Karlsruhe, Germany] 20% fetal calf serum [FCS; Hyclone Fisher Scientific, Schwerte, Germany], 1% P/S) was added to the wells containing aortic pieces. The medium was changed every 2nd day. After 4-6 days, smooth muscle cells start to migrate out of the graft. The cells were transferred to a 75 cm^2 flask for expansion. Later the cells were trypsinized according to II.3.

II.5.1 Characterization of smooth muscle cells

Aortic smooth muscle cells were characterized by immunolabelling of α-smooth muscle actin with FITC-conjugated mouse monoclonal anti-smooth muscle actin antibody (Clone 1A4; Sigma, St. Louis, USA)

II.5.2 Procedure for immunolabelling

For immunolabelling, the cells were cultured in 8-well culture slides (NUNC, New York, USA). The 80-90% confluent cells were used for immunolabelling with anti-smooth muscle actin antibody. The cells were washed with PBS and then fixed with 4% PFA for 15 min, followed by washing for 5 min with PBS. The cells were treated with 0.1% triton x-100 (Merck, Darmstadt, Germany) for 10 min to make the cell membrane permeable, and washed with PBS for 5 min. The cells were incubated with

blocking solution (5% BSA and 5% NGS in PBS) for 1 h at room temperature. The cells were incubated overnight at room temperature with FITC-conjugated anti-smooth muscle actin antibody from mouse, diluted 1:500 in PBS+NaCl+NaN_3. After overnight incubation, the cells were washed with PBS 2 x 10 min.

For nuclear labeling, the smooth muscle cells were incubated with DAPI (stock solution 1 mg/ml) 1:5000 diluted in PBS for 10 min, followed by washing with PBS 2 x 10 min. Then cells were again fixed with 4% PFA for 10 min, washed with PBS 2 x 10 min and coverslipped with mowiol 4-88. Slides were kept at 4°C until microscopy.

II.6 Exposure of vascular cells to hypoxia

Vascular cells (endothelial and smooth muscle cells) were exposed to hypoxia (1% O_2, 5% CO_2, and 94% N_2) in an incubator at 37°C. For hypoxic exposure, the cells were cultured in 6-well plates (for total RNA isolation) and in 75 cm^2 culture flasks (for protein extraction). The cells were exposed to hypoxia for 6, 12 and 24 h in an incubator at 37°C. At the same time, a normoxic (20% O_2, 5% CO_2) control was also included in each experiment. After hypoxic and normoxic exposure the samples were processed for PCR and western blotting as follows.

II.7 Polymerase chain reaction (RT-PCR)

II.7.1 RNA isolation

For total RNA isolation, Rneasy Mini Kit (Qiagen, Hilden, Germany) was used according to the instruction manual provided in the kit. After total RNA isolation, the RNA quantity was measured with a Bio photometer (Eppendorf, Hamburg, Germany) and the total RNA was stored at -80°C until further work.

II.7.2 cDNA Synthesis

For cDNA synthesis, 1 µg of total RNA was first exposed to DNase (Invitrogen GmbH, Karlsruhe, Germany) to remove any left-over traces of DNA during RNA isolation. For this purpose, 1 µg of total RNA was mixed with 1 µl DNase-I (1 U/µl, Invitrogen GmbH) and 1 µl 10x DNase I Reaction Buffer (Invitrogen GmbH, Karlsruhe), and incubated for 15 min at 25°C. The DNase reaction was stopped by adding 1 µl of EDTA (25 mM, pH 8.0; Invitrogen GmbH) and heating the mixture to 65°C for 10 min.

After this step, the mixture was immediately cooled to 4°C by placing on ice. For reverse transcription, 1 µl of oligo dTs (MWG Biotech AG, Ebersberg, Germany), and 1 µl of dNTPs (10 mM of each dNTP; Qiagen, Hilden, Germany), 2 µl dithiolthreitol (0.1 M; Invitrogen GmbH), 1 µl Superscript II Revese Transcriptase (200 U/µl, Invitrogen GmbH) and 4 µl 5x First Strand Buffer (Invitrogen GmbH) were incubated at 42°C for 2 min followed by incubation at 42°C for 50 min. At the end of cDNA synthesis reaction, the mixture was heated to 72°C for 10 min for inactivation of Superscript II. The cDNA was stored at -20°C.

II.7.3 Real-time reverse transcription-polymerase chain reaction

Real-time reverse transcription-polymerase chain reaction (real-time RT-PCR) was performed with an I-Cycler (Bio-Rad, Munich, Germany) by using iQ™ SYBR® Green Supermix (Bio-Rad, Munich, Germany). This master mix contains all the necessary ingredients required for qPCR. For setting up the reaction, 2 µl of 1:2 diluted cDNA was added to 12.5 µl of iQ™ SYBR® Green Supermix and 0.5 µl (20 pM) of intron spanning forward and reverse primer pairs (table 1) and 10 µl of H_2O .

Primer	Sequence	Product length (DNA fragment position)	Accession number
TH	Forward ACGTCCCCAAGGTTCATC Reverse TACAGCCCGAGACAAGGA	216 bp (99-314)	NM_012740
DDC	Forward AGAGGGAAGGAGATGGTGGA Reverse GTGGGGAAGTAAGCGAAGAAGT	221 bp (302-122)	NM_008890
DβH	Forward AGCCCCTTCCCTTACCACA Reverse TGCGTTCTCCATCTCACCTC	162 bp (148-309)	NM_031144
PNMT	Forward GCGAGGGTGAAGCGAGTC Reverse GGCAGAAGGCAGAGACCAAG	106 bp (495-564)	NM_012512
β_2MG	Forward TGTCTCAGTTCCACCCACCT Reverse GGGCTCCTTCAGAGTGAC	252 bp (49-262)	NM_031144
β-actin	Forward CAACCTTCTTGCAGCTCCTC Reverse AGGGTCAGGATGCCTCTCTT	191 bp (147-338)	NM_012512

Table 1: Rat primer pairs used for real-time RT-PCR (TH: tyrosine hydroxylase; DDC: dopa decarboxylase; DβH: dopamine-β-hydroxylase; PNMT: phenylethanolamine-N-methyltransferase; β_2MG: β-2-microglobulin)

The conditions for real-time RT-PCR were as follows: The mixture was incubated for 10 min at 95°C for activation of DNA polymerase, followed by 45 cycles (20 s at 95°C, 20 s at 60°C and 20 s at 72°C) for the extension. At the end of the PCR cycles, melting curves of the products were analyzed. All the samples were run in triplicate and the mean cycle threshold (CT) values were taken for further analysis.

Primer	Sequence	Product length (DNA fragment position)	Accession number
TH	Forward ACCCTGACCTGGACTTGG Reverse CAATCTCCTCGGCGGTGT	138 bp (663-800)	NM_199292
DDC	Forward AGAGGGAAGGAGATGGTGGA Reverse AGTGGGGAAGTAGGCGAAGA	222 bp (226-442)	NM_001082971
DβH	Forward CTCTCGGCACCACATTATCA Reverse TCGGGTTTCATCTTGGAGTC	147 bp (732-878)	NM_000787
PNMT	Forward GCAGCCACTTTGAGGACATC Reverse CAAGCAGAAGGCAGAGACCA	281 bp (494-774)	NM_002686
β_2MG	Forward TTCACCCCCACTGAAAAAGA Reverse AGCAAGCAAGCAGAATTTGG	160 bp (328-487)	NM_004048

Table 2: Human primer pairs used for real-time RT-PCR (TH: tyrosine hydroxylase; DDC: dopa decarboxylase; DβH: dopamine-β-hydroxylase; PNMT: phenylethanolamine-N-methyltransferase; β_2MG: β-2- microglobulin)

II.7.4 Gel electrophoresis

The PCR product size was analyzed by gel electrophoresis in 2% agarose gel (Genegarose L.E.; iNNO-TRAIN Diagnostik GmbH, Kronberg, Germany) in Tris-acetate-EDTA buffer (482 g/l TRIS [USB, Cleveland, USA], 104.2 ml/l glacial acetic acid [Merck, Darmstadt, Germany], 200 ml/l 0.5 M EDTA [Invitrogen, Karlsruhe, Germany] up to 1 l with distilled H_2O, pH 8.0). Ethidium bromide 1 µl (1%; Roth GmbH, Karlsruhe, Germany) was added to label the PCR product for visualization with an UV transilluminator (Biometra, Göttingen, Germany)

II.7.5 Data analysis

The real-time RT-PCR data was analyzed by comparative method or ΔΔCT method of relative quantification. In this method amounts of target are calculated by using CT values as described below.

First of all, the ΔCT value for each sample is determined by calculating the difference between the CT value of the target gene and the CT value of the house keeping gene. In this study β-2 microglobulin (β2MG) was used as house keeping gene.

ΔCT (sample) = CT target gene – CT β2MG

To compare normoxic with hypoxic samples, ΔΔCT was calculated by the following formula:

ΔΔCT = ΔCT (sample) - ΔCT (control)

Control is normoxic and sample is hypoxia exposed.

From this ΔΔCT value, relative expression was calculated by following the formula $2^{-\Delta\Delta CT.}$ This gives the gene expression relative to normoxic conditions.

The data were analyzed for significance by Kruskal-Wallis test and Mann-Whitney-U test, and data are presented as box plots by using the software program SPSS Version 15.0 (SPSS GmbH Software, Munich, Germany). Probability (P) values of less than 0.05 were considered significant ($P<0.05$).

II.8 Western blot

II.8.1 Protein extraction

Protein extract from tissue/cells was made by urea extraction buffer (8 M urea [Merck], 10 % glycerol [Merck], 5% SDS [Merck], 1 M Tris pH 6.8 [Merck], 1 M DTT [dithiotheritol, Sigma], 100 mM PMSF [phenylmethylsulphonyl fluoride, Sigma]) and one tablet of complete protease inhibitor cocktail (Roche Diagnostics GmbH, Mannheim, Germany) per 10 ml of buffer.

Tissue/cells were extracted in a five fold excess (v/w) of extraction buffer. The tissue/cells were homogenized by a ball mill homogenizer (Retsch, Haan, Germany) for 5 min at maximum speed (30 strokes/s). Later, the extract was centrifuged for 2-3 min at 6800xg to get a clear extract.

II.8.2 Protein gel electrophoresis

Protein electrophoresis was done by SDS-PAGE. The seperating gel containing 10% acrylamide was made by 10 ml of 30% acrylamid (Roth, Karlsruhe, Germany), 5.6 ml 2 M TRIS-HCl, pH 8.8, 150 µl 20% SDS (Serva, Heidelberg, Germany), 160 µl 10% ammoniumpersulfate (APS; Merck, Darmstadt, Germany), 12 µl TEMED (TEMED; Tetramethylethylenediamine, Roth, Karlsruhe, Germany) and 9.25 ml H_2O. The

stacking gel consisted of 1 ml 30% acrylamide, 50 µl 20% SDS, 1.25 ml 1 M TRIS-HCl, pH 6.8, 80 µl 10% APS, 10 µl TEMED and 7.7 ml H_2O.

Before loading, the protein extracts were mixed with 5x concentrated sample buffer (320 mM Tris-HCl, pH 6.8, 5% SDS, 50% glycerol, and 0.25 mg/ml bromphenolblue and 1% β-2-mercaptoethanol) and heated to 95°C for 5 min. Protein extracts were applied 5-10 µl per lane. For reference, 10 µl of prestained protein marker (Biorad, Munich, Germany) was also applied in one lane as reference of molecular weight of protein. The running buffer consisted of 0.025 M TRIS, 0.192 M glycine and 2.5 ml 20% SDS in one litre water. The stacking gel was electrophoresed for 15-20 min at 100 V (Power supply from Hoefer Scientific Instruments, San Francisco, USA) for separation of proteins; the separation gel was electrophoresed at 200 V for 40-50 min. After electrophoresis, the proteins were transfered from the gel to a polyvinylidene fluoride (PVDF) membrane (Millipore, Schwalbach, Germany) in semi-dry conditions (Semi-dry electroblotter; Sartorius, Goettingen, Germany). Before transfer, the PVDF membrane was activated according to the manufacturer's protocol. For transfer, filter paper, PVDF membrane and the gel were soaked in a blotting buffer (NuPAGE Transfer Buffer, Invitrogen, Karlsruhe, Germany). The transfer was done for 90 min at 6 V.

After transfer, the PVDF membrane was incubated for 1 h at room temperature in blocking buffer consisting of 10% milk powder (Roth, Karlsruhe, Germany) in tween-tris-buffered saline (TTBS; 0.01 M Tris-HCl [pH 8.0], 0.2 NaCl and 0.05% Tween-20).

After blocking, the membrane was incubated with primary antibody (mouse anti-tyrosine hydroxylase antibody; ms-α-TH, clone 2/40/50; Chemicon international, Temecula, USA) diluted 1:2,000 in 5% milk powder TTBS overnight at room temperature. After overnight incubation, the membrane was washed with TTBS 6x5 min and incubated with peroxidase-conjugated secondary antibody (goat anti-mouse-IgG, 1:10,000 dilution; Pierce, Bonn, Germany) in 2.5% milk powder TTBS for 1 h at room temperature. Membranes were washed again with TTBS 6x5 min. For visualizing the protein, chemiluminescence substrate (Super Signal West Pico Chemiluminescence Substrate, Pierce, Bonn, Germany) was applied to the membranes for 5 min according to the instructions of manufacturer. For the visualization of the chemiluminescence reaction, the membranes were exposed to x-ray films (Amersham, Munich, Germany) for various periods of time.

II.9 Dissection of rat vessels for real-time RT-PCR and western blotting

To isolate various vessels, adult female wistar rats weighing 240-260 g (for real-time RT-PCR n=5, and for western blotting n=4) were used. The rats were obtained from the animal facility of the Institute for Physiology, Justus-Liebig-University Giessen.

The rats were sacrificed by inhalation of isoflurane (Baxter). The thorax was opened and 0.2 ml of heparin (5,000 IU/ml, Ratiopharm) was injected into the left ventricle of the heart. Rat thoracic aorta, abdominal aorta, superior mesenteric and femoral were removed, given a quick wash in ice-cold saline, and frozen at -80°C. Later, these samples were processed for real-time RT-PCR (III) and western blot (IV).

II.10 Primary human vascular cell culture

Primary human vascular cells were obtained from Lonza (Verviers, Belgium). Human microvascular endothelial cells of the lung (HMVEC-L; cat # CC-2527), human aortic endothelial cells (HAEC; cat # CC-2535) and human pulmonary artery endothelial cells (HPAEC; cat # CC-2530) were cultured in the endothelial cell basal medium (cat# CC-3121, Lonza) supplemented with the various growth factors (cat # CC-4147; Lonza) according to the instructions from the supplier and were characterized according to protocols (II.4).

Human aortic smooth muscle cells (HAOSMC; cat # CC-2571) were cultured in the smooth muscle cell growth medium (Lonza) according to the instructions from the supplier and were characterized according to protocols (II.5.1).

II.11 Exposure of primary human vascular cells to hypoxia

Primary human vascular cells were exposed to hypoxia according to protocol (II.6).

II.12 Western blotting and real-time RT-PCR

Western blotting from primary human vascular cells exposed to normoxia and hypoxia was done according to protocol (II.7), and qPCR was done according to (II.8)

II.13 Immunohistochemistry

II.13.1 Dissection, fixation and processing of vessels

Adult female wistar rats weighing 240-260 g (n= 3) were used. The rats were obtained from the animal facility of the Institute for Physiology, Justus-Liebig-University Giessen.

The rats were sacrificed by inhalation of isoflurane (Baxter). The thorax was opened and 0.2 ml of heparin (5,000 IU/ml, Ratiopharm) was injected into the left ventricle of the heart. Rat thoracic aorta, abdominal aorta, superior mesenteric and femoral was removed, given a quick wash in ice cold saline and placed immediately in 4% paraformaldehyde (PFA; Roth, Karlsruhe, Germany) in 0.1 M phosphate buffer, pH 7.4, for fixation for 4 h. Later, the tissues were washed overnight in 0.1 M phosphate buffer, pH 7.4.

After overnight wash, the vessels were placed overnight in 18% sucrose (Roth, Karlsruhe, Germany) in 0.1 M phosphate buffer. The next day, fixed tissues were shock-frozen in liquid nitrogen and stored at -20 °C.

The frozen PFA-fixed tissues were cut with a cryostat to 10 μm thick sections. The sections were fixed with histo block solution (10% horse serum, 0.5% tween and 0.1 % BSA in PBS, pH 7.4) for 1 hour at room temperature.

Then, the sections were incubated overnight at room temperature with rabbit anti-tyrosine hydroxylase antibody (Biotrend) diluted 1:400 in PBS+NaCl+NaN_3. The sections were washed with PBS 2x10 min and incubated with Cy3-conjugated donkey anti-mouse-IgG antibody (Dianova, Hamburg, Germany) diluted 1:1000 in PBS+NaCl+NaN_3 for 1 h at room temperature. After incubation with secondary antibody, the sections were again washed with PBS 2x10 min and post-fixed with 4% PFA for 10 min.

The sections were washed again 2x10 min with PBS, coverslipped with mowiol-488 and stored at 4°C.

II.13.2 Preabsorption test

The specificity of the primary antibody labelling was tested by incubating the primary antibody (rabbit anti-tyrosine hydroxylase antibody) with the antigen (tyrosine hydroxylase, 1 μg/μl; Biotrend, Cologne, Germany) for 1 h at room temperature. This

mixture was used in immunohistochemistry. As positive control, primary antibody without antigen was used.

II.13.3 Microscopy/Epifluorescence microscopy

The slides with fluorescence labeled tissue sections were analyzed by an epifluorescence microscope (Axioplan 2 Imaging, Zeiss, Jena, Germany) fitted with a camera (Axio Cam, Zeiss). The images were captured by the camera with the help of Axiovision 4 and 4.7 software (Zeiss).

The filters with specific wavelength for excitation and absorption spectra for various fluorochromes/fluorophores are listed in table 3.

Fluorochrome	**Excitation filter (nm)**	**Barrier filter (nm)**
Cyanine 3 (Cy3)	525-560	570-650
DAPI	360-370	420-460
Fluorescein isothiocyanate (FITC)	460-490	515-550

Table 3: The filters used for immunohistochemistry.

III Results

III.1 Cell culture

III.1.1 Endothelial cell culture from rat

Rat lung microvascular and aortic EC were isolated, expanded and characterized by uptake of DiI-Ac-LDL (Fig. 4 A, B) and by immunoreactivity to vWF. Immunolabeled cells showed dot-like structures within the cytoplasm (Fig. 4 C, D). The labeling was absent when the cells were incubated without primary antibody (Fig. 4 E).

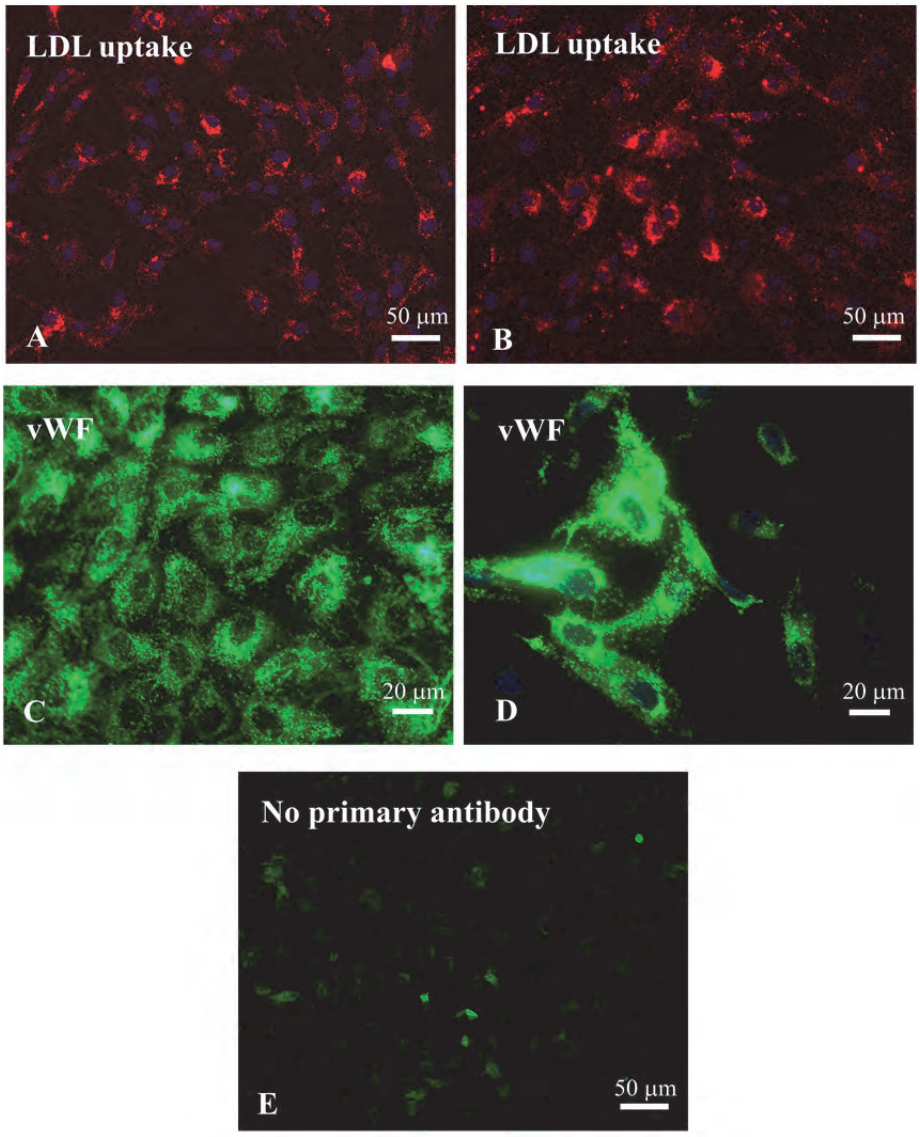

Fig. 4: The purity of isolated EC was controlled by use of specific EC markers. (A) Rat lung microvascular EC and (B) aortic EC show uptake of DiI-Ac-LDL. (C) Rat lung EC, (D) rat aortic EC were immunolabeled with anti-vWF antibody. (E) The negative control, lung EC incubated with secondary antibody only, showed absence of labeling.

III.1.2 Endothelial cell culture from human

Primary human EC (lung microvascular, aortic and pulmonary artery) were purchased from Lonza, cultured and characterized by uptake of DiI-Ac-LDL (Fig. 5 A, B, C).

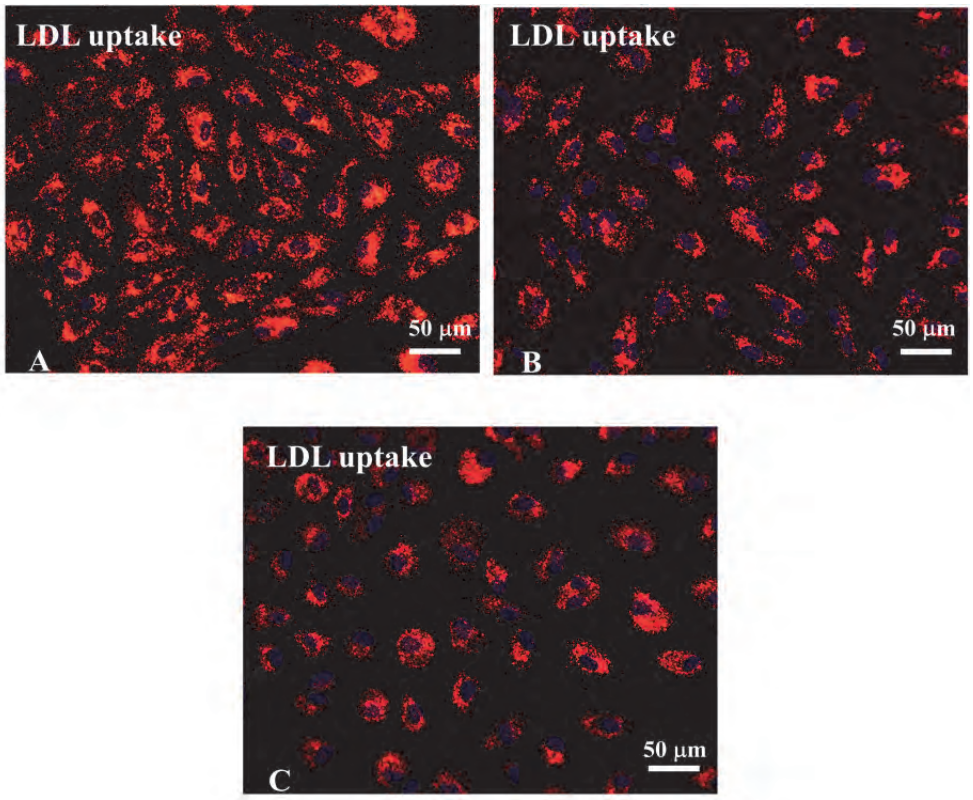

Fig. 5: The purity of EC was controlled by use of specific EC markers. (A) Human lung microvascular EC, (B) human aortic EC and (C) human pulmonary artery EC, showed uptake of DiI-Ac-LDL.

The cells were further characterized by immunoreactivity to vWF. Immunolabeled cells showed dot-like structures within the cytoplasm (Fig. 6 A, B, C). The labeling was absent when the cells were incubated without primary antibody (Fig. 6 D).

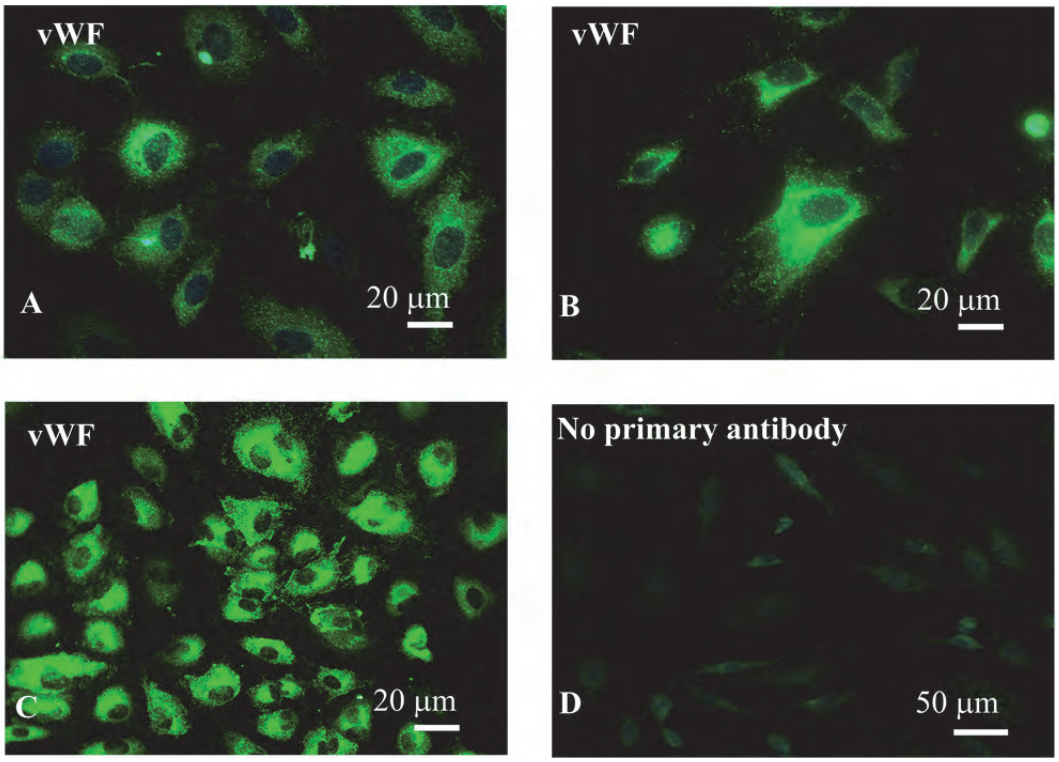

Fig. 6: The purity of EC was controlled by use of specific EC markers. (A) Human lung microvascular EC, (B) human aortic EC and (C) human pulmonary artery EC were immunolabeled with anti-vWF antibody. (D) The negative control, human lung EC incubated only with secondary antibody showed absence of labeling.

III.1.3 Smooth muscle cell culture from rat

Smooth muscle cells were isolated and cultured from rat thoracic and abdominal aorta. These cells were characterized by immunolabelling of α-smooth muscle actin (sm-actin) in smooth muscle cells (Fig. 7 A, B).

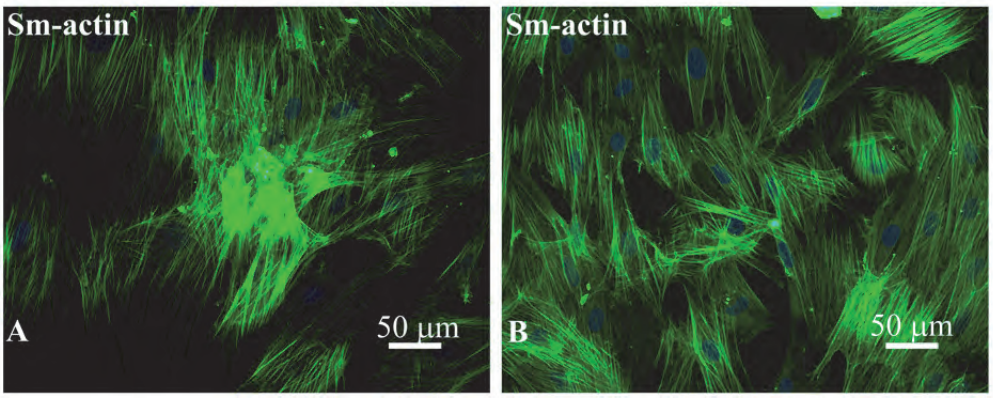

Fig. 7: Smooth muscle cells were immunolabeled with FITC-conjugated mouse monoclonal α-smooth muscle actin-antibody. (A) Rat thoracic aortic and (B) rat abdominal aortic smooth muscle cells were immunolabeled.

III.1.4 Smooth muscle cell culture from human

Human aortic smooth muscle cells were purchased from Lonza, cultured and characterized by immunoreactivity to α-smooth muscle actin in smooth muscle cells (Fig. 8).

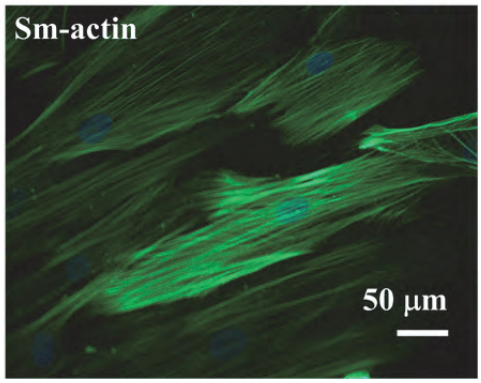

Fig. 8: Human aortic smooth muscle cells were immunolabeled with FITC-conjugated mouse monoclonal α-smooth muscle actin-antibody.

III.2 Immunohistochemistry of rat arteries

III.2.1 Thoracic and abdominal aorta

TH, the rate limiting enzymatic step of catecholamine biosynthesis, was detected by immunohistochemistry in sections of rat thoracic and abdominal aorta. The EC and the smooth muscle cells of the both parts of aorta were immunolabeled. No nerve fiber labeling was observed in both cases (Fig. 9 A, C). This labeling was not detectable when the TH-antibody has been preabsorbed with its cognate antigen (Fig. 9 B, D) and when the primary antibody was omitted (Fig. 9 E).

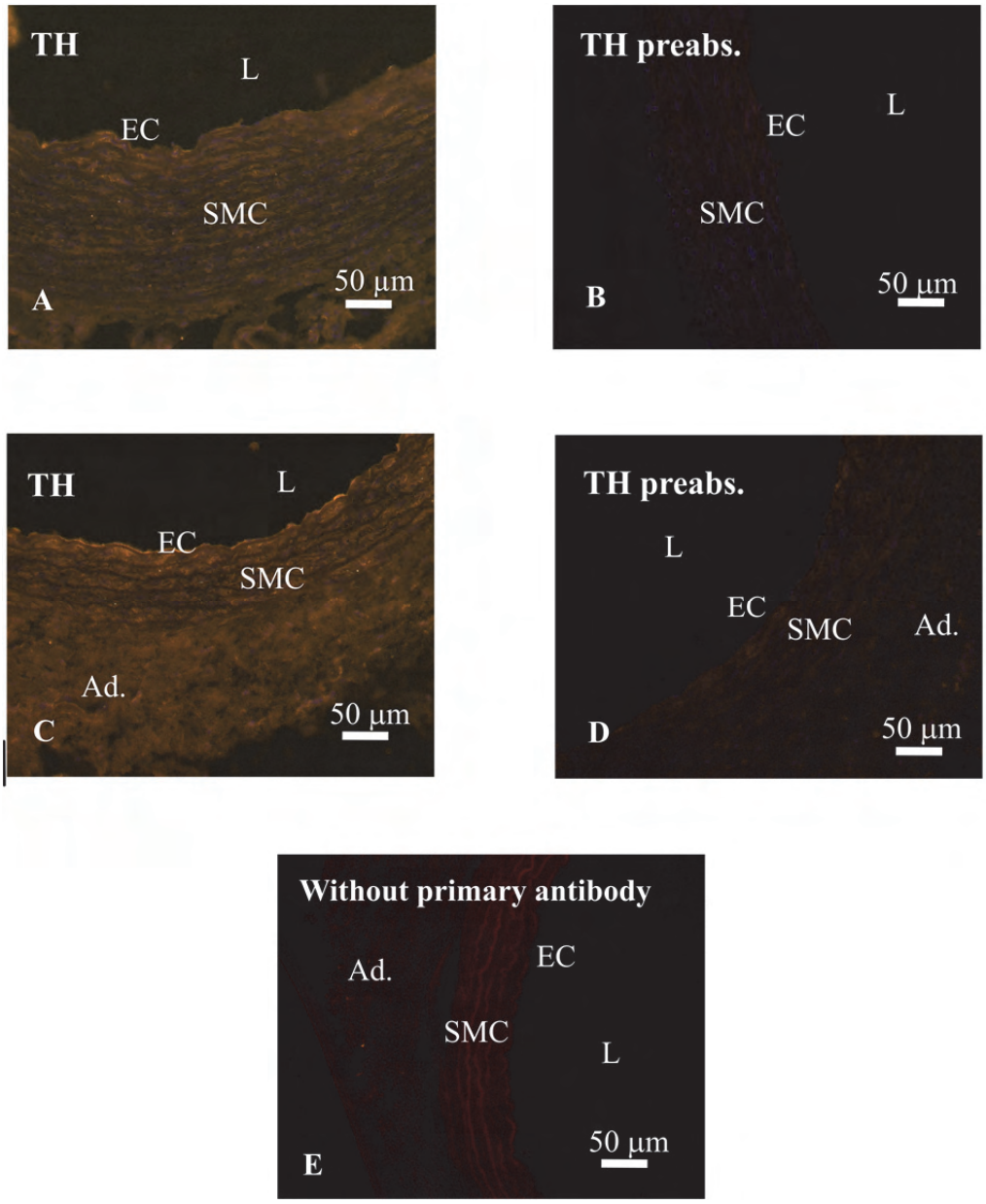

Fig. 9: TH-Immunolabelling, rat aorta. Rat thoracic (A) and abdominal aorta (C) are labeled with rabbit polyclonal anti TH-antibody. (B, D) Immunolabelling was absent after preabsorption of the antibody with corresponding peptide. (E) No immunolabelling was detectable in negative control, when sections were incubated without primary antibody. L: Lumen; EC: Endothelial cells; SMC: smooth muscle cells and Ad: adventitia.

III.2.2 Femoral artery

TH was detected in sections of rat femoral artery by immunohistochemistry. The EC and the smooth muscle cells of the artery were immunolabeled as well as sympathetic nerve fibers (Fig. 10 A). This labeling was not detectable when the TH-

antibody has been preabsorbed with its cognate antigen (Fig. 10B). This labeling was also not detectable when the primary antibody was omitted (Fig. 10 C).

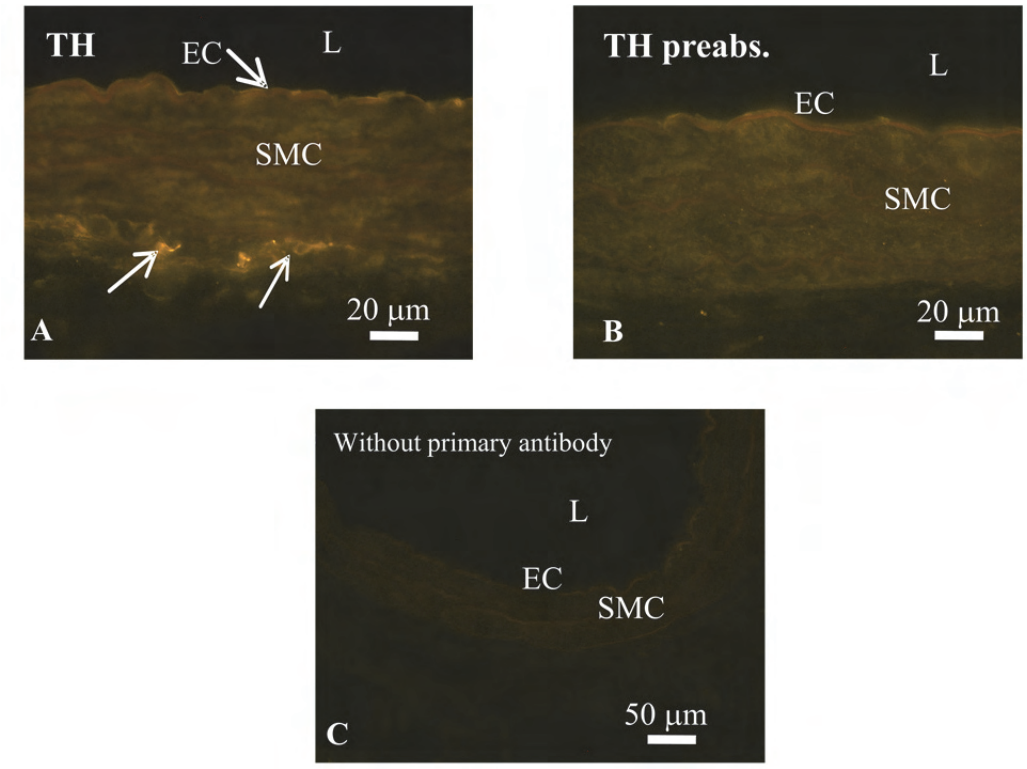

Fig. 10: TH-Immunolabelling, rat femoral artery. Rat femoral artery (A) was immunolabeled with rabbit polyclonal anti TH-antibody. (B) Immunolabelling was absent after preabsorption of the antibody with corresponding peptide (C) No immunolabelling was detectable in negative control, when sections were incubated without primary antibody. L: Lumen; EC: Endothelial cells; SMC: smooth muscle cells and "→" is for nerve fibers.

III.2.3 Superior mesenteric artery

TH was detected in sections of rat superior mesenteric artery by immunohistochemistry. The EC and the smooth muscle cells of the artery were immunolabeled as well as sympathetic nerve fibers (Fig. 11 A). In EC and smooth muscle cells, this labeling was not detectable when the TH-antibody has been preabsorbed with its cognate antigen (Fig. 11 B). The labeling was not detectable when the primary antibody was omitted (Fig. 11 C).

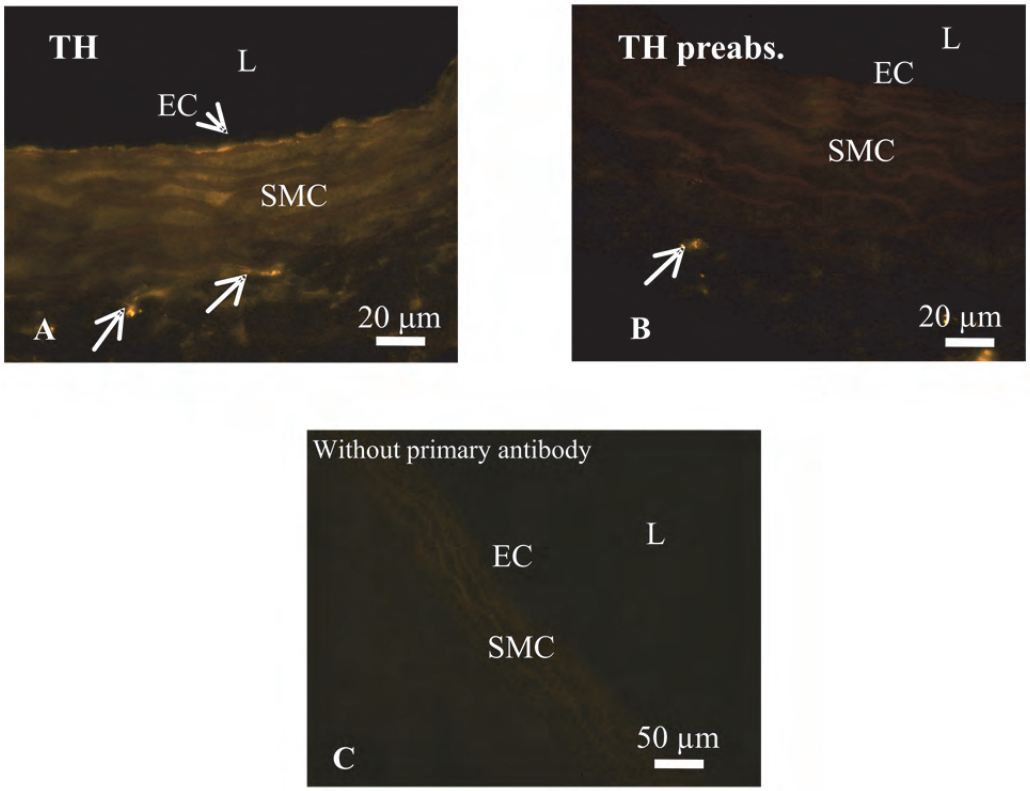

Fig. 11: TH-immunolabeling in rat superior mesenteric artery. (A) Rat superior mesenteric artery was immunolabeled with rabbit polyclonal anti TH-antibody. (B) Immunolabelling was absent after preabsorption of the antibody with corresponding peptide, nerve fibers were still labeled. (C) No immunolabelling was detectable in negative control, when sections were incubated without primary antibody. L: Lumen; EC: Endothelial cells; SMC: smooth muscle cells and "⟶" is for nerve fibers.

III.2 Western blot

III.2.1 Rat arteries

TH, the rate limiting enzyme in catecholamine synthesis, was also detected by western blot of the protein extracts from rat vessels (thoracic and abdominal aorta and femoral artery). A TH-immunoreactive band was detected at 56 kDa by a mouse monoclonal anti-TH antibody (Fig. 12). Adrenal gland protein extract was used as the positive control and a negative control was run without primary antibody. Other visible bands were might be phosphorylated forms of TH.

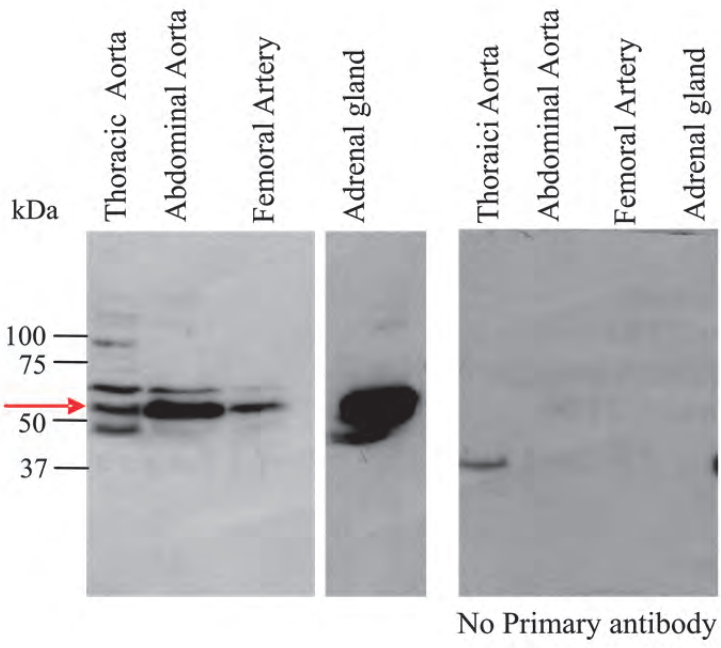

Fig. 12: Western blot analysis of the protein extracts from rat thoracic and abdominal aorta and femoral artery, while rat adrenal gland protein extract was used as positive control. TH was detected by western blot in all arteries with the expected molecular weight of 56 kDa, marked with red arrow. The strongest signal was observed in adrenal gland extract. A negative control was run without primary antibody from protein extract of each sample.

III.2.2 Rat lung EC

Rat lung EC were exposed to hypoxia (1% O_2) for 6, 12 and 24 hours, and a normoxic control was also included in this setup. The protein extracts from these EC were analyzed by western blotting for the expression of TH. Hypoxia causes an up-regulation of TH expression in rat lung EC (Fig. 13).

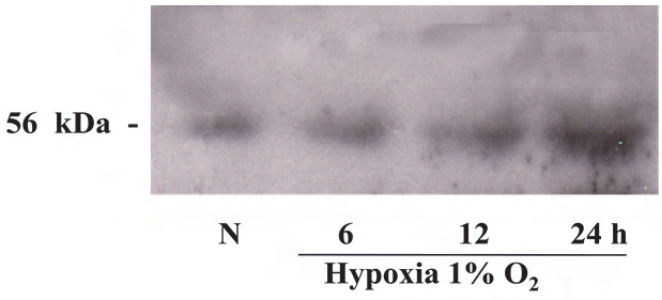

Fig. 13: Expression of TH in rat lung EC exposed to hypoxia and normoxia. A 56 kDa band was detected which corresponds to the expected size of the TH protein. There was up-regulation of TH protein expression with increasing hypoxic exposure.

III.3 Real-time RT-PCR

III.3.1 PCR Efficiency curves

PCR efficiency curves were made by serial dilution of rat adrenal gland cDNA, as this organ expresses high amount of catecholamine synthesizing enzymes. The PCR efficiencies calculated were 89.2% for TH (Fig. 14 A), 102.6% for DDC (Fig. 15 A), 104.5% for DβH (Fig. 16 A) and 95.2% for PNMT (Fig. 17 A). The cDNA from rat adrenal gland was serially diluted (e.g. 1:10, 1:100, 1:1000 and 1:10,000). Every dilution resulted in a 3-4 cycle difference in CT values (Fig. 14 B, Fig. 15 B, Fig. 16 B and Fig. 17 B). The melting curves for the respective targets also showed single melting peaks in all serially diluted samples (Fig. 14 C, Fig. 15 C, Fig. 16 C and Fig. 17 C).

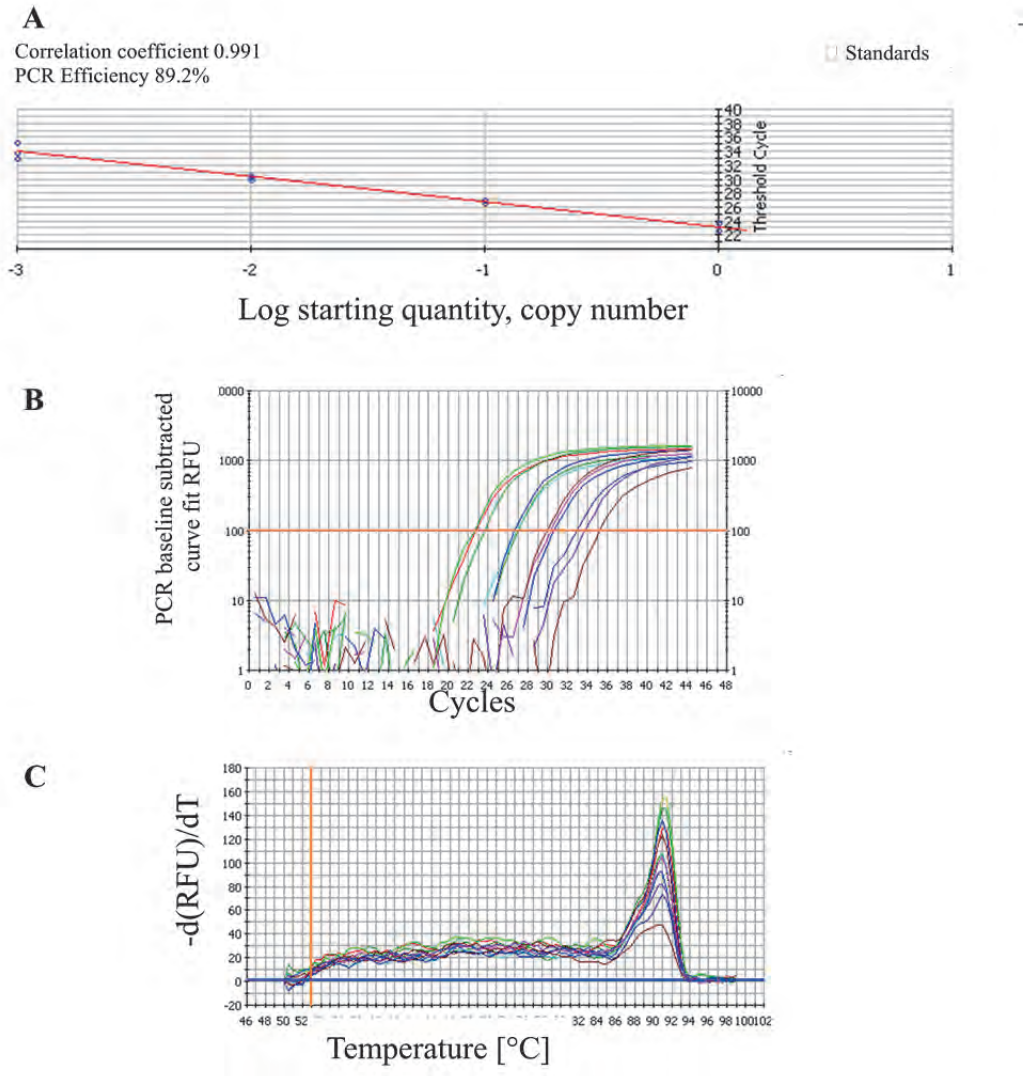

Fig. 14: (A) PCR efficiency curve for TH from rat adrenal gland. The PCR efficiency curved made by dilution series of adrenal gland showed 89.2% PCR efficiency, which is within acceptable limits. (B) Graph showing CTs from pure and serially diluted (1:10,

1:100 and 1:1000) cDNA samples. (C) A single melt peak was observed at all dilutions, confirming the specificity and efficiency of primer pairs. Temperature is plotted on the x-axis while -d(RFU)/dT, the difference in relative fluorescence units divided by difference in temperature, is plotted on the y-axis.

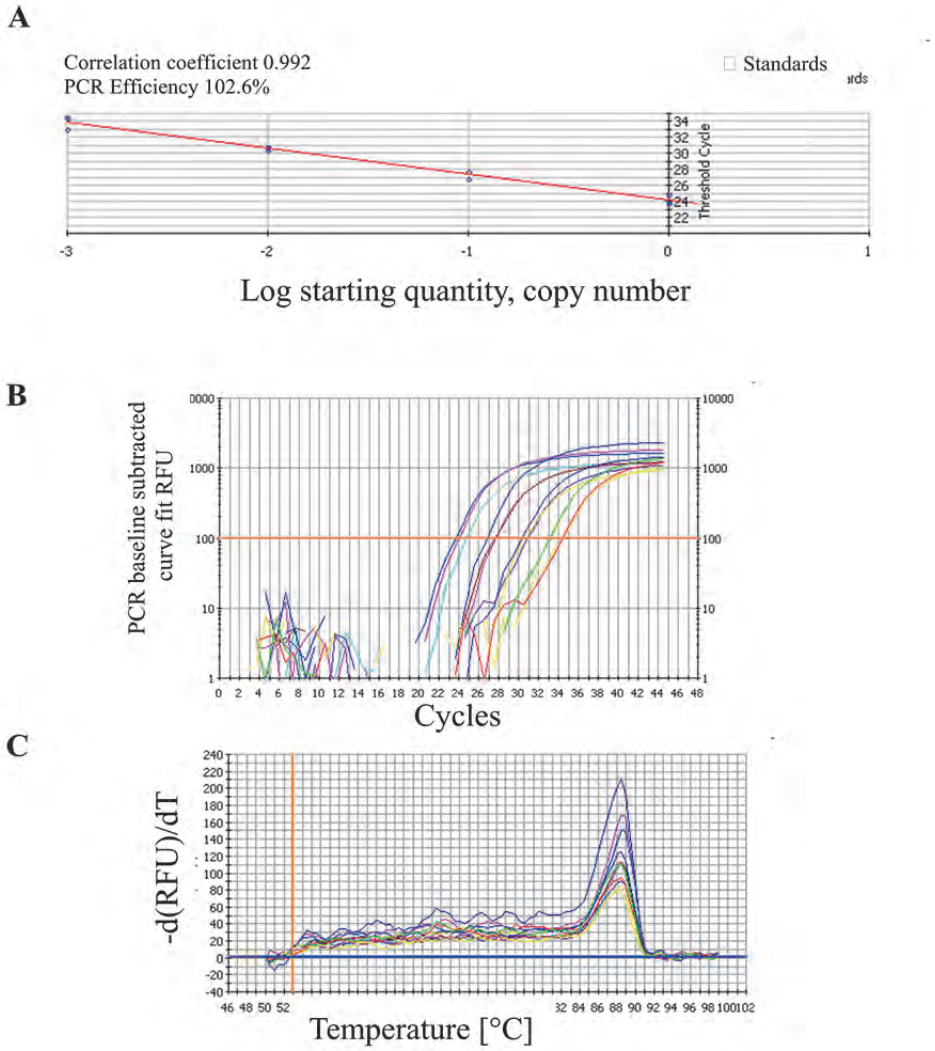

Fig. 15: (A) PCR efficiency curve for DDC from rat adrenal gland. The PCR efficiency curved made by dilution series of adrenal gland showed 102.6% PCR efficiency, which is within acceptable limits. (B) Graph showing CTs from pure and serially diluted (1:10, 1:100 and 1:1000) cDNA samples. (C) A single melt peak was observed at all dilutions, confirming the specificity and efficiency of primer pairs. Temperature is plotted on the x-axis while -d(RFU)/dT, the difference in relative fluorescence units divided by difference in temperature, is plotted on the y-axis.

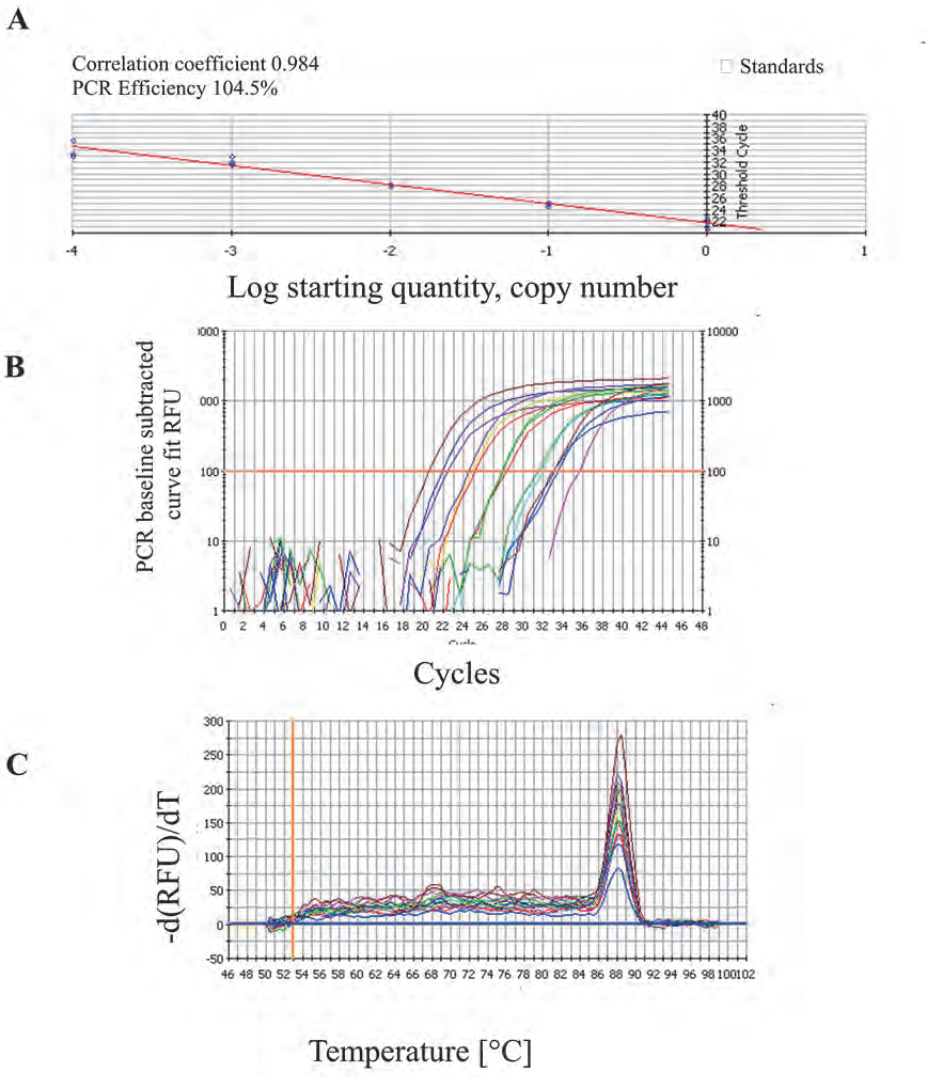

Fig. 16: (A) PCR efficiency curve for DβH from rat adrenal gland. The PCR efficiency curved made by dilution series of adrenal gland showed 104.5% PCR efficiency, which is within acceptable limits. (B) Graph showing CTs from pure and serially diluted (1:10, 1:100, 1:1000 and 1:10000) cDNA samples. (C) A single melt peak was observed at all dilutions, confirming the specificity and efficiency of primer pairs. Temperature is plotted on the x-axis while -d(RFU)/dT, the difference in relative fluorescence units divided by difference in temperature, is plotted on the y-axis.

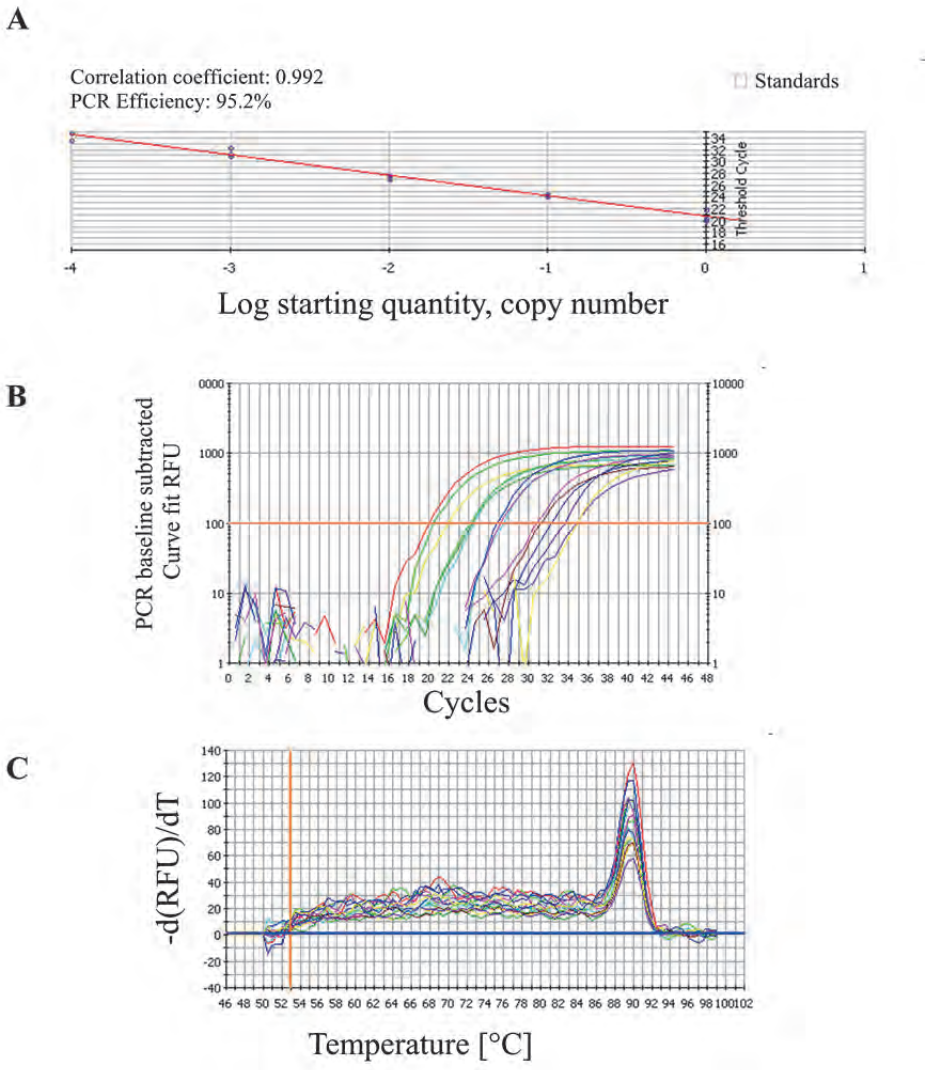

Fig. 17: (A) PCR efficiency curve for PNMT from rat adrenal gland. The PCR efficiency curved made by dilution series of adrenal gland showed 95.2% PCR efficiency, which is within acceptable limits. (B) Graph showing CTs from pure and serially diluted (1:10, 1:100, 1:1000 and 1:10000) cDNA samples. (C) A single melt peak was observed at all dilutions confirming the specificity and efficiency of primer pairs. Temperature is plotted on the x-axis while -d(RFU)/dT, the difference in relative fluorescence units divided by difference in temperature, is plotted on the y-axis.

III.3.2 Real-time RT-PCR from rat arteries

The expression of mRNA for catecholamine synthesizing enzymes was studied in the rat thoracic and abdominal aorta, superior mesenteric artery and femoral artery by real-time RT-PCR. The mRNA expression of all of these four enzymes involved in catecholamine synthesis was detected by real-time RT-PCR using intron spanning specific primers. Amplicon sizes were 216 bp for TH, 221 bp for DDC, 162 bp for DβH and 106 bp for PNMT and 252 bp for the house keeping gene β-actin. The cleanliness

of PCR reaction was confirmed by running water control (water was added in place of cDNA) and reverse transcriptase control (no reverse transcriptase was added while making cDNA) which showed no product amplification and subsequent detection on agarose gel (Fig. 18). By using real-time RT-PCR, mRNA expression levels were also studied quantitatively. In each real-time RT-PCR experiment, melting curves were also analyzed. Each target, in each artery, showed only one peak in the melting curve, corresponding to a single PCR product amplified in that particular PCR reaction (Figs. 19,20,21,22).

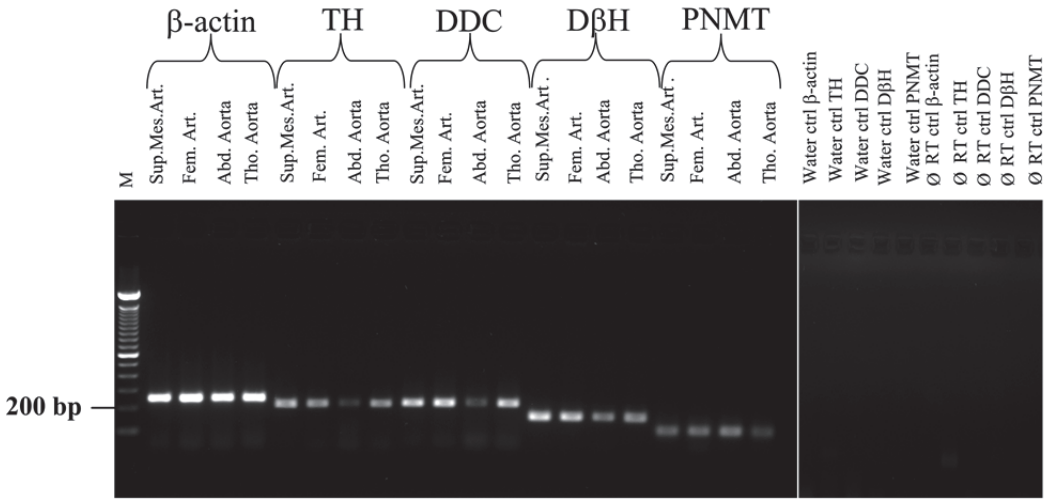

Fig. 18: Agarose gel electrophoresis of real-time RT-PCR products for the catecholamine synthesizing enzymes. Sup. Mes. Art.: superior mesenteric artery; Fem. Art.: Femoral artery; Abd. Aorta: Abdominal aorta; Tho. Aorta: Thoracic aorta. The control reactions were carried out as ø RT control: without reverse transcription reaction and water control: water in place of cDNA template, which showed no PCR product amplification.

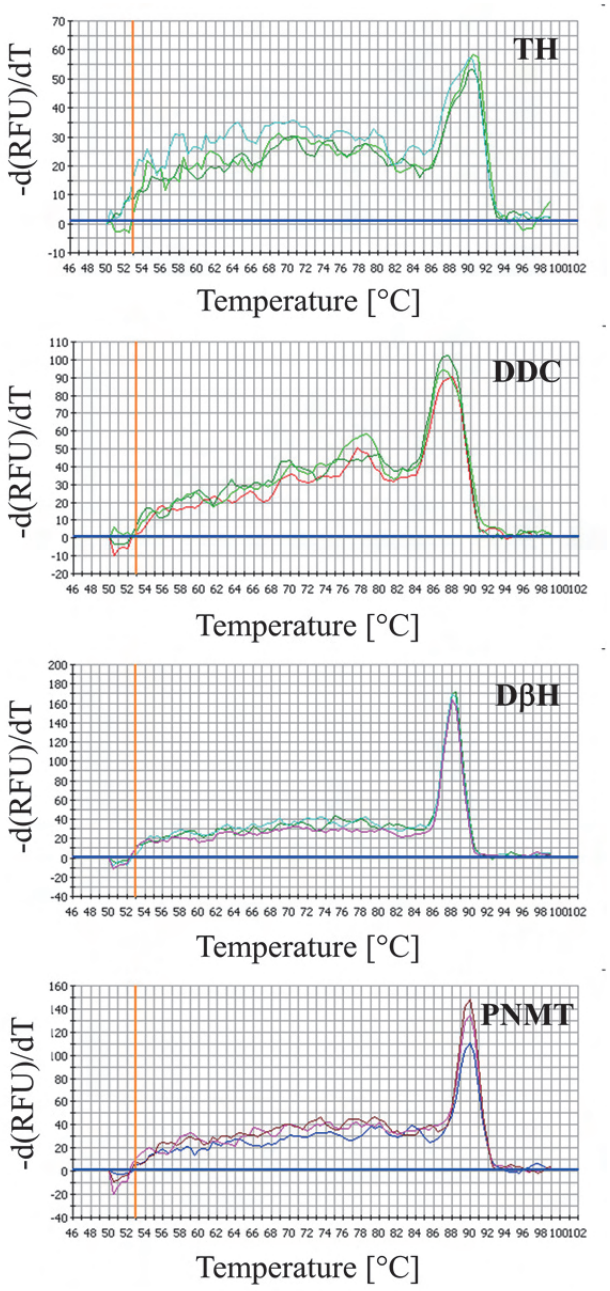

Fig. 19: Melting curves of real-time RT-PCR of catecholamine synthesizing enzymes from the real-time RT-PCR products from thoracic aorta, a representative picture for all the enzymes. In every experiment, each target was run in triplicate and showed a single peak in the melting curve. The peaks show the melting point of the amplified PCR product. Temperature is plotted on the x-axis while -d(RFU)/dT, the difference in relative fluorescence units divided by difference in temperature, is plotted on the y-axis.

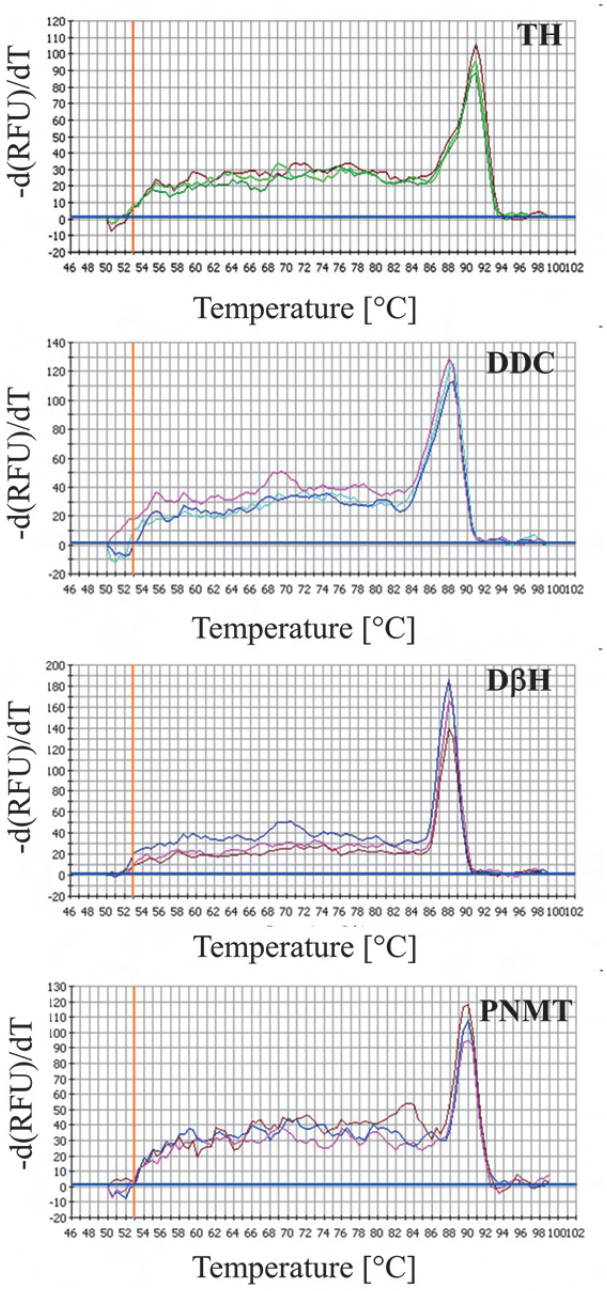

Fig. 20: Melting curves of real-time RT-PCR of catecholamine synthesizing enzymes from the real-time RT-PCR products from abdominal aorta, a representative picture for all the enzymes. In every experiment, each target was run in triplicate and showed a single peak in the melting curve. The peaks show the melting point of the amplified PCR product. Temperature is plotted on the x-axis while -d(RFU)/dT, the difference in relative fluorescence units divided by difference in temperature, is plotted on the y-axis.

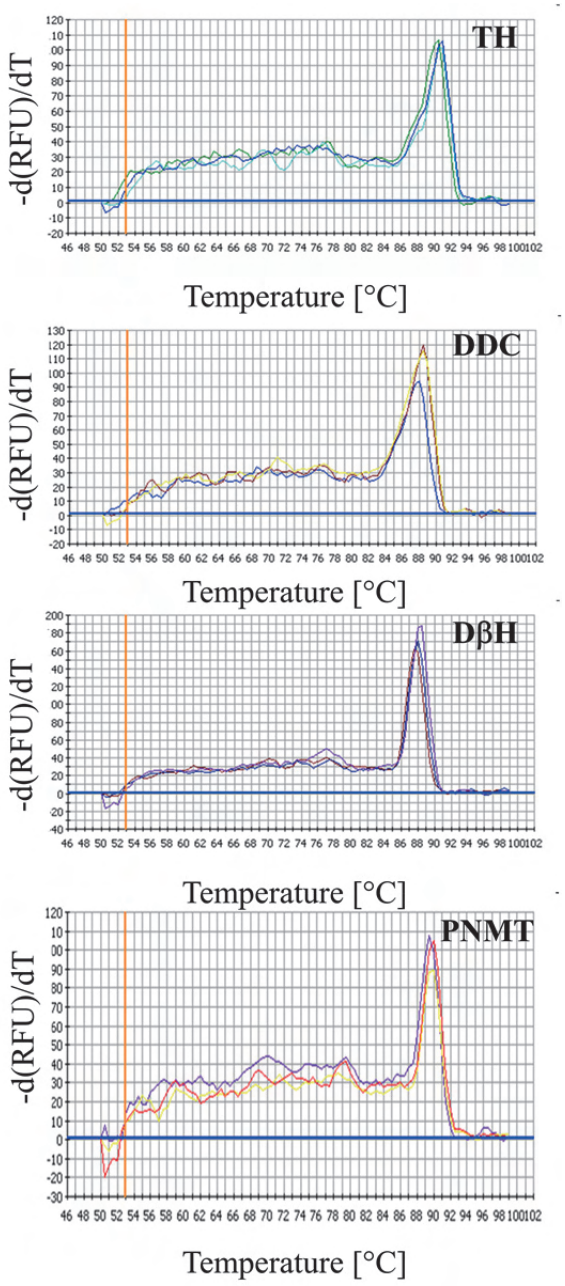

Fig. 21: Melting curves of real-time RT-PCR of catecholamine synthesizing enzymes from the real-time RT-PCR products from superior mesenteric artery, a representative picture for all the enzymes. In every experiment, each target was run in triplicate and showed a single peak in the melting curve. The peaks show the melting point of the amplified PCR product. Temperature is plotted on the x-axis while -d(RFU)/dT, the difference in relative fluorescence units divided by difference in temperature, is plotted on the y-axis.

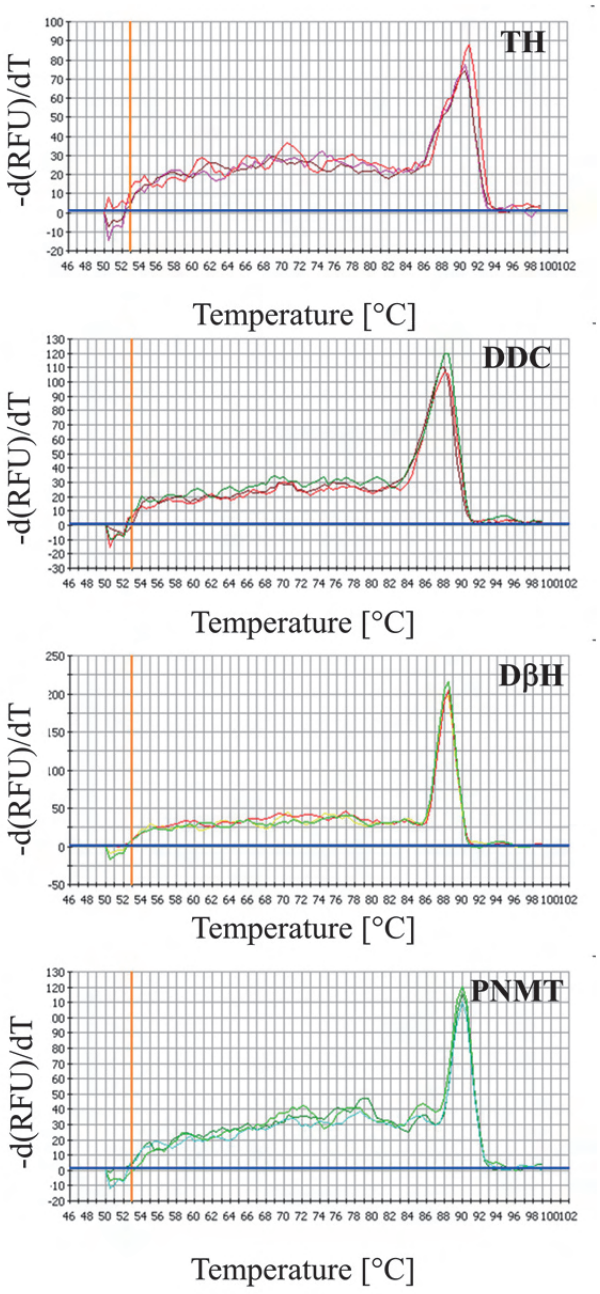

Fig. 22: Melting curves of real-time RT-PCR of catecholamine synthesizing enzymes from the real-time RT-PCR products from femoral artery, a representative picture for all the enzymes. In every experiment, each target was run in triplicate and showed a single peak in the melting curve. The peaks show the melting point of the amplified PCR product. Temperature is plotted on the x-axis while -d(RFU)/dT, the difference in relative fluorescence units divided by difference in temperature, is plotted on the y-axis.

Real-time RT-PCR was used to compare expression levels of these four enzymes involved in catecholamine synthesis in these arteries. In the thoracic aorta, TH was significantly higher expressed as compared to DDC, DβH and PNMT. In the abdominal aorta, TH expression was significantly higher than PNMT and DβH expression. In the superior mesenteric artery, PNMT expression was highly significantly

lower than that of DDC and PNMT, while DβH was stronger expressed than DDC. In the femoral artery, TH, DDC and DβH expression were highly significantly stronger than PNMT expression (Fig. 23).

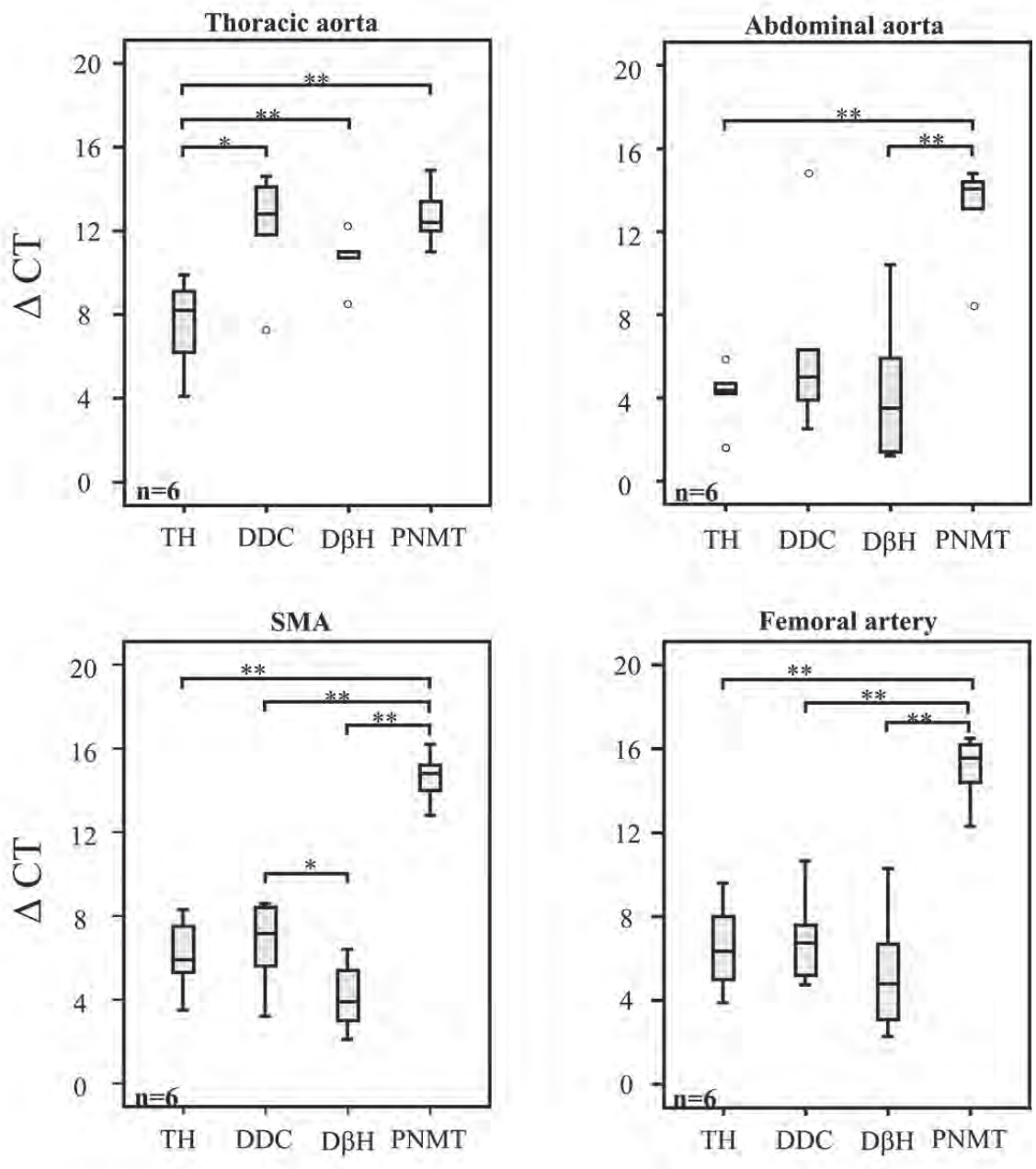

Fig. 23: Box plots showing the delta CT values of the mRNA expression of catecholamine synthesizing enzymes in different arteries. A high delta CT value means that the gene is relatively low expressed, while a low delta CT value corresponds to a high expression of that particular gene. Data are presented as box plots with percentiles 0, 25, 50 (median, indicated by horizontal line within the box) 75 and 100. Data was analyzed statistically by the non-parametric Kruskal-Wallis test and, if P≤0.05, further analysis among the groups was performed by Mann-Whitney test. Significance level was set as P≤0.05 (significant:*****), P≤0.01 (highly significant:******) and P≤0.001 (very highly significant:*******). The symbol "°" represents an outlier value.

In a next step, differences in enzyme expression between arteries were evaluated. TH mRNA expression was not significantly different between all the arteries. DDC mRNA expression was lowest in the thoracic aorta, being significantly different from the femoral and superior mesenteric artery. DβH mRNA expression was lowest in the thoracic aorta. PNMT expression was significantly higher in the thoracic aorta than in the superior mesenteric artery and femoral artery (Fig. 24)

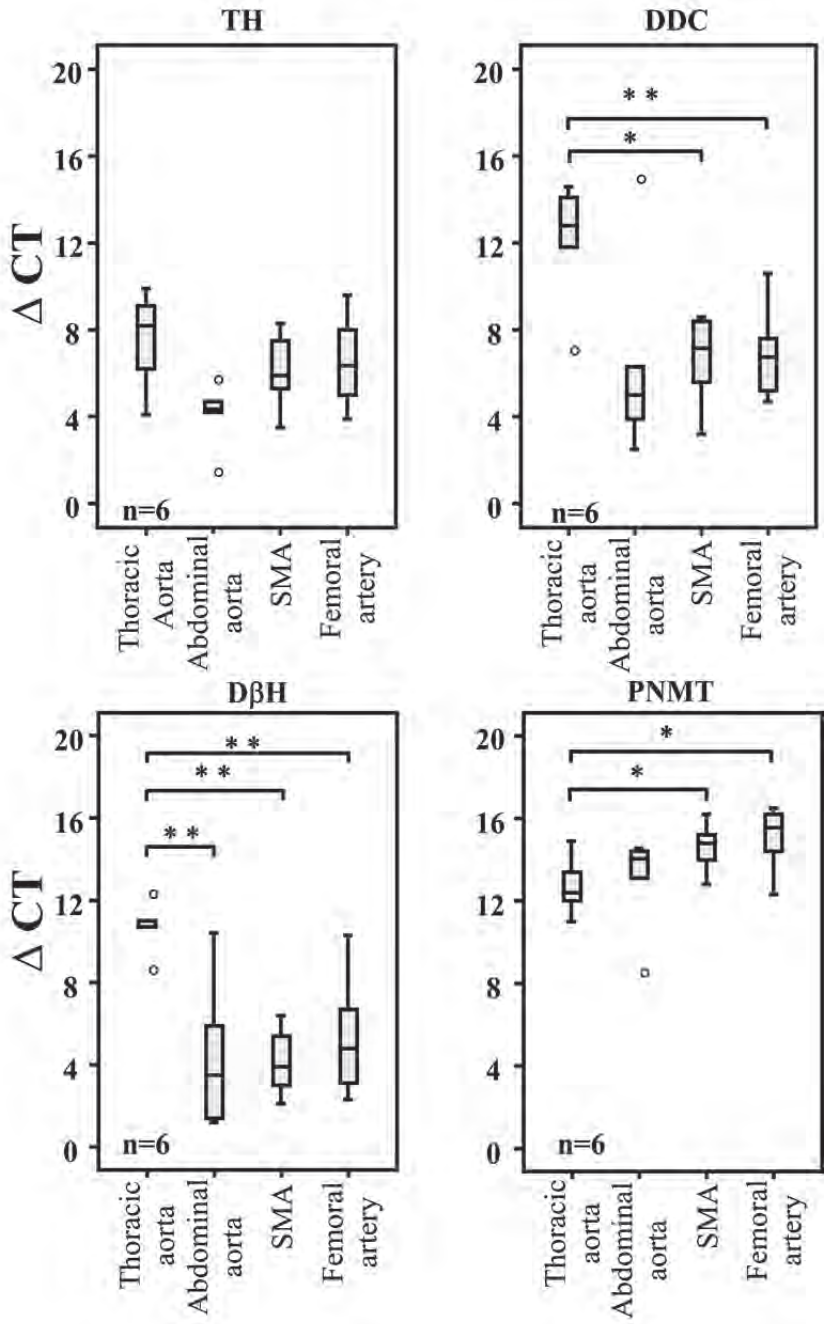

Fig. 24: Box plots showing the delta CT values of the mRNA expression of catecholamine synthesizing enzymes in different arteries. A high delta CT value means that the gene is relatively low expressed, while a low delta CT value corresponds to a

high expression of that particular gene. Data are presented as box plots with percentiles 0, 25, 50 (median, indicated by horizontal line within the box) 75 and 100. Data was analyzed statistically by Kruskal-Wallis test and, if P≤0.05, further analysis with the groups was performed by Mann-Whitney test. Significance level was set as P≤0.05 (significant:*), P≤0.01 (highly significant:**) and P≤0.001 (very highly significant:***). The symbol "°" represents an outlier value.

III.3.3 Rat lung EC

Rat lung EC were investigated for the expression of mRNA for TH, DDC, DβH, and PNMT. All of the four enzymes involved in catecholamine synthesis were detected in rat lung EC. The amplified PCR products were detected by agarose gel electrophoresis (Fig. 25), amplicon sizes were 216 bp for TH, 221 bp for DDC, 162 bp for DβH and 106 bp for PNMT. The house keeping genes β2-MG 191 bp and β-actin 252 bp were also detected on the gel.

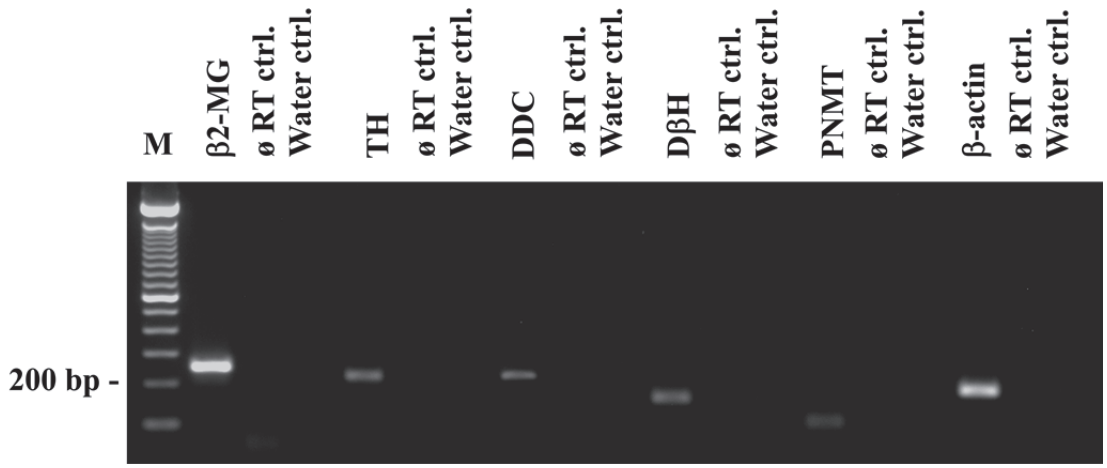

Fig. 25: RT-PCR for the catecholamine synthesizing enzymes in lung EC, agarose gel electrophoresis. The control reactions were carried out as ø RT ctrl.: without reverse transcription reaction and water ctrl.: water in place of cDNA template, which showed absence of PCR product amplification.

The lungs EC were exposed to hypoxia (1% O_2) for 6, 12 and 24 hours, and a control was maintained at normoxic condition (21% O_2). Real-time PCR was performed and melting curves were analyzed showing specificity of PCR reaction and no amplification of unspecific products (Fig. 26).

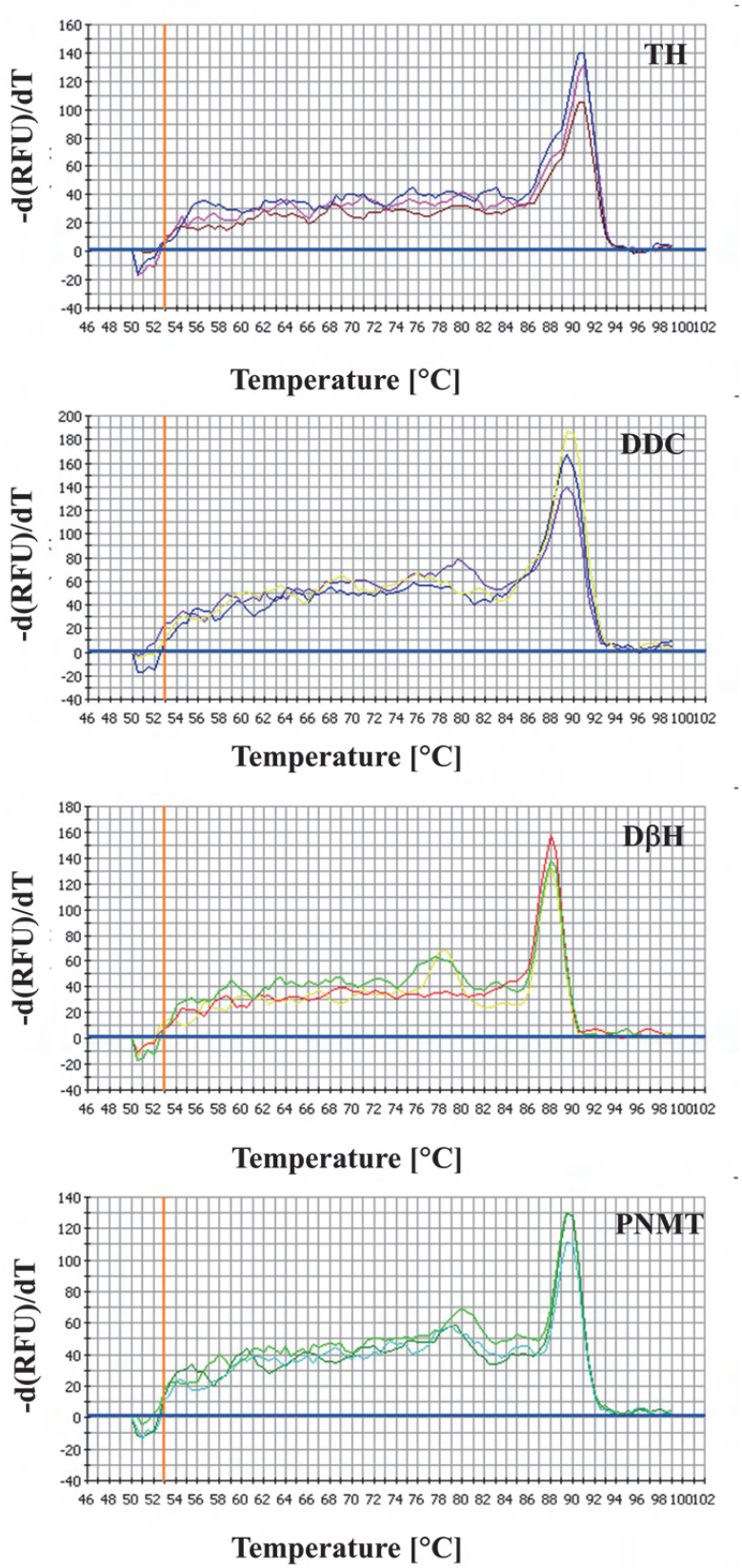

Fig. 26: Melting curves of real-time RT-PCR of catecholamine synthesizing enzymes from the rat lung EC, representative picture for all the enzymes. In each experiment, each target was run in triplicate and showed only a single peak. The peaks show the melting point of the amplified product. Temperature is plotted on the x-axis while -

d(RFU)/dT, the difference in relative fluorescence units divided by difference in temperature, is plotted on the y-axis.

Hypoxia caused an up-regulation in TH mRNA expression by 25-fold after 24 hours of exposure. There was no significant difference in DDC mRNA expression (Fig. 27).

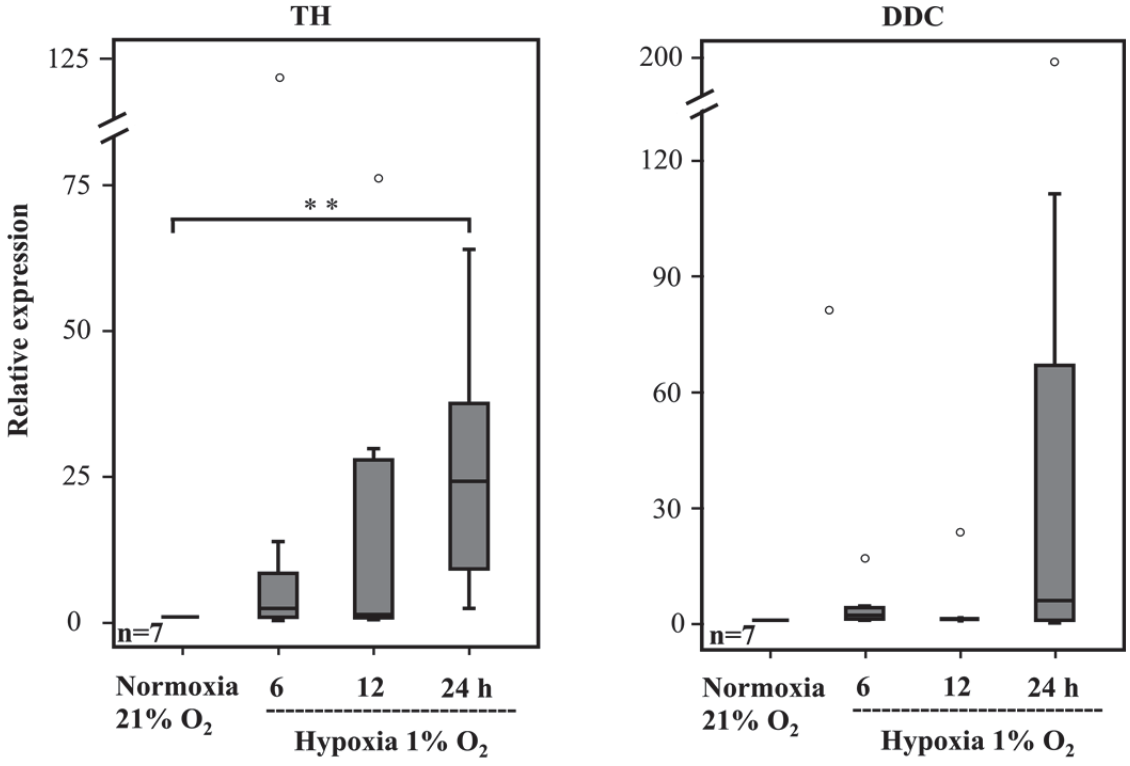

Fig. 27: Effect of hypoxia on the expression of TH and DDC mRNA in rat lung EC. There was a highly significant increase in TH mRNA expression after 24 h of hypoxic exposure, while there was no significant change in DDC mRNA expression. Data are presented as box plots with percentiles 0, 25, 50 (median, indicated by horizontal line within the box) 75 and 100. Data was analyzed statistically by Kruskal-Wallis test and, if $P \leq 0.05$, further analysis with the groups was performed by Mann-Whitney test. Significance level was set as $P \leq 0.05$ (significant:*****), $P \leq 0.01$ (highly significant:******) and $P \leq 0.001$ (very highly significant:*******). The symbol "°" represents an outlier value.

DβH mRNA expression was upregulated after 6 and 24 h of hypoxic exposure as compared to normoxia (Fig. 28).

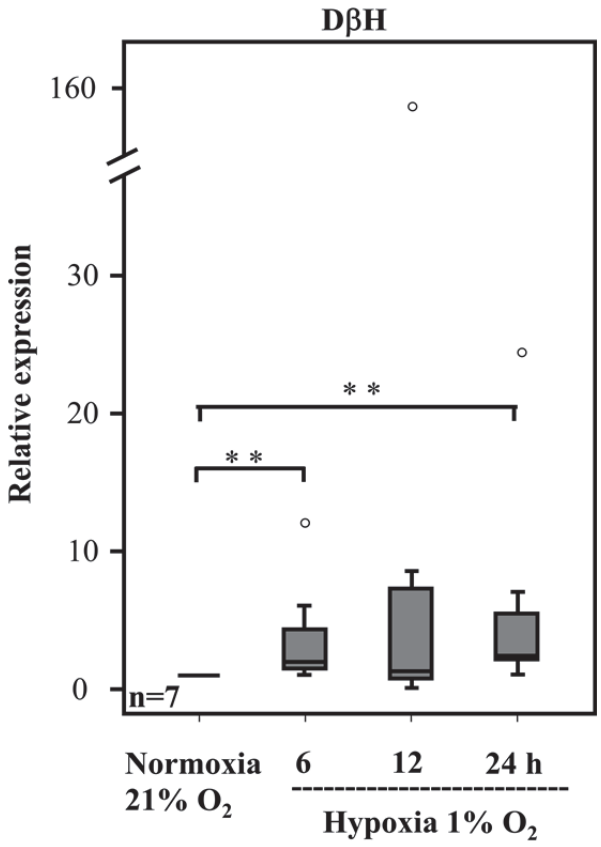

Fig. 28: Effect of hypoxia on the expression of DβH mRNA in rat lung EC. There was a highly significant increase in DβH mRNA expression after 6 and 24 h of hypoxic exposure. Data are presented as box plots with percentiles 0, 25, 50 (median, indicated by horizontal line within the box) 75 and 100. Data was analyzed statistically by Kruskal-Wallis test and, if P≤0.05, further analysis with the groups was performed by Mann-Whitney test. Significance level was set as P≤0.05 (significant:*), P≤0.01 (highly significant:**) and P≤0.001 (very highly significant:***). The symbol "°" represents an outlier value.

There was no significance change in PNMT mRNA expression after hypoxic exposure (Fig. 29).

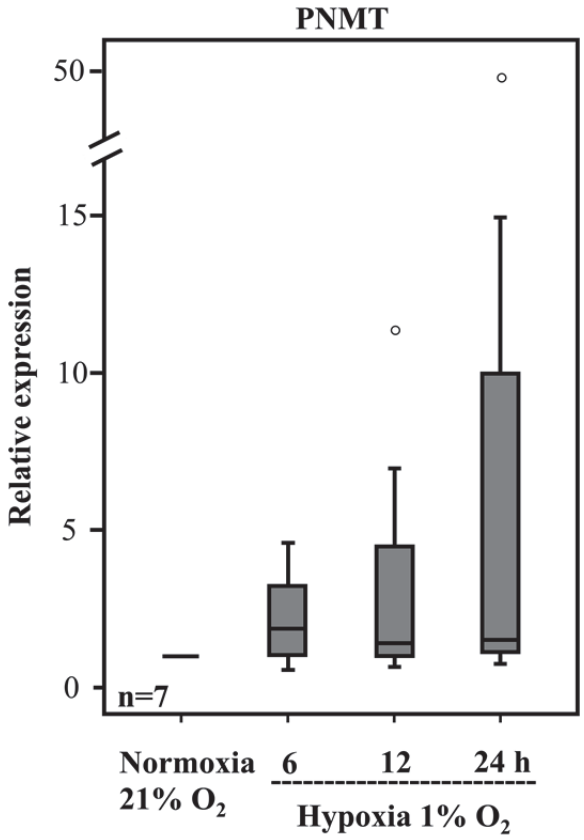

Fig. 29: Effect of hypoxia on the expression of PNMT mRNA in rat lung EC. There was no significance change in PNMT mRNA expression after hypoxic exposure. Data are presented as box plots with percentiles 0, 25, 50 (median, indicated by horizontal line within the box) 75 and 100. The symbol "°" represents an outlier value.

III.3.4 Rat aortic EC

The EC from rat aorta were investigated for the expression of mRNA for TH, DDC, DβH, and PNMT. All of the four enzymes involved in catecholamine synthesis were detected in RT-PCR. The amplified PCR products were detected by agarose gel electrophoresis (Fig. 30), amplicon sizes were 216 bp for TH, 221 bp for DDC, 162 bp for DβH and 106 bp for PNMT. The house keeping genes β2-MG 191 bp and β-actin 252 bp were also detected on the gel.

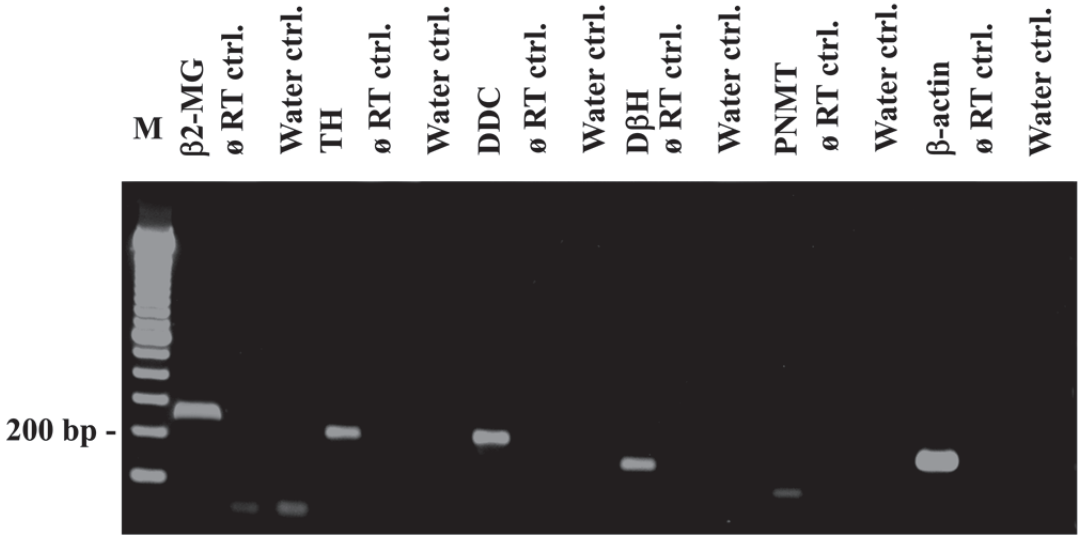

Fig. 30: RT-PCR for the catecholamine synthesizing enzymes from rat aortic EC, agarose gel electrophoresis. M: base pair marker. The control reactions were carried out as ø RT ctrl.: without reverse transcription reaction, and water ctrl.: water in place of cDNA template, which showed absence of PCR product amplification. In case of water and RT control for β2-MG, a weak single band is visible which is caused by primer dimers.

Aortic EC were exposed to hypoxia (1% O_2) for 6, 12 and 24 hours and a control was maintained at normoxic condition (21% O_2). Total RNA was isolated from normoxic and hypoxic cells and the cDNA was synthesized. Real-time PCR was performed and melting curves were analyzed, showing specificity of PCR reaction and no amplification of unspecific products (Fig. 31).

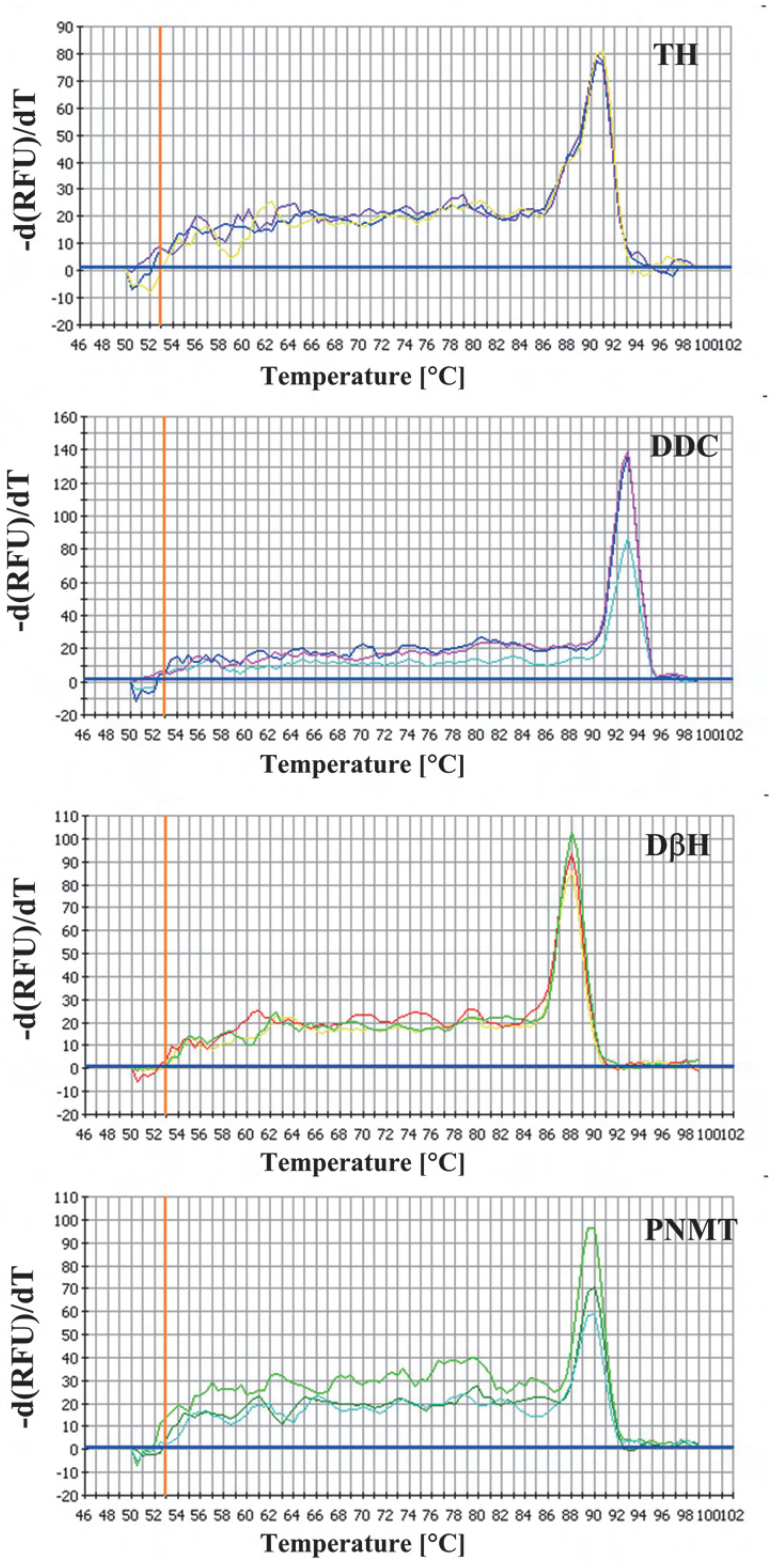

Fig. 31: Melt curves of real-time RT-PCR of catecholamine synthesizing enzymes from the rat aortic EC, a representative picture for all the enzymes. In each experiment, each target was run in triplicate and shows no extra peaks. Peak shows the melting point of the amplified product. Temperature is plotted on the x-axis while -d(RFU)/dT, the difference in relative fluorescence units divided by difference in temperature, is plotted on the y-axis.

Hypoxic exposure did not cause a significant change in the mRNA expression of the enzymes involved in catecholamine synthesis (Fig. 32).

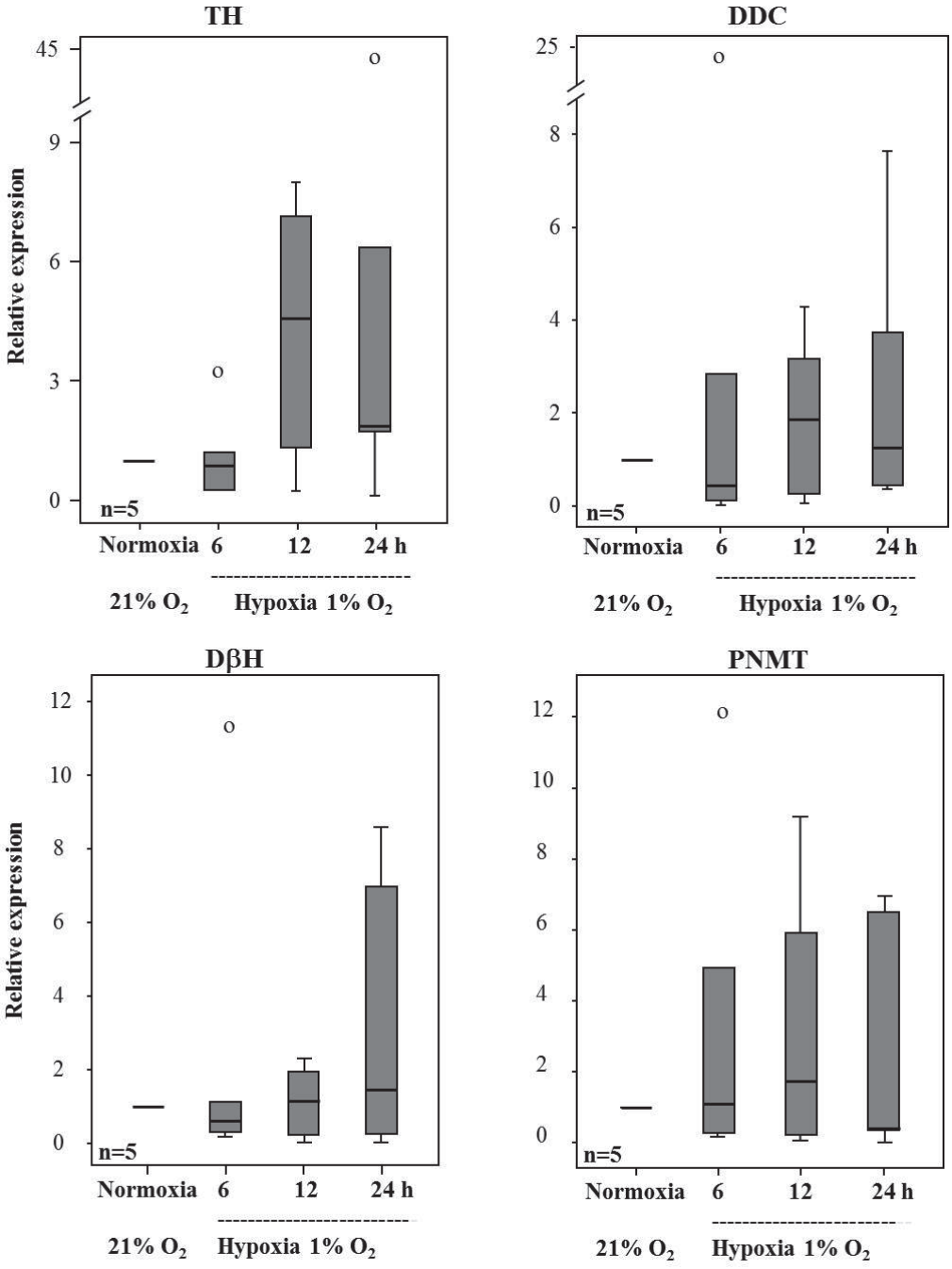

Fig. 32: Effect of hypoxia on the expression of TH, DDC, DβH and PNMT mRNA in rat aortic EC. There was no significance difference in mRNA expression of any of the enzymes after hypoxic exposure for 6, 12 and 24 h. Data are presented as box plots with percentiles 0, 25, 50 (median, indicated by horizontal line within the box) 75 and 100. Data was analyzed statistically by Kruskal-Wallis test, significance was set as $P \leq 0.05$. The symbol "°" represents an outlier value.

III.3.5 Rat aortic smooth muscle cells

Rat aortic smooth muscle cells (thoracic and abdominal aorta) were investigated for the expression of mRNA for TH, DDC, DβH, and PNMT. All mRNAs were readily detectable except that for DDC. The amplified PCR products were detected by agarose gel electrophoresis (Fig. 33), amplicon sizes were 216 bp for TH, 221 bp for DDC, 162 bp for DβH and 106 bp for PNMT. The house keeping genes β2-MG (191 bp) and β-actin (252 bp) were also detected on the gel.

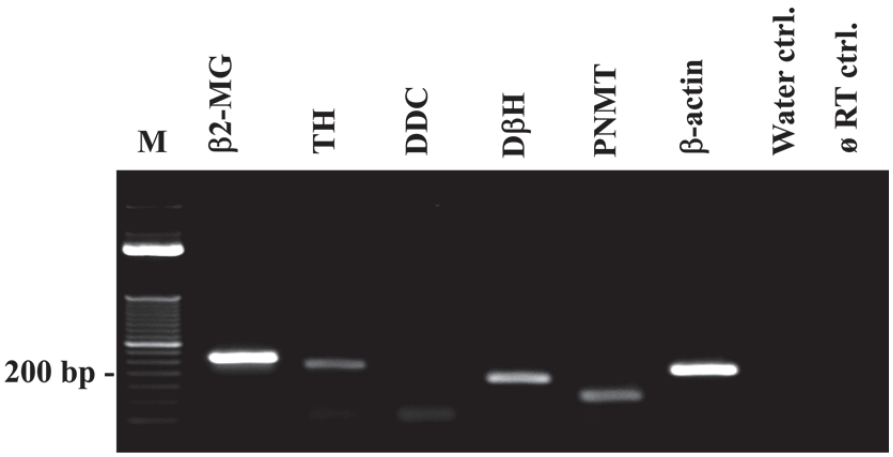

Fig. 33: Real-time RT-PCR for the catecholamine synthesizing enzymes from rat thoracic aortic smooth muscle cells, agarose gel electrophoresis. M: base pair marker. The control reactions were carried out for TH, as ø RT ctrl. without reverse transcription reaction and water ctrl. water in place of cDNA template, which showed no PCR product amplification.

Aortic smooth muscle cells were exposed to hypoxia (1% O_2) for 6, 12 and 24 hours and a control was maintained at normoxic condition (21% O_2). Real-time PCR was performed and melting curves were analyzed, showing specificity of PCR reaction and no amplification of unspecific products (Figs. 34 & 35).

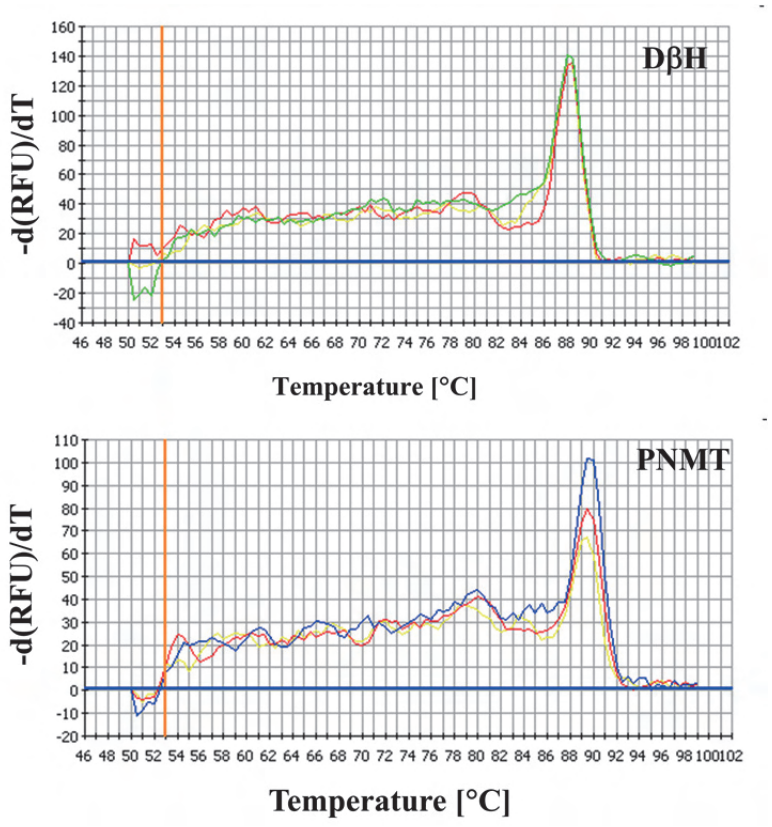

Fig. 34: Melting curves of real-time RT-PCR of catecholamine synthesizing enzymes from the rat thoracic aortic smooth muscle cells, a representative picture. In each experiment, each target was run in triplicate and shows no extra peaks. The peaks show the melting point of the amplified PCR product. Temperature is plotted on the x-axis while -d(RFU)/dT, the difference in relative fluorescence units divided by difference in temperature, is plotted on the y-axis.

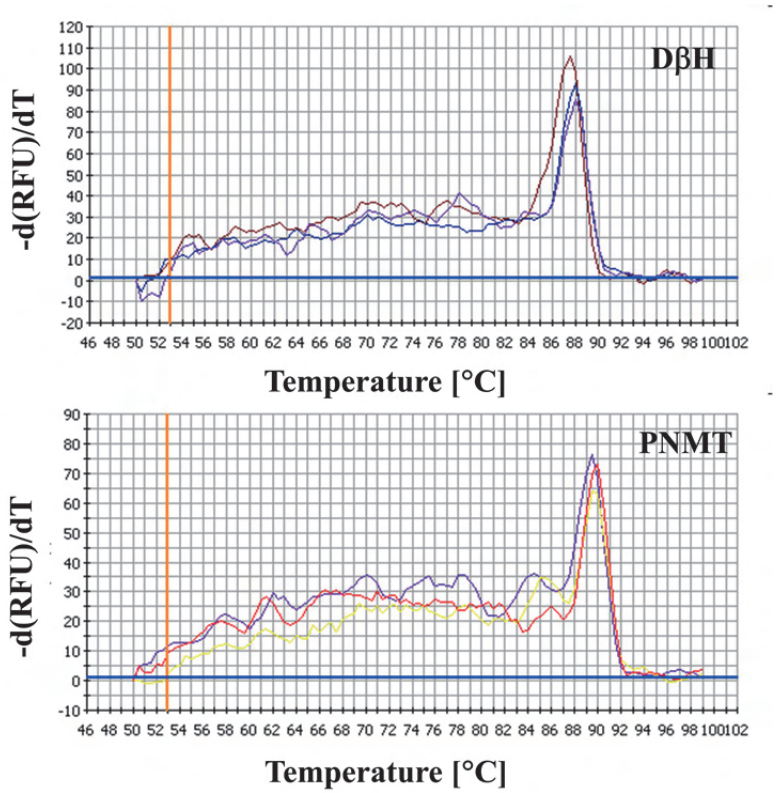

Fig. 35: Melting curves of real-time RT-PCR of catecholamine synthesizing enzymes from the rat abdominal aortic smooth muscle cells, a representative picture. In each experiment, each target was run in triplicate and shows no extra peaks. The peaks show the melting point of the amplified PCR product. Temperature is plotted on the x-axis while -d(RFU)/dT, the difference in relative fluorescence units divided by difference in temperature, is plotted on the y-axis.

In thoracic aortic smooth muscle cells, hypoxic exposure did not cause a significant change in the mRNA expression of DβH and PNMT (Fig. 36). The expression of TH and DDC mRNA was too low to be quantified, although TH was qualitatively detectable (Fig. 33).

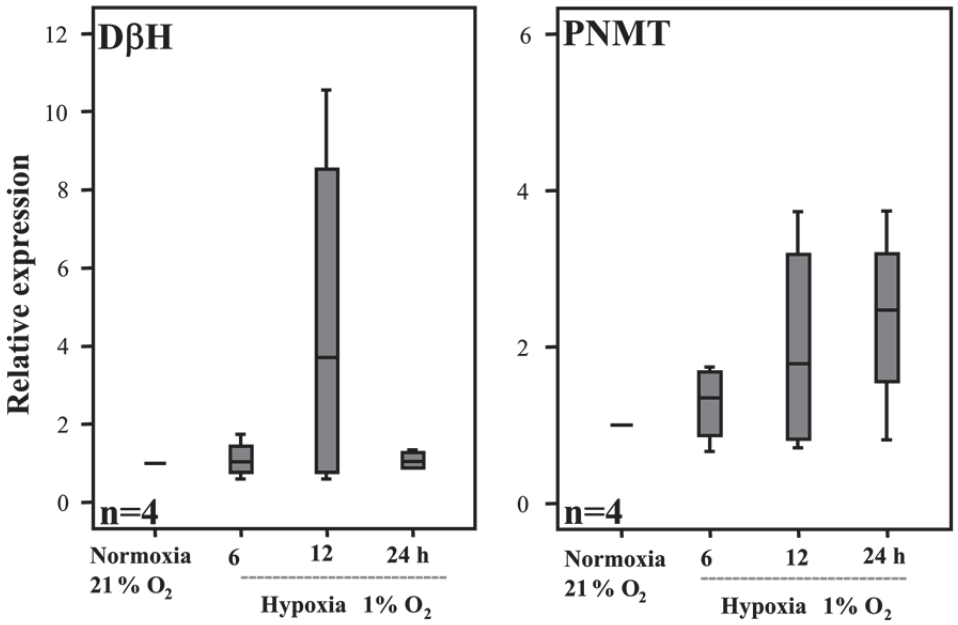

Fig. 36: Effect of hypoxia on the expression of DβH and PNMT mRNA in rat thoracic aortic smooth muscle cells. There was no significance difference in mRNA expression of any of the enzymes after hypoxic exposure for 6, 12 and 24 h. Data are presented as box plots with percentiles 0, 25, 50 (median, indicated by horizontal line within the box) 75 and 100. Data was analyzed statistically by Kruskal-Wallis test. Significance level was set as $P \leq 0.05$.

In abdominal aortic smooth muscle cells, hypoxic exposure did not cause a significant change in the mRNA expression of DβH and PNMT (Fig. 37). The expression of TH and DDC mRNA was too low to be quantified, although TH was qualitatively detectable (Fig. 33).

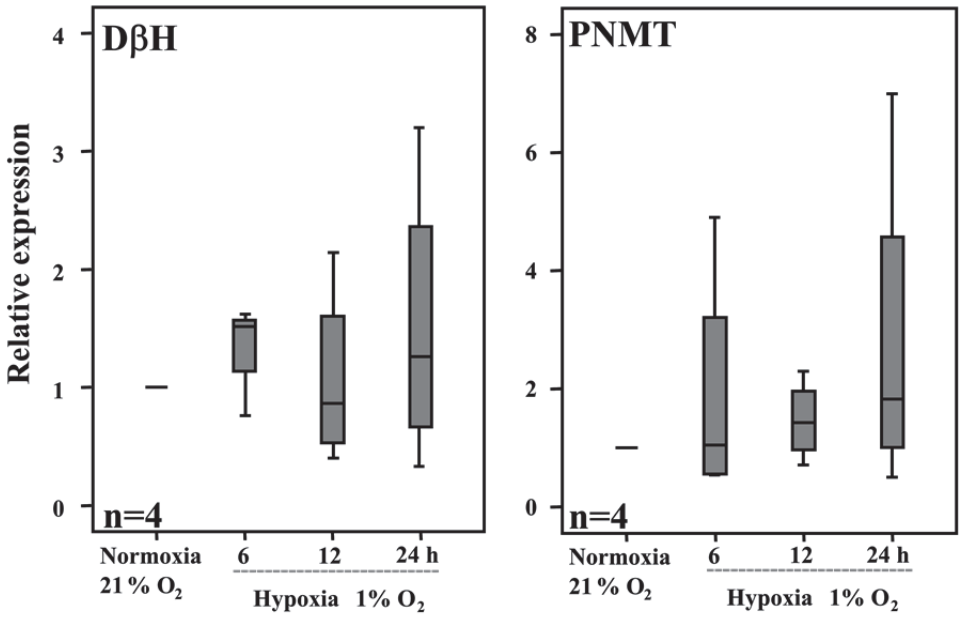

Fig. 37: Effect of hypoxia on the expression of DβH and PNMT mRNA in rat abdominal aortic smooth muscle cells. There was no significance difference in mRNA expression of any of the enzymes after hypoxic exposure for 6, 12 and 24 h. Data are presented as box plots with percentiles 0, 25, 50 (median, indicated by horizontal line within the box) 75 and 100. Data was analyzed statistically by Kruskal-Wallis test. Significance level was set as $P \leq 0.05$.

III.3.6 Catecholamine synthesis in human cells

To study catecholamine synthesizing in human cells, intron spanning primer pairs were designed and PCR conditions were optimized by using cDNA from a pheochromocytoma. Single peaks in the melting curves indicated specific PCR product amplification (Fig. 38). This was further confirmed by agarose gel electrophoresis (Fig. 39). All the four mRNAs coding for catecholamine synthesis enzymes were detected in the gel. Amplicon sizes were 138 bp for TH, 222 bp for DDC, 157 bp for DβH, 281 bp for PNMT, and 160 bp for the housekeeping gene β2-MG.

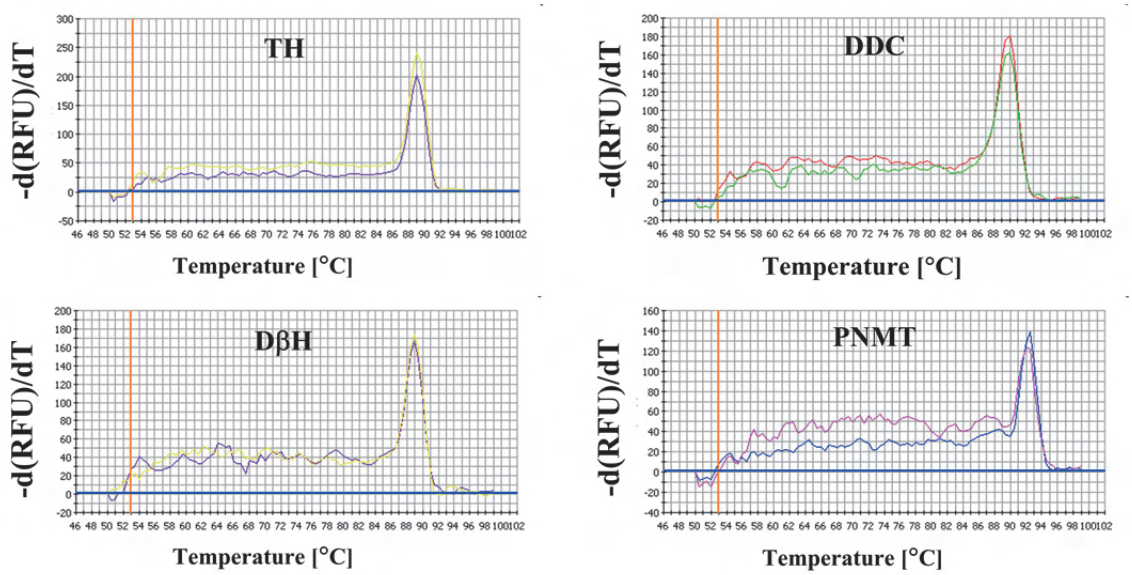

Fig. 38: Melting curves from cDNA of a human pheochromocytoma subjected to PCR, a representative picture for catecholamine synthesizing enzyme. In each experiment, each target was run in duplicate and showed only a single melting peak. The peaks show the melting point of the amplified PCR product. Temperature is plotted on the x-axis while -d(RFU)/dT, the difference in relative fluorescence units divided by difference in temperature, is plotted on the y-axis.

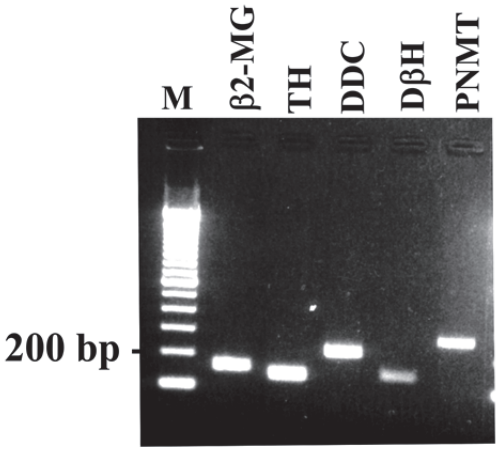

Fig. 39: Real-time RT-PCR for the catecholamine synthesizing enzymes from a pheochromocytoma, agarose gel electrophoresis. M: base pair marker.

As an additional positive control, real-time RT-PCR was run from a human sympathetic trunk ganglion. All the four mRNAs coding for catecholamine synthesis enzymes were detected in the gel, except for PNMT which was not detectable (Fig. 40), much in line with the inability of principal sympathetic neurons to convert noradrenaline into adrenaline.

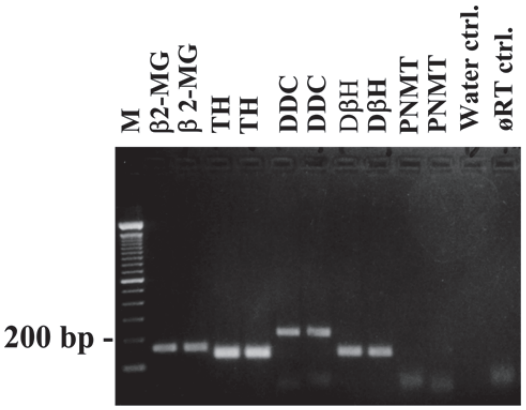

Fig. 40: Real-time RT-PCR for the catecholamine synthesizing enzymes from human sympathetic trunk, agarose gel electrophoresis. M: base pair marker. The control reactions were carried out for TH, as ø RT ctrl. without reverse transcription reaction) and water ctrl. water in place of cDNA template, which showed absence of PCR product amplification.

Primary HAEC, HMVEC-L, HPAEC and HAoSMC were purchased from Lonza, cultured and characterized. These cells were exposed to hypoxia (1% O_2) for 6, 12 and 24 h, and to normoxia (21% O_2). In real-time RT-PCR, mRNA of none of the enzymes was detected. Only the house keeping gene β2-MG (amplicon size: 160 bp) was detectable, showing the functionality of PCR conditions (Fig. 41).

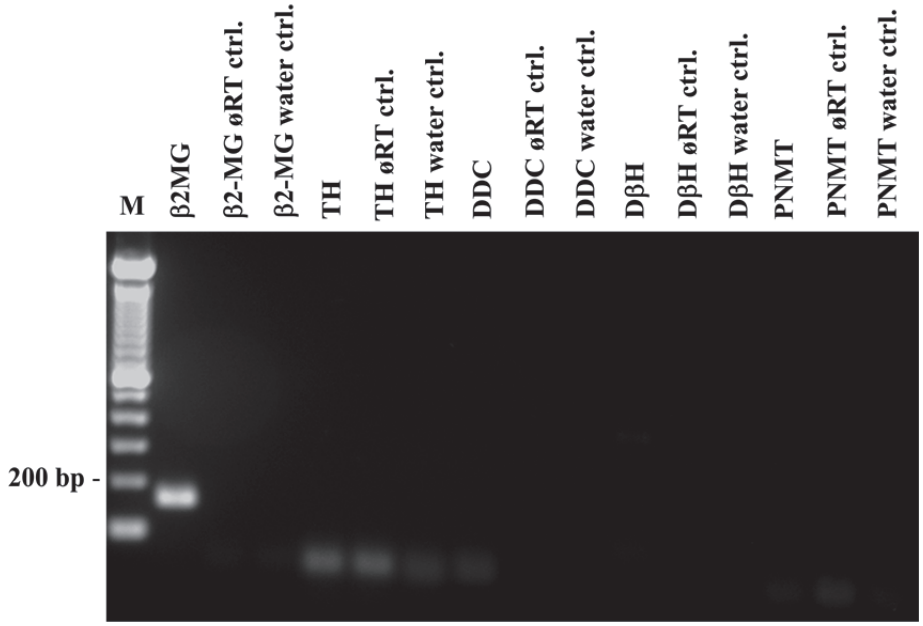

Fig. 41: Real-time RT-PCR for the catecholamine synthesizing enzymes from HMVEC-L, agarose gel electrophoresis. M: base pair marker. The control reactions were carried out, as “ø RT ctrl.” without reverse transcription reaction, and “water ctrl.” water in place of cDNA template, which showed absence of PCR product amplification.

IV Discussion

IV.1 Non-neuronal catecholamine synthesis in arteries

Catecholamines (dopamine, norepinephrine and epinephrine) play a vital role in the regulation of various body functions by the nervous system. Dopamine is a transmitter in the CNS, norepinephrine in the CNS and of postganglionic sympathetic neurons, and epinephrine is both a hormone released from the adrenal gland and also serves as neurotransmitter of brain stem neurons. Still, they are not restricted to the CNS (Kuhar et al., 2006). The present study elaborated on the synthesis and hypoxic regulation of catecholamines in vascular cells with particular reference to dopamine, which might act as local vasodilator.

Vascular tone of peripheral arteries, (e.g. SMA) is mediated by three types of nerve fibers innervating the vascular wall: sympathetic nerve fibers (releasing NE and causing vasoconstriction), parasympathetic nerve fibers (cholinergic fibers and nitregic fibers, causing vasodilation) and sensory fibers (C-fibers releasing substance P and calcitonin gene-related peptide, causing vasodilation) (Morris et al., 1995). Furthermore other factors such as circulating and locally produced hormones, e.g. bradykinin, also play an important role in the regulation of vascular tone (Auch-Schwelk et al., 1993).

Little is known about catecholamine synthesis within the vascular wall, which is mainly composed of ECs, VSMC and adventitial connective tissue cells. This is the first study providing a detailed evidence of catecholamine synthesis within the vascular wall. In the present study, expression of mRNA of all of four enzymes of the catecholamine synthesis pathway was detected and quantified in rat thoracic and abdominal aorta, SMA and femoral artery. It was observed that these arteries express different levels of mRNA of these enzymes. TH is the rate limiting enzyme of the pathway which converts L-tyrosine to L-DOPA (Nagatsu et al., 1964); its mRNA is highly expressed in all of these arteries. TH protein was also detected in these arteries by immunolabelling and western blot analysis. TH mRNA and protein expression in these arteries suggests active synthesis of dopamine and/or other catecholamines in these vessels. TH mRNA expression and enzyme activity have been already been reported in 1999 in various non-neuronal and non-adrenal tissues of rat, e.g. aorta, vas deferens, stomach, lung, duodenum, pancreas, spleen and salivary gland (Kawamura et al., 1999). After chemical sympathectomy (6-hydroxydopamine) of young adult rats, catecholamine levels (NE, dopamine), TH mRNA and enzyme activity were reduced in most organs such as vas

deferens, stomach and salivary gland whereas they remained unchanged in the abdominal aorta. This persistence of catecholamines and their synthesizing enzyme in the aorta was interpreted by the authors as being due to the presence of sympathetic nerve cell bodies or extra-adrenal paraganglia, e.g. organ of Zuckerkandl (Kawamura et al., 1999). The present study, however, clearly demonstrates non-neuronal and non-paraganglionic sources of TH in the arterial wall, since 1) this enzyme was consistently found also in arteries that are not accompanied by paraganglia (e.g. femoral artery and thoracic descending aorta), 2) paraganglia were never observed in the specimens processed for immunohistochemistry, and 3) TH mRNA and protein were also detected in cultured cells from the vascular wall, i.e. EC and VSMC.

DDC is the second enzyme of the catecholamine synthesis pathway. DDC mRNA expression, as well as that of DβH mRNA, was lower in the thoracic aorta than in the other arteries investigated in the present study. These quantitative differences might suggest less active synthesis of catecholamines in this particular arterial segment. However, there are no direct data addressing this issue and it is noteworthy that no significant differences were observed in expression of the rate limiting enzyme, TH. Structurally, the thoracic aorta differs from the other arteries being investigated in this study by its highly elastic wall. Generally, there are two types of arteries: elastic and conducting arteries. The highly elastic wall of arteries close to the heart allows them to store part of the ejected volume during systole and maintain blood flow at diastole. The VSMC of these arteries synthesize elastin and other extracellular matrix components and are classified as metabolic VSMC. The tunica media of distributing or muscular arteries, is mainly composed of SMC of the contractile type and these arteries are mainly involved in the regulating the distribution of blood to various organs according to physiological needs, e.g. low pO_2 causes vasodilation to accommodate more blood supply to the organ. The differences in DDC and DβH mRNA content observed in the present study might reflect differences in catecholamine synthesis by metabolic and contractile VSMC although this has further to be confirmed by direct investigation.

NE and E are synthesized by the actions of DβH and PNMT. Messenger RNAs coding for both of these enzymes were also consistently detected in all arteries in this study. Expression of DβH and PNMT within the vascular wall suggests local synthesis of NE and E. Supportively, NE and E levels are largely reduced in chemically

sympathectomized aorta and SMA but 20% still persisted in our accompanying experiments (Kuncová et al., 2007).

Non-neuronal NE and E have also been reported in the heart. In the human heart, NE has been reported to account for 88% out of total synthesized catecholamines, whereas the balance of 12 % is dopamine (Eisenhofer et al., 1997). On the other hand, the human heart contains also PNMT protein and activity (Kennedy et al., 1995). In the rat heart, there is significant expression of PNMT also. Here, PNMT mRNA expression persists after chemical sympathectomy, and immunofluorescence identified cardiomyocytes as a source of this non-neuronal PNMT (Kvetnanský et al., 2006).

PNMT is predominantly present in brain and adrenal gland (Ziegler et al, 2002). This enzyme has also been previously reported to be present in various non-neuronal organs, e.g. spleen (Pendleton et al., 1978), lung (Pendleton et al., 1978; Kennedy et al., 1990), kidney (Ziegler et al., 1989), and heart (Axelrod, 1962; Pendleton et al., 1978; Kennedy and Ziegler, 1991; Eisenhofer et al., 1997). In the present study of arteries, PNMT mRNA content was significantly lower than that of the other enzymes which also fits to our observation that, after sympathectomy, vascular E levels were lowest among the catecholamines (Kuncová et al., 2007).

Collectively, the present data demonstrate that the machinery for synthesis of non-neuronal catecholamine, predominantly dopamine and synthesis occurs also in intact arteries where these locally synthesized catecholamines might play an important role in various vascular functions.

IV.2 Expression and regulation of catecholamine synthesizing enzyme mRNAs in vascular cells

The dominant cells of vascular intima and media are EC and VSMC, respectively. EC are present on the inner most surfaces and form a monolayer of flat and compactly packed cells. They play a vital role in vascular injury repair mechanisms and help to maintain the vascular tone and hemostasis. EC release different mediators in response to various stimuli, e.g. vWF, prostaglandins, growth factors, cytokines and nitric oxide (Augustin, 2007). VSMC are the contractile end-effectors of the vascular wall, which receive input from the endothelium and also from the nervous system. They regulate the vascular diameter according to the inputs. Furthermore, they are also involved in the synthesis and secretion of extracellular matrix which also plays an important role in vascular function (Handa et al., 2007).

This is the first study providing evidence of expression of catecholamine synthesis enzymes in isolated vascular cells. Under normoxic conditions, EC express mRNAs coding for all of the enzymes involved in catecholamine synthesis. In rat pulmonary EC, hypoxia caused an up-regulation of TH mRNA by 25-fold after 24 h, of DβH mRNA by 8-fold after 6 and 24 h, whereas DDC and PNMT mRNA content were not significantly different after hypoxic exposure. Other studies have also shown up-regulation of TH mRNA expression after hypoxic exposure. Hypoxia causes up-regulation of TH mRNA transcription, and this effect can be inhibited by protein kinase C inhibitors (Millhorn et al., 1997; Raymond and Millhorn, 1997). It has been shown that TH mRNA expression is up-regulated by hypoxia in cultured rat mesencephalic cells by 4-5 fold, and dopamine content was also increased by 5-fold (Leclere et al., 2004). In PC12 cells, a rat pheochromocytoma cell line, TH and PNMT mRNA and protein expression are up-regulated in response to hypoxia (Czyzyk-Krzeska et al., 1994; Norris and Millhorn, 1995; Höhler et al., 1999; Evinger et al., 2000). The duration of hypoxia also plays an important role on the expression and stability of TH mRNA. It has been reported that the rate of TH mRNA transcription increases rapidly after hypoxic exposure with peak levels at ~6 h. This higher expression is maintained over a time period of >12 h in PC12 cells (Czyzyk-Krzeska et al., 1994).

In contrast to the reported hypoxic regulation of TH expression in several cell types including rat pulmonary EC in the present study, hypoxic exposure of rat aortic EC did not cause a significant change in the mRNA expression of any of these enzymes. It remains to be determined whether this reflects different properties of the systemic versus pulmonary circulation or microvascular - the isolation procedure of lung EC favors enrichment of microvascular EC - versus arterial EC.

Rat aortic VSMC also express the mRNAs for TH, DβH and PNMT while DDC mRNA expression was too low to be detected in these cells. This apparent lack or paucity of DDC might imply that L-DOPA instead of catecholamines is the major product in VSMC. Alternatively, synthesis may proceed towards dopamine via low levels of DDC below detection level of the present approach, or by DDC from other sources.

L-DOPA from VSMC might be taken up by EC to be converted to dopamine. L-type amino acid transporters are likely candidates for accomplishing this release and uptake. Rat brain EC have a sodium independent L-type amino acid transporter (LAT) which is involved in the transport of L-DOPA from blood stream to the neurons

(Sampaio-Maia et al., 2001). This transporter is reported to work as importer and exporter of L-DOPA. Such transporter is also reported in EC of other parts of the vascular tree such as rat retinal microvasculature (Tomi et al., 2005) and human aorta (Haase et al., 2007).

L-DOPA might act as a regulator of dopamine synthesis in EC. In the previous years it has been shown that externally applied L-DOPA can increase the dopamine synthesis rate and activity of DDC. It has been shown that treatment of PC12 cells with L-DOPA (20-200 µM) results in increased dopamine synthesis by 226-504% by increasing the enzymatic activity of TH and DDC (Jin et al., 2008).

DβH and PNMT mRNA expression indicates that VSMCs are capable of NE and E synthesis. Dopamine released from EC might serve as a substrate for DβH and PNMT in VSMC. In addition, DDC also circulates in plasma (Boomsma et al., 1986; Lee et al., 1986), so that sufficient L-DOPA converting activity in the vascular wall can be assumed. In this scenario, conversion of dopamine into NE by VSMC requires dopamine uptake. Several dopamine transporters are known, among them being most important the plasma monoamine transporter PMAT (Okura et al., 2011), the dopamine transporter (DAT) (Mignini et al., 2006), and organic cation transporter-2 (OCT-2) (Gründemann et al., 1998). While plasma monoamine transporter (PMAT) and DAT are considered to be preferentially expressed in the nervous system, DAT immunoreactivity in arterial walls also has been reported (Mignini et al., 2006). Detailed studies on potential dopamine transporters in VSMC have not been reported yet.

This locally synthesized NE and E might also play an important role in physiological functions of VSMC or the vascular wall in general, but unlike catcholamine synthesis in various other cells including pulmonary EC, synthesis appears not to be significantly regulated by hypoxia and indicated from the present real-time RT-PCR experiments.

Collectively, these data indicated that there are two sources of catecholamines - neuronal and non-neuronal - in the vascular wall, with the non-neuronal catecholamine synthesis not being restricted to a single cell type. In addition to EC and VSMC directly addressed in the present study, various cells of the immune system are also regular constituents of the vascular wall, and they provide additional sources of intrinsic non-neuronal catecholamines (Flierl et al., 2007).

IV.2.1 Expression in human vascular cells

The data obtained from human vascular cells differed considerably from those of isolated vascular cells from rat. None of the four enzymes were detectable by PCR from cDNA of human vascular cells, despite the housekeeping gene (β2-MG) was readily detected, proving efficiency of RNA isolation and reverse transcription. We had optimized the PCR conditions for the primer pairs addressing catecholamine synthesizing enzymes by using total RNA from human pheochromocytoma. Human pheochromocytomas express high levels of mRNA of TH, DDC and DβH while mRNA for PNMT is lower as compared to healthy persons (Isobe et al., 1998). In our pheochromocytoma sample we were able to detect mRNA of TH, DDC and DβH by using RT-PCR, suggesting that our primer pairs and PCR conditions are well optimized. In order to further support our results we used total RNA from human sympathetic trunk as another positive control. Again, all four enzyme mRNAs were detectable by using the same primer pairs as were used for human vascular cells.

In human brain, four splice variants for human TH are reported while in rodent only one variant exists and there are 2 variants in monkey (Lewis et al., 1993). In this study, primer pairs were selected to be able to detect any of the four human variants. Thus, the negative results in human vascular cells are unlikely to be explained by presence of an unusual splice variant.

Consequently, the most likely explanation for the negative findings is that cultured human vascular cells do not express the classical catecholamine synthesizing enzymes. It has to be considered that these human vascular cells were purchased from a commercial provider using different isolation protocols than we used for isolation of rat cells. However, even when TH, DDC, DβH and PNMT are indeed not expressed in human vascular cells, this does not rule out the possibility of catecholamine synthesis by these cells. An alternative pathway for the catecholamine synthesis has also been reported, mediated by an enzyme tyrosinase, mainly present in melanocytes, which can convert tyrosine to L-DOPA. This L-DOPA can be released and can be taken up by other cells expressing DDC to make dopamine (Sanchez-Ferrer et al., 1995).

IV.3 Catecholamines, hypoxia and vasodilation

Catecholamines function as neurotransmitters and neuro-hormones and play an important role in the regulation of various physiological and metabolic processes in

body. All three catecholamines (E, NE and dopamine) are found in plasma. Plasma NE originates from sympathetic neuronal activity while E mainly comes from the adrenal medulla, whereas plasma dopamine content has been ascribed to originate mainly from sympathetic noradrenergic nerve terminals (Goldstein and Holmes, 2008). These circulating catecholamines might play important role in various physiological functions. In clinical practice dopamine is administered in acute hypotension illness. At low dose, dopamine acts on vascular β-adrenergic and dopamine receptors while at high doses it also stimulates α_1 and α_2 adrenergic receptors. Low dose dopamine has many beneficial effects; it increases cardiac output and heart rate and selectively increases the blood flow in renal and hepato-splanchnic arteries, decreases pulmonary resistance and enhances oxygen supply (Hoffman et al., 1990; Philip-Joet et al., 1988; Chan, 1995). The body responds to hypoxia by increasing the hyperventilation (acute) and by polycythemia (chronically) by increased production of red blood cells, to enhance the O_2 carrying capacity of blood. Hyperventilation is mediated by the carotid body chemoreceptors. The type I cells of carotid body are reported to be O_2 sensitive and release dopamine in the event of low pO_2. During hypoxia, TH enzymatic activity and expression is also increased in these cells (Czyzyk-Krzeska et al., 1994).

In parallel studies (Kuncová et al., 2007), we have observed that lowering of pO_2 causes vasodilation in isolated and perfused rat SMA. This vasodilator response is blocked by the D_1 receptor agonist SCH-23990, suggesting an endogenous release of dopamine in the vascular wall. After removal of the endothelial cell layer, this vasodilator response is still present, although less than with an intact endothelial cell layer, and still can be blocked by the D_1 receptor agonist SCH-23990. It is well known that smooth muscle cells express dopamine receptors D_1 and D_3. Dopamine acts via D_1 and D_3 receptors located on rat mesenteric artery smooth muscle cells. Furthermore, these receptors interact physically and are probably involved in regulation of blood pressure and flow in this artery (Zeng et al., 2004). Vasodilation by D_1 receptors is mediated by cAMP/PKA signaling pathway. Stimulation of these receptors also increases intracellular levels of cAMP (Hussain and Lokhandwala, 1998; Jose et al., 1998; Jose et al., 2002).

The observations on endothelial denuded SMA support the hypothesis that there are two sources of dopamine in the vascular wall: EC and SMC. This conclusion derives from the finding that D_1 receptor mediated hypoxic relaxation was diminished but not abolished by removal of the endothelium. The current work also supports this, as EC

express mRNA of all of the four enzymes, and under hypoxic conditions regulation for TH and DβH mRNAs was also observed. The rat VSMC expresses mRNAs for TH, DβH and PNMT while DDC mRNA expression was too low to be detected. It already has been discussed that they still may possess the ability of catecholamine synthesis by up-take of dopamine. The same transporters that mediate uptake of dopamine, i.e. PMAT, DAT and OCT-2 (Gründemann et al., 1998; Mignini et al., 2006; Okura et al., 2011), can also serve as release mechanisms. In rat endothelial cell lines and brain capillaries, PMAT expression has recently been reported (Okura et al., 2011) but more studies are needed to elucidate endothelial dopamine release mechanisms in more detail.

IV.4 Other non-neuronal functions of dopamine

Recently it has been reported that catecholamines are involved in a broader variety of physiological and pathophysiological functions than previously thought. New evidences are emerging that they are synthesized by other tissues or cells in the body having diverse functions. Catecholamine synthesis in the gastrointestinal tract is well reported (Eisenhofer et al., 1997) and it is suggested that in catecholamines are probably involved in exocrine secretion from the pancreas (Iwatsuki et al., 1992), bicarbonate secretion regulation in stomach and duodenum (Flemstrom et al., 1993). The pancreas is reported to be actively involved particularly in dopamine synthesis and release; the dopamine is usually released into the duodenum along with other secretions. It is postulated that dopamine acts as a self defense mechanism in the gastrointestinal tract against harmful agents (Mezey et al., 1996).

Tumor hypoxia is an important feature of advanced solid tumors (Vaupel and Harrison, 2004). It has been reported that tumor cells can synthesize dopamine under hypoxic conditions thereby decreasing angiogenesis by acting in a paracrine manner via D_2 receptors located on EC of the tumor vessels (Basu et al., 2001; Chakroborty et al., 2008). The expression of dopamine synthesis machinery and its hypoxic regulation in vascular cells might be an indigenous protective mechanism to prevent tumor invasion and metastasis.

Dopamine is also reported to modulate the exocytosis in EC in response to thrombin or histamine by inhibiting the release of vWF (Zarei et al., 2006). Immune cells are also reported to be equipped with catecholamine synthesizing machinery. Particularly, monocytes are reported to be able to synthesize and release catecholamines

(Cosentino et al., 1999; Brown et al., 2003). This synthesis and release is increased in response to inflammatory mediators such as LPS in alveolar macrophages and blood monocytes (Flierl et al., 2007).

Finally, it also has to be considered that dopamine might not only act via dopamine receptors but also can be converted into other active, non-catecholaminergic compounds. N-Arachidonoyl-dopamine is an endocannabinoid that acts as a vasodilator through vanniloid and cannabinoid receptors (O'Sullivan et al., 2004).

V Conclusions

Endothelial cells express the enzymatic machinery for catecholamine synthesis and, upon hypoxia or low pO_2, this machinery is activated and produces dopamine and possibly other catecholamines, too. The locally synthesized dopamine stimulates the D_1 receptors on underlying smooth muscle cells, causing relaxation/vasodilation, ultimately resulting in increased blood supply to affected organ. Smooth muscle cells also have the machinery to synthesize NE and E once dopamine is provided. Possibly, they can take up dopamine from EC via membrane transporters. Upon lowered pO_2, this stored dopamine is released and acts on dopamine receptors on smooth muscle cells and results in vasodilation (Fig. 42).

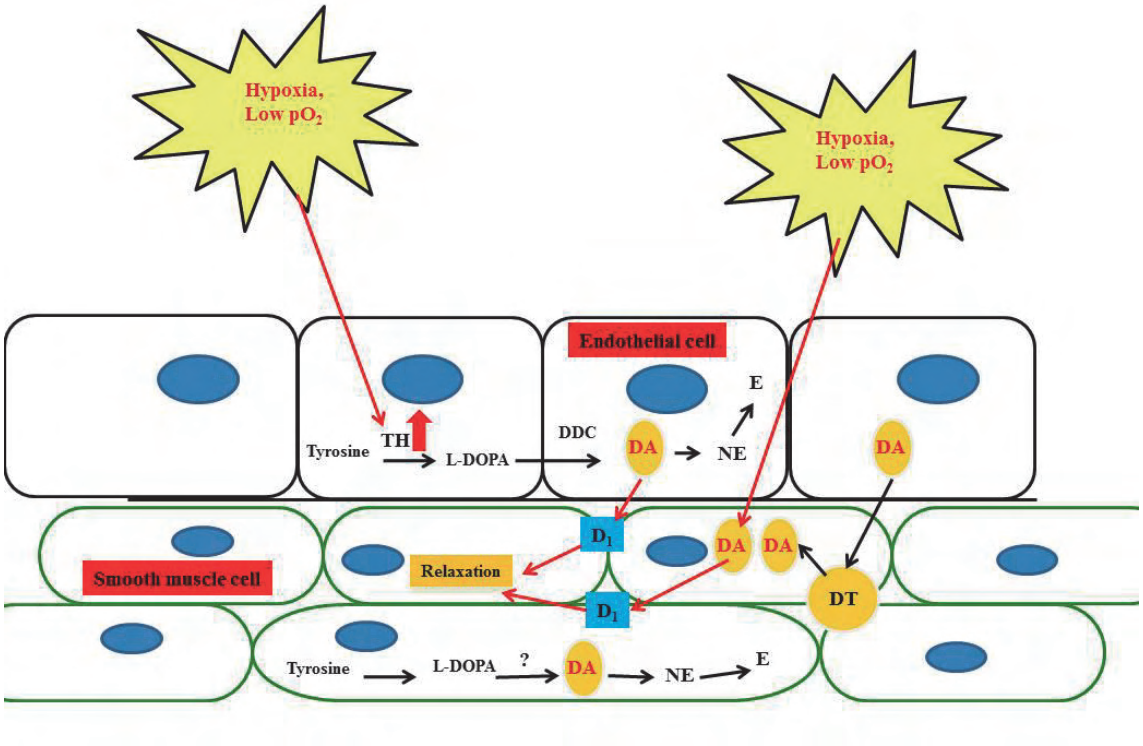

Fig. 42: Proposed scenario of regulation of catecholamine synthesis in vascular cells.
DT: dopamine transport mechanisms, e.g. PMAT, DAT or OCT-2,
DA: Dopamine

VI References

1. Adam WR, Culvenor AJ, Hall J, Jarrott B, Wellard RM. Aromatic L-amino acid decarboxylase: histochemical localization in rat kidney and lack of effect of dietary potassium or sodium loading on enzyme distribution. Clin Exp Pharmacol Physiol 13:47–53, 1986
2. Ahlquist R. A study of adrenotropic receptors. Am J Physiol 153:586-600, 1948
3. Andreassi II JL, Eggleston WB, Stewart JK. Phenylethanolamine N-methyltransferase mRNA in rat spleen and thymus. Neurosci Lett 241:75–78, 1998
4. Auch-Schwelk W, Bossaller C, Claus M, Graf K, Gräfe M, Fleck E. ACE inhibitors are endothelium dependent vasodilators of coronary arteries during submaximal stimulation with bradykinin. Cardio Res *27*:312–317, 1993
5. Augustin HG. Endothelial Cell Input. In: Arid WC (Ed.) Endothelial Biomedicine Cambridge University Press Pp. 227-229, 2007
6. Axelrod J. Purification and properties of phenylethanolamine-N-methyltransferase. J Biol Chem 237:1657-1660, 1962
7. Basu S, Nagy JA, Pal S, Vasile E, Eckelhoefer IA, Bliss VS, Manseau EJ, Dasgupta PS, Dvorak HF, Mukhopadhyay D. The neurotransmitter dopamine inhibits angiogenesis induced by vascular permeability factor/vascular endothelial growth factor. Nat Med 7:569-574, 2001
8. Bell C, Stubbs A. Localization of vasodilator dopamine receptors in the canine hind limb. Br J Pharmacol 64:253-258, 1978
9. Bello-Reuss E, Higashi Y, Kaneda Y. Dopamine decreases fluid reabsorption in straight portions of rabbit proximal tubule. Am J Physiol 242:634-640, 1982
10. Bergquist J, Tarkowski A, Ekman R and Ewing A. Discovery of endogenous catecholamines in lymphocytes and evidence for catecholamine regulation of lymphocyte function via an autocrine loop. Proc Natl Acad Sci USA 91:12912-12916, 1994
11. Berne RM. Effect of epinephrine and norepinephrine on coronary circulation. Cir Res 6:644-655, 1958
12. Blaschko H. The specific action of L-dopa decarboxylase. J Physiol (Lond) 96:50-51, 1939

13. Bohn MC, Bloom E, Goldstein M, Black IB. Glucocorticoid regulation of phenylethanolamine N-methyl-transferase (PNMT) in organ culture of superior cervical ganglia. Dev Biol 105:130-136, 1984
14. Boomsma F, van der Hoorn FA, Schalekamp MA. Determination of aromatic-L-amino acid decarboxylase in human plasma. Clin Chim Acta 159:173-183, 1986
15. Brodde OE. $Beta_1$- and $beta_2$-adrenoceptor polymorphisms and cardiovascular diseases. Fundam Clin Pharmacol 22:107-125, 2008
16. Brown SW, Meyers RT, Brennan KM, Rumble JM, Narasimhachari N, Perozzi EF, Ryan JJ, Stewart JK, Fischer-Stenger K. Catecholamines in a macrophage cell line. J Neuroimmunol 135:47-55, 2003
17. Chakroborty D, Chowdhury UR, Sarkar C, Baral R, Dasgupta PS, Basu S. Dopamine regulates endothelial progenitor cell mobilization from mouse bone marrow in tumor vascularization. J Clin Invest 118:1380-1389, 2008
18. Chan TY. Low-dose dopamine in severe right heart failure and chronic obstructive pulmonary disease. Ann Pharmacother 29:493-6, 1995
19. Chan YL. Cellular mechanisms of renal tubular transport of L-dopa and its derivatives in the rat: microperfusion studies. J Pharmacol Exp Ther 199:17-24, 1976
20. Chandel NS, Maltepe E, Goldwasser E, Mathieu CE, Simon MC, Schumaker PT. Mitochondrial reactive oxygen species trigger hypoxia-induced transcription. Proc Natl Acad Sci USA 95:11715-11720, 1998
21. Cheung PY and Barrington KJ. Renal dopamine receptors: Mechanisms of action and developmental aspects. Cardiovasc Res 31:2-6, 1996
22. Cosentino M, Marino F, Bombelli R, Ferrari M, Lecchini S, Frigo G. Endogenous catecholamine synthesis, metabolism, storage and uptake in human neutrophils. Life Sci 64(11):975-981, 1999
23. Cummins EP, Taylor CT. Hypoxia-responsive transcription factors. Pflugers Arch-Eur J Physiol 450: 363-371, 2005
24. Czyzyk-Krzeska MF, Bayliss DA, Lawson EE, Millhorn DE. Regulation of tyrosine hydroxylase gene expression in the rat carotid body by hypoxia. J Neurochem 58:1538-1546, 1992
25. Czyzyk-Krzeska MF, Furnari BA, Lawson EE, Millhorn DE. Hypoxia increases rate of transcription and stability of tyrosine hydroxylase mRNA in pheochromocytoma (PC12) cells. J Biol Chem 269:760-764, 1994

26. Dearry A, Gingrich JA, Falardeau P, Fremeau RT, Bates MD, Caron MG. Molecular cloning and expression of the gene for a human D_1 dopamine receptor. Nature 347:72-76, 1990

27. DiMarco GS, Vio CP, Dos Santos OF, Schor N, Casarini DE. Catecholamine production along the nephron. Cell Physiol Biochem 20:919-924, 2007

28. Dunkley PR, Bobrovskaya L, Graham ME, von Nagy-Felsobuki EI, Dickson PW. Tyrosine hydroxylase phosphorylation: regulation and consequences. J Neurochem 91:1025-1043, 2004

29. Ebert SN, Baden JM, Mathers LH, Siddall BJ, Wong DL. Expression of phenylethanolamine N-methyltransferase in the embryonic rat heart. J Mol Cell Cardiol 28:1653-1658, 1996

30. Eisenhofer G, Aneman A, Friberg P, Hooper D, Fåndriks L, Lonroth H, Hunyady B, Mezey E. Substantial production of dopamine in the human gastrointestinal tract. J Clin Endocrinol Metab. 82:3864-3871, 1997

31. Elliott J. Alpha-adrenoceptors in equine digital veins: evidence for the presence of both α_1- and α_2-receptors mediating vasoconstriction. J Vet Pharmacol Ther 20: 308-317, 1997

32. Ema M, Hirota K, Mimura J, Abe H, Yodoi J, Sogawa K, Poellinger L, Fujii-Kuriyama Y. Molecular mechanisms of transcription activation by HLF and HIF1α in response to hypoxia: their stabilization and redox signal-induced interaction with CBP/p300. EMBO J 18:1905-1914, 1999

33. Evinger MJ, He R, Powers J, Tischler AS. Hypoxia stimulates expression of PNMT gene. Proc Soc Neurosci 26:19.2, 2000

34. Feldman RS, Meyer JS, Quenzer LF. Catecholamines, Principles of neuropsychopharmacology. Sunderland, MA: Sinauer Associates, Inc. Pp. 277-344, 1997

35. Flemström G, Säfsten B, Jedstedt G. Stimulation of mucosal alkaline secretion in rat duodenum by dopamine and dopaminergic compounds. Gastroenterology. 104:825-833, 1993

36. Flierl MA, Rittirsch D, Nadeau BA, Chen AJ, Sarma JV, Zetoune FS, McGuire SR, List RP, Day DE, Hoesel LM, Gao H, Van Rooijen N, Huber-Lang MS, Neubig RR, Ward PA. Phagocyte-derived catecholamines enhance acute inflammatory injury. Nature 449:721-725, 2007

37. Fremeau RJ, Duncan GE, Fornaretto MG, Dearry A, Gingrich JA, Breese GR, Caron MG. Localization of D_1 dopamine receptor mRNA in brain supports a role in cognitive, affective and neuroendocrine aspects of dopaminergic neurotransmission. Proc Natl Acad Sci USA 91:12564-12568, 1991
38. Garcia-Fernandez M, Ortega-Saenz P, Castellano A, Lopez-Barneo J. Mechanisms of low-glucose sensitivity in carotid body glomus cells. Diabetes 56: 2893–2900, 2007
39. Gardner LB, Corn PG. Hypoxic regulation of mRNA expression. Cell Cycle 7:1916-1924, 2008
40. Goldberg LI, Volkman PH, Kohli JD. A comparison of the vascular dopamine receptors with other dopamine receptors. Annu Rev Pharmacol Toxicol 18:57-79, 1978
41. Goldstein DS, Holmes C. Neuronal source of plasma dopamine. Clin Chem 54:1864-1871, 2008
42. Greene LA, Tischler AS. Establishment of a noradrenergic clonal line of rat adrenal pheochromocytoma cells which respond to nerve growth factor. Proc Natl Acad Sci USA 73:2424-2428, 1976
43. Gründemann D, Köster S, Kiefer N, Breidert T, Engelhardt M, Spitzenberger F, Obermüller N, Schömig E. Transport of monoamine transmitters by the organic cation transporter type 2, OCT2. J Biol Chem 273:30915-30920, 1998
44. Haase C, Bergmann R, Fuechtner F, Hoepping A, Pietzsch J. L-type amino acid transporters LAT1 and LAT4 in cancer: uptake of 3-O-methyl-6-18F-fluoro-L-dopa in human adenocarcinoma and squamous cell carcinoma in vitro and in vivo. J Nucl Med 48:2063-2071, 2007.
45. Handa S, Kolodziejska and Husain, M. Vascular Smooth Muscle Cells: The Muscle behind Vascular Biology. In: Arid WC (Ed.) Endothelial Biomedicine Cambridge. University Press Pp. 454-561, 2007
46. Head RJ, Hempstead J, Berkowitz BA. Catecholamines in the vasculature of the rat and rabbit: dopamine, norepinephrine, epinephrine. Blood Vessels 19:135-147, 1982
47. Hoffman B, Lefkowitz R. Catecholamines and sympathomimetic drugs. In: Gilman A, Rall T, Nies A, Taylor P, editors. Goodman and Gilman’s the Pharmacological Basis of Therapeutics. New York: Pergamon Press pp. 187–220, 1990

48. Hoffmann A, Gloe T, Pohl U. Hypoxia-induced up-regulation of eNOS gene expression is redox-sensitive: a comparison between hypoxia and inhibitors of cell metabolism. J Cell Physiol 188:33–44, 2001

49. Höhler B, Lange B, Holzapfel B, Goldenberg A, Hänze J, Sell A, Testan H, Möller W, Kummer W. Hypoxic up-regulation of tyrosine hydroxylase gene expression is paralleled, but not induced, by increased generation of reactive oxygen species in PC12 cells. FEBS Lett 457:53-56, 1999

50. Huang LE, Gu J, Schau M, Bunn HF. Regulation of hypoxia-inducible factor 1 alpha is mediated by an O2-dependent degradation domain via the ubiquitin-proteasome pathway. Proc Natl Acad Sci USA 95:7987-799, 1998

51. Hussain T and Lokhandwala M. Renal dopamine receptors and hypertension. Exp Biol Med (Maywood) 228:134–142, 2003

52. Hussain T, Lokhandwala MF. Renal dopamine receptor function in hypertension. Hypertension 32:187–197, 1998

53. Isobe K, Nakai T, Yukimasa N, Nanmoku T, Takekoshi K, Nomura F. Expression of mRNA coding for four catecholamine-synthesizing enzymes in human adrenal pheochromocytomas. Eur J Endocrinol 138:383-387, 1998

54. Iwatsuki K, Ren LM, Chiba S. Effects of YM435, a novel dopamine D_1 receptor agonist, on pancreatic exocrine secretion in anesthetized dogs. Eur J Pharmacol 218:237-241, 1992

55. Jiang BH, Semenza GL, Bauer C, Marti HH. Hypoxia-inducible factor 1 levels vary exponentially over a physiologically relevant range of O_2 tension. Am J Physiol Cell Physiol 271:C1172–C1180, 1996

56. Jin CM, Yang YJ, Huang HS, Lim SC, Kai M, Lee MK. Induction of dopamine biosynthesis by L-DOPA in PC12 cells: implications of L-DOPA influx and cyclic AMP. Eur J Pharmacol 591:88-95, 2008

57. Jose PA, Eisner GM and Felder RA. Dopamine receptor-coupling defect in hypertension. Curr Hypertens Rep 4:237-244, 2002

58. Jose PA, Eisner GM, Felder RA. Renal dopamine receptors in health and hypertension. Pharmacol Ther 80:149–182, 1998

59. Kameda, Y. Mash1 is required for glomus cell formation in the mouse carotid body. Dev Biol 283:128–139, 2005

60. Kawamura M, Schwartz JP, Nomura T, Kopin IJ, Goldstein DS, Huynh TT, Hooper DR, Harvey-White J, Eisenhofer G. Differential Effects of Chemical

Sympathectomy on Expression and Activity of Tyrosine Hydroxylase and Levels of Catecholamines and DOPA in Peripheral Tissues of Rats. Neurochem Res 24:25-32, 1999

61. Kebabian JW and Calne DB. Multiple receptors for dopamine. Nature 277:93-96, 1979
62. Kennedy B, Elayan H, Ziegler M. Lung epinephrine synthesis. Am J Physiol 258: L227-L231, 1990
63. Kennedy B, Ziegler M. Cardiac epinephrine synthesis. Circulation 84: 891-895, 1991
64. Kennedy B, Elayan H, Ziegler MG. Glucocorticoid elevation of mRNA encoding epinephrine-forming enzyme in lung. Am J Physiol 265:117–120, 1993
65. Kennedy B, Bigby TD, Ziegler MG. Nonadrenal epinephrine-forming enzymes in humans. Characteristics, distribution, regulation, and relationship to epinephrine levels. J Clin Invest 95:2896–2902, 1995
66. Kokkinou I, Nikolouzou E, Hatzimanolis A, Fragoulis EG, Vassilacopoulou D. Expression of enzymatically active L-DOPA decarboxylase in human peripheral leukocytes. Blood Cells Mol Dis 42:92-98, 2009
67. Kroll SL, Paulding WR, Schnell PO, Barton MC, Conaway JW, Czyzyk-Krzeska, MF. Hippel-Lindau protein induces hypoxia regulated arrest of tyrosine hydroxylase transcript elongation in pheochromocytoma cells. J Biol Chem 274:30109–30114, 1999
68. Kubovcáková L, Micutková L, Sabban EL, Krizanová O, Kvetnanský R. Identification of tyrosine hydroxylase gene expression in rat spleen. Neurosci Lett 310:157-160, 2001
69. Kuhar MJ, Minneman K, Muly EC. Catecholamines. In: Siegel G, Albers RW, Brady S, Price D (Eds). Basic Neurochemistry 7th ed. Elsevier Academic Press. Pp. 211–226, 2006
70. Kuncová J, Pfeil U, Brüggmann D, Paddenberg R, Rafiq A, Schluter KD, Mewe M, Middendorff R, Slaviková J, Kummer W. Dopamine is an endothelium-derived vasodilator in hypoxic vessels. Autonomic Neuroscience 135:Pp. 146, 2007
71. Kvetnanský R, Kubovcáková L, Tillinger A, Micutkova L, Krizanova O, Sabban EL. Gene expression of phenylethanolamine N-methyltransferase in

corticotropin-releasing hormone knockout mice during stress exposure. Cell Mol Neurobiol 26:735-754, 2006

72. Kvetnanský R, Sabban EL, Palkovits M. Catecholaminergic systems in stress: structural and molecular genetic approaches. Physiol Rev 89:535-606, 2009
73. Leclere N, Andreeva N, Fuchs J, Kietzmann T, Gross J. Hypoxia-induced long-term increase of dopamine and tyrosine hydroxylase mRNA levels. Prague Med Rep 105:291-300, 2004
74. Lee M, Nohta H, Ohkura Y. Occurrence of aromatic L-amino acid decarboxylase in human plasma and its assay by high-performance liquid chromatography with fluorescence detection. J Chromatogr 378:329-336, 1986
75. Lewis DA, Melchitzky DS, Haycock JW.Four isoforms of tyrosine hydroxylase are expressed in human brain. Neuroscience 54:477-492, 1993
76. Lewis-Tuffin LJ, Quinn PG, Chikaraishi DM. Tyrosine hydroxylase transcription depends primarily on cAMP response element activity, regardless of the type of inducing stimulus. Mol Cell Neurosci 25:536-547, 2004
77. Lindström P, Sehlin J. Mechanisms underlying the effects of 5-hydroxytryptamine and 5-hydroxytryptophan in pancreatic islets. A proposed role for L-aromatic amino acid decarboxylase. Endocrinology 112:1524-1529, 1983
78. Lokhandwala MF, Hegde S. Cardiovascular pharmacology of dopamine receptor agonist. In: Amenta, F. (Ed.) Peripheral Dopamine Pathophysiology. CRC Press, Boca Raton, Pp. 63-77, 1990
79. Lopez-Barneo J, Pardal R, Ortega-Saenz P. Cellular mechanisms of oxygen sensing. Annu Rev Physiol 63:259-287, 2001
80. Lovenberg W, Weissbach H, Udenfriend S. Aromatic L-amino acid decarboxylase. J Biol Chem 237:89-93, 1962
81. Maxwell PH, Pugh CW, Ratcliffe PJ. Inducible operation of the erythropoietin 30 enhancer in multiple cell lines: evidence for a widespread oxygensensing mechanism. Proc Natl Acad Sci USA 90:2423-2427, 1993
82. Maxwell PH, Wiesener MS, Chang GW, Clifford SC, Vaux EC, Cockman ME, Wykoff CC, Pugh CW, Maher ER, Ratcliffe, PJ. The tumor suppressor protein VHL targets hypoxia-inducible factors for oxygen dependent proteolysis. Nature 399:271-275, 1999

83. McDonald RH, Goldberg LI, McNay JL, Tuttle EP. Effects of dopamine in man: augmentation of sodium excretion, glomerular filtration rate, and renal plasma flow. J Clin Invest 43:1116-1124, 1964

84. McNay JL, Goldberg LI. Comparison of the effects of dopamine, isoproterenol, norepinephrine and bradykinin on canine renal and femoral blood flow. J Pharmacol Exp Ther 151:23-31, 1966

85. McNay JL, McDonald RM, Goldberg LI. Direct renal vasodilation produced by dopamine in the dog. Circ Res 16:510-517, 1965

86. Mezey E, Eisenhofer G, Harta G, Hansson S, Gould L, Hunyady B, Hoffman BJ. A novel nonneuronal catecholaminergic system: exocrine pancreas synthesizes and releases dopamine. Proc Natl Acad Sci USA 93: 10377-10382, 1996

87. Mignini F, Traini E, Tomassoni D, Amenta F. Dopamine plasma membrane transporter (DAT) in rat thymus and spleen: an immunochemical and immunohistochemical study. Auton Autacoid Pharmacol 26:183-189, 2006.

88. Millhorn DE, Czyzyk-Krzeska M, Bayliss DA, Lawson EE. Regulation of gene expression by hypoxia. Sleep 16:44-48, 1993

89. Millhorn DE, Raymond R, Conforti L, Zhu W, Beitner-Johnson D, Filisko T, Genter MB, Kobayashi S, Peng M. Regulation of gene expression for tyrosine hydroxylase in oxygen sensitive cells by hypoxia. Kidney Int 51:527-535, 1997

90. Missale C, Nash SR, Robinson SW, Jaber M, Caron MG. Dopamine receptors: from structure to function. Physiol Rev 78:189-225, 1998

91. Morris JL, Gibbins IL, Kadowitz PJ, Herzog H, Kreulen DL, Toda N, Claing A. Roles of peptides and other substances in cotransmission from vascular autonomic and sensory neurons. Can J Physiol Pharmacol 73:521-532, 1995

92. Muhlbauer B, Kuster E and Luippold G. Dopamine D3 receptors in the rat kidney: role in physiology and pathophysiology. Acta Physiol Scand 168:219-223, 2000

93. Musso NR, Brenci S, Setti M, Indiveri F, Lotti G. Catecholamine content and in vitro catecholamine synthesis in peripheral human lymphocytes. J Clin Endocrinol Metab 81:3553-3557, 1996

94. Nagatsu T, Levitt M and Udenfriend S. Tyrosine hydroxylase: the initial step in norepinephrine biosynthesis. J Biol Chem 239:2910-2917, 1964

95. Norris ML, Millhorn DE. Hypoxia-induced protein binding to O_2-responsive sequences on the tyrosine hydroxylase gene. J Biol Chem 270: 23774-23779, 1995

96. Nurse C. Neurotransmission and neuromodulation in the chemosensory carotid body. Auton Neurosci 120:1–9, 2005

97. Okura T, Kato S, Takano Y, Sato T, Yamashita A, Morimoto R, Ohtsuki S, Terasaki T, Deguchi Y. Functional characterization of rat plasma membrane monoamine transporter in the blood-brain and blood-cerebrospinal fluid barriers. J Pharm Sci 100:3924-3938, 2011

98. O'Sullivan SE, Kendall DA, Randall MD. Characterisation of the vasorelaxant properties of the novel endocannabinoid N-arachidonoyl-dopamine (NADA). Br J Pharmacol 141:803-812, 2004

99. Pardal R, Lopez-Barneo J. Low glucose sensing cells in the carotid body. Nat Neurosci 5:197-198, 2002

100. Peers C, Buckler KJ. Transduction of chemostimuli by the type I carotid body cell. J Membr Biol 144:1-9,1995

101. Pendleton R, Gessner G, Sawyer J. Studies on the distribution of phenylethanolamine-N-methyltransferase and epinephrine in the rat. Res Commun Chem Path Pharm 2: 315-325, 1978

102. Philip-Joet F, Saadjian A, Vestri R, Tran GA, Arnaud A. Hemodynamic effects of a single dose of dopamine and L-dopa in pulmonary hypertension secondary to chronic obstructive lung disease. Respiration 53:146–152, 1988

103. Rahman MK, Nagatsu T, Kato T. Determination of aromatic L-amino acid decarboxylase in serum of various animals by high-performance liquid chromatography with electrochemical detection. Life Sci 28:485-492, 1981

104. Raymond R, Millhorn D. Regulation of tyrosine hydroxylase gene expression during hypoxia: role of Ca^{2+} and PKC. Kidney Int 51:536-541, 1997

105. Ricci A, Bronzetti E, Fedele F, Ferrante F, Zaccheo D, Amenta F. Pharmacological characterization and autoradiographic localization of a putative dopamine D_4 receptor in the heart. J Auton Pharmacol 18:115-121, 1998

106. Ricci A, Escaf S, Vega JA and Amenta F. Autoradiographic localization of dopamine D_1 receptors in the human kidney. J Pharmacol Exp Ther 264: 431-437, 1993

107. Rump LC and Schollmeyer P. Dopamine receptor modulation of neurotransmission in rat and human kidney. In: Soares-da-Silva, P. (Ed.), Cardiovascular and Renal actions of Dopamine. Pergamon Press. Pp 88:91–98, 1993

108. Sagrada A, Fargeas MJ, Bueno L. Involvement of α_1- and α_2-adrenoceptors in the postlaparotomy intestinal motor disturbances in the rat. Gut 28:955–959, 1987

109. Salceda S, Caro J. Hypoxia inducible factor 1α (HIF-1α) protein is rapidly degraded by the ubiquitin proteasome system under normoxic conditions. Its stabilization by hypoxia depends on redox-induced changes. J Biol Chem 272:22642–22647, 1997

110. Salnikow K, Kluz T, Costa M, Piquemal D, Demidenko ZN, Xie K, Blagosklonny MV. The regulation of hypoxic genes by calcium involves c-Jun/AP-1, which cooperates with hypoxia-inducible factor 1 in response to hypoxia. Mol Cell Biol 22:1734–1741, 2002

111. Sampaio-Maia B, Serrao MP, Soares-da-Silva P. Regulatory pathways and uptake of L-DOPA by capillary cerebral endothelial cells, astrocytes, and neuronal cells. Am J Physiol Cell Physiol 280:C333-C342, 2001

112. Sanchez-Ferrer A, Rodriguez-Lopez J, Garcia-Canovas F, Garcia-Carmona F Tyrosinase: a comprehensive review of its mechanism. Biochim Biophys Acta 1247:1-11, 1995

113. Schnell PO, Ignacak ML, Bauer AL, Striet JB, Paulding WR, Czyzyk-Krzeska MF. Regulation of tyrosine hydroxylase promoter activity by the von Hippel-Lindau tumor suppressor protein and hypoxia-inducible transcription factors. J Neurochem 85:483-491, 2003

114. Semenza GL, Wang GL. A nuclear factor induced by hypoxia via *de novo* protein synthesis binds to the human erythropoietin gene enhancer at a site required for transcriptional activation. Mol Cell Biol 12:5447-5454, 1992

115. Semenza GL. HIF-1: mediator of physiological and pathophysiological responses to hypoxia. J Appl Physiol 88:1474-1480, 2000

116. Semenza GL. Regulation of mammalian O_2 homeostasis by hypoxia-inducible factor 1. Annu Rev Cell Dev Biol 15:551-578, 1999

117. Shaulian E, Karin M. AP-1 in cell proliferation and survival. Oncogene 20:2390–2400, 2001

118. Silva P, Landsberg L, Besarab A. Excretion and metabolism of catecholamines by the isolated perfused rat kidney. J Clin Invest 64:850-857, 1979

119. Tomi M, Mori M, Tachikawa M, Katayama K, Terasaki T, Hosoya K. L-type amino acid transporter 1-mediated L-leucine transport at the inner blood-retinal barrier. Invest Ophthalmol Vis Sci. 46:2522-2530, 2005

120. Vallone D, Picetti R, Borrelli W. Structure and function of dopamine receptors. Neurosci Biobehav Rev 24:125-132, 2000

121. Vargovic P, Ukropec J, Laukova M, Cleary S, Manz B, Pacak K, Kvetnansky R. Adipocytes as a new source of catecholamine production. FEBS Lett 585:2279-84, 2011

122. Vaupel P, Harrison L. Tumor hypoxia: causative factors, compensatory mechanisms, and cellular response. Oncologist Suppl 5:4-9, 2004

123. Wallace EF, Krantz MJ and Lovenberg W. Dopamine-β-hydroxylase: a tetrameric glycoprotein. Proc Nat Acad Sci USA 70:2253-2255, 1973

124. Wang GL, Semenza GL. Characterization of hypoxia-inducible factor 1 and regulation ofDNA binding activity by hypoxia. J Biol Chem 268:21513–21518, 1993

125. Weiner DM, Levey AI, Sunhara RK, Niznik HH, O'Dowd BF, Brann MR. Dopamine D_1 and D_2 receptor mRNA expression in rat brain. Proc Natl Acad Sci USA 88:1859-1863, 1991

126. Wenger RH. Mammalian oxygen sensing, signaling and gene regulation. J Exp Biol 203:1253-1263, 2000

127. Woodman OL, Vatner SF. Coronary vasoconstriction mediated by α_1- and α_2-adrenoceptors in conscious dogs. Am J Physiol 253:388-393, 1987

128. Zarei S, Frieden M, Rubi B, Villemin P, Gauthier BR, Maechler P, Vischer UM. Dopamine modulates von Willebrand factor secretion in endothelial cells via D_2-D_4 receptors. J Thromb Haemost 4:1588-1595, 2006

129. Zeng C, Wang D, Yang Z, Wang Z, Asico LD, Wilcox CS, Eisner GM, Welch WJ, Felder RA, Jose PA. Dopamine D_1 receptor augmentation of D_3 receptor action in rat aortic or mesenteric vascular smooth muscles. Hypertension 43:673-679, 2004

130. Zhang M, Buttigieg J, Nurse CA. Neurotransmitter mechanisms mediating low-glucose signaling in co-cultures and fresh tissue slices of rat carotid body. J Physiol 578: 735-750, 2007

131. Zhu H, Jackson T, Bunn HF. Detecting and responding to hypoxia. Nephrol Dial Transplant 17:3-7, 2002

132. Ziegler MG, Bao X, Kennedy BP, Joyner A, Enns R. Location, development, control, and function of extra adrenal phenylethanolamine N-methyltransferase. Ann N Y Acad Sci 971:76-82, 2002

133. Ziegler MG, Kennedy B, Elayan H. Rat renal epinephrine synthesis. J Clin Invest 84:1130-1133, 1989

VII Summary

Catecholamines (dopamine, norepinephrine and epinephrine) are physiologically important as they are involved in a number of body functions and also act as neurotransmitters. Dopamine is a metabolic intermediate in the formation of norepinephrine and epinephrine and a well known neurotransmitter in the central nervous system. In most of the mammalian systemic arteries, dopamine acts as a potent vasodilator. The vascular effects of dopamine are mediated via specific G protein-coupled receptors (D_1-D_5).

The present study aimed to look for the presence of enzymatic machinery (tyrosine hydroxylase = TH; DOPA-decarboxylase = DDC; dopamine-β-hydroxylase = DβH; phenylethanolamine-N-methyltransferase = PNMT) required to synthesize catecholamines in rat arteries, and their regulation in response to hypoxia (1% O_2) in endothelial (EC) and vascular smooth muscle cells (VSMC). Quantitative RT-PCR served to estimate mRNA content, and western blotting was used to test for TH protein expression. Furthermore, we also looked for the expression of the rate-limiting enzyme of catecholamine synthesis, TH, by quantitative RT-PCR, immunohistochemistry and western blotting in the intact vessels (rat thoracic aorta, abdominal aorta, superior mesenteric artery [SMA] and femoral artery).

Expression of mRNA of all four enzymes of the catecholamine synthesis pathway was detected and quantified in rat thoracic and abdominal aorta, SMA and femoral artery. It was observed that these arteries express different levels of mRNA content of these enzymes with PNMT being least abundant. TH protein was also detected in these arteries by immunolabelling and western blot analysis. TH expression in these arteries suggests active synthesis of dopamine and/or other catecholamines in these vessels. Previously, TH mRNA expression has been reported in rat aorta and it has been suggested that this might be the result of paraganglia contamination during sampling process. No paraganglia were detectable in immunohistochemical preparation of rat aorta suggesting that this part of vascular tree is itself capable of synthesizing catecholamines.

Rat pulmonary and aortic EC were isolated and cultured. These cells were characterized by DiI-Ac-LDL uptake and by immunolabeling with anti-vWF antibody. VSMC were isolated and cultured from thoracic and abdominal aorta and characterized by immunolabeling with anti α-smooth muscle actin antibody. Under normoxic conditions, EC and VSMC express mRNAs coding for all of the enzymes involved in

catecholamine synthesis. These vascular cells were exposed to hypoxia (1% O_2) for 6, 12 and 24 hours. Using real-time RT-PCR we detected the mRNAs for the complete or partial enzymatic machinery necessary for catecholamine synthesis in these cells. In rat pulmonary EC, hypoxia caused an up-regulation of TH mRNA by 25-fold after 24 h, of DβH mRNA by 8-fold after 6 and 24 h, whereas DDC and PNMT mRNA content were not significantly different after hypoxic exposure. In contrast, no significant effect of hypoxia on the regulation of the enzymatic machinery was observed in rat aortic EC. In VSMC, TH mRNA was qualitatively detectable while DDC mRNA content was too low to be detected. No statistically significant regulation of DβH and PNMT mRNA content was observed after hypoxic exposure in VSMC. This suggests that vascular cells are capable of catecholamine synthesis and this synthesis is differentially regulated under hypoxic conditions.

This is the first study providing evidence of expression of catecholamine synthesis enzymes in isolated vascular cells. Previously, Kuncova et al., 2007, had shown that the presence of catecholamines in rat aorta and SMA. Chemical sympathectomy with the neurotoxin, 6-hydroxydopamine, significantly reduced norepinephrine and epinephrine levels, while dopamine content was unaffected. Functional studies using rat SMA showed an endothelium-dependent vasodilation in response to fall of PO_2 ~ -25 mm Hg, which could be blocked by the specific dopamine D_1 receptor antagonist SCH23990, suggesting possible role of locally produced dopamine in the vasodilation.

This study suggests that there are two sources of catecholamines, in particular dopamine - neuronal and non-neuronal - and the non-neuronal synthesis is carried out by both principal cell types of vascular wall, i.e. EC and VSMC. Catecholamines produced by vascular cells are released in the event of hypoxia. This locally synthesized and released dopamine mediates vasodilation and might help in an increased O_2 and nutrient supply to the affected organ.

VIII Zusamenfassung

Katecholamine (Dopamine, Noradrenalin und Adrenalin) spielen eine physiologisch wichtige Rolle als Neurotransmitter sowie in der Regulation verschiedenster Körperfunktionen. Dopamin ist ein Zwischenprodukt in der Synthese von Noradrenalin und Adrenalin sowie auch selbst ein Neurotransmitter im zentralen Nervensystem. In den systemischen Arterien des Säugers ist Dopamin zumeist ein potenter Vasodilatator. Die vaskulären Effekte von Dopamin werden über spezifische G Protein-gekoppelte Rezeptoren (D_1 - D_5) vermittelt.

In der vorliegenden Studie wurde das Vorkommen der enzymatischen Maschinerie zur Katecholaminsynthese (Tyrosinhydroxylase = TH, DOPA-Decarboxylase = DDC; Dopamin-β-Hydroxylase = DβH, Phenyläthanolamin-N-Methyltransferase = PNMT) in Arterien der Ratte untersucht sowie auch deren Hypoxie abhängige Regulation in Endothel-(EC) und vaskulären glatten Muskelzellen (VSMC). Der Gehalt an mRNA wurde über quantitative RT-PCR untersucht, TH-Proteinexpression wurde mittels Western Blot bestimmt. Weiterhin wurde die Expression des geschwindigkeitsbestimmenden Enzyms der Katecholaminsynthese (TH) mittels quantitativer RT-PCR, Immunhistochemie und Western Blot in intakten Gefäßen (Brustaorta, abdominale Aorta, obere Mesenterialarterie und Femoralarterie) untersucht.

Expression der mRNA für alle vier Enzyme war nachweisbar und wurde in allen untersuchten Arterien quantifiziert. Hierbei zeigten sich für die einzelnen Enzyme unterschiedliche mRNA-Mengen, wobei PNMT die niedrigste Expression aufwies. TH-Protein wurde in diesen Arterien immunhistochemisch und im Western Blot nachgewiesen. Die TH-Expression in diesen Arterien lässt eine aktive Synthese von Dopamin und/oder anderen Katecholaminen erwarten. In einer früheren Arbeit wurde TH-mRNA-Expression in der Aorta der Ratte gezeigt und es wurde angenommen, dass dies durch eine Kontamination durch Paraganglien während der Probengewinnung beruhte. In den immunhistochemischen Untersuchungen in dieser Arbeit waren Paraganglien nicht nachweisbar, was darauf hinweist, dass die Aorta selbst zur Katecholaminsynthese in der Lage ist.

EC wurden aus der Aorta und Lungenarterie der Ratte isoliert und kultiviert. Sie wurden durch den Nachweis der DiI-Ac-LDL-Aufnahme und durch Immunmarkierung mit anti-vWF-Antikörpern charakterisiert. VSMC wurden von der Brust und der Abdominalaorta isoliert und kultiviert, ihre Charakterisierung erfolgte durch

Immunmarkierung mit anti α-smooth muscle actin Antikörper. Unter normoxischen Kulivierungsbedingungen exprimieren EC und VSMC mRNA für alle Enzyme der Katecholaminsynthese. Diese Gefäßzellen wurden dann für 6, 12 und 24 Stunden hypoxischer (1% O_2) Atmosphäre exponiert. Real-time RT-PCR zeigte die mRNA für alle oder einen Teil der Enzyme der Katecholaminsynthese in diesen Zellen. In den Lungen-EC der Ratte bewirkte Hypoxie-Exposition eine Hochregulation der TH-mRNA um das 25-fache nach 24 Stunden und der DβH mRNA um das 8-fache nach 6 und 24 Stunden, wohingegen DDC- und PNMT-mRNA Gehalt sich nicht signifikant veränderten. Im Gegensatz dazu zeigten sich keine signifikanten Veränderungen in Aorten-EC der Ratte nach hypoxischer Exposition. In VSMC war TH-mRNA qualitativ nachweisbar, wohingegen der DDC-mRNA-Gehalt unter der Nachweisgrenze lag. Hypoxie-Exposition der VSMC resultierte nicht in einer statistisch signifikant nachweisbaren Regulation des DβH- und PNMT-mRNA-Gehalts. Diese Ergebnisse zeigen, dass Zellen der Gefäßwand zur Katecholaminsynthese in der Lage sind und dass diese Synthese unter hypoxischen Bedingungen unterschiedlich reguliert wird.

Dies ist die erste Studie, die einen direkten Nachweis der Expression der Katecholaminsynthese-Enzyme in isolierten Gefäßwandzellen liefert. Kuncova und Mitarbeiter zeigten zuvor in 2007 das Vorkommen von Katecholaminen in der Aorta und oberen Mesenterialarterie der Ratte. Chemische Sympathektomie mit dem Neurotoxin 6-Hydroxydopamin führte zu einer signifikanten Reduktion des Noradrenalin- und Adrenalingehaltes, während der Dopamingehalt konstant blieb. Funktionelle Studien an der oberen Mesenterialarterie der Ratte zeigten eine endothelabhängige Vasodilatation bei einem Abfall des PO_2 um 25 mmHg, welche durch den spezifischen Dopamin D_1 Rezeptorantagonisten SCH23990 aufgehoben wurde. Dies weist auf eine wahrscheinliche Rolle des lokal produzierten Dopamin in der Vasodilatation hin.

Die Ergebnisse dieser Studie lassen zwei verschiedene Quellen von Katecholaminen, insbesondere Dopamin, in der Gefäßwand annehmen – neuronal und nicht-neuronal – und die nicht-neuronale Synthese kann von den beiden vorherrschenden Zellen der Gefäßwand (EC und VSMC) bewerkstelligt werden. Von Gefäßmuskelzellen hergestellte Katecholamine können unter hypoxischen Bedingungen freigesetzt werden. Dieses lokal synthetisierte und freigesetzte Dopamin vermittelt Gefäßerweiterung und trägt wahrscheinlich zu einer verbesserten Sauerstoff- und Nährstoffversorgung der abhängigen Organe bei.

IX Ehrenwörtliche Erklärung

„Hiermit erkläre ich, dass ich die vorliegende Arbeit selbständig und ohne unzulässige Hilfe oder Benutzung anderer als der angegebenen Hilfsmittel angefertigt habe. Alle Textstellen, die wörtlich oder sinngemäß aus veröffentlichten oder nichtveröffentlichten Schriften entnommen sind, und alle Angaben, die auf mündlichen Auskünften beruhen, sind als solche kenntlich gemacht. Bei den von mir durchgeführten und in der Dissertation erwähnten Untersuchungen habe ich die Grundsätze guter wissenschaftlicher Praxis, wie sie in der „Satzung der Justus-Liebig-Universität Gießen zur Sicherung guter wissenschaftlicher Praxis“ niedergelegt sind, eingehalten. Ich versichere, dass Dritte von mir weder unmittelbar noch mittelbar geldwerte Leistungen für Arbeiten erhalten haben, die im Zusammenhang mit dem Inhalt der vorgelegten Dissertation stehen, und dass die vorgelegte Arbeit weder im Inland noch im Ausland in gleicher oder ähnlicher Form einer anderen Prüfungsbehörde zum Zweck einer Promotion oder eines anderen Prüfungsverfahrens vorgelegt wurde. Alles aus anderen Quellen und von anderen Personen übernommene Material, das in der Arbeit verwendet wurde oder auf das direkt Bezug genommen wird, wurde als solches kenntlich gemacht. Insbesondere wurden alle Personen genannt, die direkt an der Entstehung der vorliegenden Arbeit beteiligt waren.“

Datum 11.10.2011

Amir Rafiq

Der Lebenslauf wurde aus der elektronischen Version der Arbeit entfernt.

The curriculum vitae was removed from the electronic version of the paper.

Research Publications

1. Aslam M, Pfeil U, Gündüz D, **Rafiq A**, Kummer W, Piper HM, Noll T. Intermedin/adrenomedullin2 stabilises endothelial barrier and antagonizes thrombin-induced barrier failure. Br J Pharmacol. 2011 Jun 15. doi: 10.1111/j.1476-5381.2011.01540.x. [Epub ahead of print]
2. Pfeil U, Aslam M, Paddenberg R, Quanz K, Chang CL, Park JI, Gries B, **Rafiq A**, Faulhammer P, Goldenberg A, Papadakis T, Noll T, Hsu SY, Weissmann N, Kummer W. Intermedin/adrenomedullin-2 is a hypoxia-induced endothelial peptide that stabilizes pulmonary microvascular permeability. Am J Physiol Lung Cell Mol Physiol. 2009 Nov;297(5):L837-845

Published Abstracts

1. **Rafiq A**, Paddenberg R, Pfeil U, Brüggmann D, Kummer W. Catecholamine biosynthesis and its hypoxic regulation in vascular cells. Annual Meeting of the Society for Microcirculation and Vascular Biology, Aachen, September 25-27, 2008 (Poster presentation)

2. **Rafiq A**, Paddenberg R, Pfeil U, Brüggmann D, Kummer W. Catecholamine biosynthesis and its hypoxic regulation in vascular cells.103rd international meeting of Anatomische Gesellschaft, Innsbruck, Austria March 2008 (Oral presentation) DOI 10.337/anatges.2008.0005

3. Kuncova J, Pfeil U, Brüggmann D, Paddenberg R, **Rafiq A,** Schluter KD, Mewe M, Middendorff R, Slavikova J, Kummer W. Dopamine is an endothelium-derived vasodilator in hypoxic vessels. **Autonomic Neuroscience**, Volume 135, Issues 1-2, 30 September 2007, Pp. 146 (Poster Presentation)

4. Pfeil U, Kuncova J, Brüggmann D, Paddenberg R, **Rafiq A**, Schlüter KD, Mewe M, Middendorff R, Slavikova J, Kummer W. Dopamine is an endothelium-derived vasodilator in hypoxic vessels. 102nd international meeting of Anatomische Gesellschaft, Giessen 2007 (Oral presentation) DOI 10.337/anatges.2007.0002

5. Vargova L, **Rafiq A**, Sykova E. Extracellular space volume and tortuosity in the cortical slices of tenascin-R knockout mice. Program No. 386.12. *2005 Abstract Viewer/Itinerary Planner*. Washington, DC: Society for Neuroscience, 2005. Online. (Poster presentation)

6. **Rafiq A,** Vargová L, Syková E. The effect of lack of tenascin-R on the extracellular space diffusion parameters and potassium-evoked cell swelling in mouse cortical slices. Fifth Conference of the Czech Neuroscience Society, Prague 19-21, 2005 (Poster presentation)

X Acknowledgements

I am extremely thankful to my mentor Prof. Dr. Wolfgang Kummer for offering me a great opportunity to do my doctoral research thesis in his department. He always supported me with his highly scientific attitude, encouragement, extreme kindness, constructive criticism and useful suggestions. I am also thankful to him for offering me a chance to be a member of the graduate college GRK 534 “Biological basics of vascular medicine.”

I am indebted to Dr. Renate Paddenberg and Dr. Uwe Pfeil for their guidance and help throughout my work. They were always there to solve my lab work problems.

I am also thankful to Deutsche Forschung Gemenschaft for providing me stipend and funding for my doctoral work through GRK 534 “Biological basics of vascular medicine.” I would also like to thank to graduate college speakers, Prof. Dr. H. M. Piper and Prof. Dr. Thomas Noll of graduate college for organizing excellent seminars to improve my basic and advance knowledge in cardiovascular biology.

I am especially thankful to all my colleagues at my department specially Dr. Gabriela Krasteva, Martin, Tamara, Silke, Anna, Petra Faulhammer and all others for their timely help and support during my lab work. I am also thankful to my doctoral colleague Miriam, Gitte, Heike, Andrea and Murtaza for their support nice company and team work to accomplish lab work. It was really nice work in a team with all the colleagues.

I am especially thankful to my parents and my brothers Wasim, Shahid and Waqas for their continuous moral support and help to achieve my goal to become a doctor.

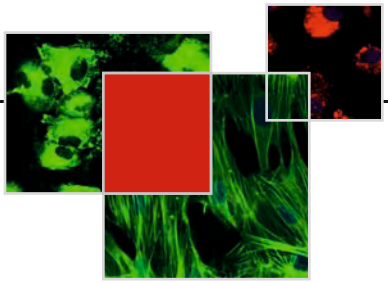

édition scientifique
VVB LAUFERSWEILER VERLAG

VVB LAUFERSWEILER VERLAG
STAUFENBERGRING 15
D-35396 GIESSEN

Tel: 0641-5599888 Fax: -5599890
redaktion@doktorverlag.de
www.doktorverlag.de

ISBN: 978-3-8359-5888-3